

THE CONTRIBUTIONS OF MIR-155 IN OBESITY, METABOLIC SYNDROME,
AND ATHEROSCLEROSIS DEVELOPMENT

A Dissertation
Submitted
To the Temple University Graduate Board

In Partial Fulfillment
Of the Requirements for the Degree of
DOCTOR OF PHILOSOPHY

By
Anthony Virtue
May, 2014

Examining Committee Members:

Dr. Xiao-Feng Yang (Advisor), Department of Pharmacology, Temple University
Dr. Hong Wang (Co-Advisor), Department of Pharmacology, Temple University
Dr. Barrie Ashby, Department of Pharmacology, Temple University
Dr. Michael Autieri, Department of Physiology, Temple University
Dr. Madesh Muniswamy, Department of Biochemistry, Temple University
Dr. Xiaolu Yang, (External Examiner), University of Pennsylvania

©
Copyright
2014
By
Anthony Virtue
All Rights Reserved

ABSTRACT

THE CONTRIBUTIONS OF MIR-155 IN OBESITY, METABOLIC SYNDROME, AND ATHEROSCLEROSIS DEVELOPMENT

Anthony Virtue

Doctor of Philosophy

Temple University, 2014

Doctoral Advisory Committee Chair: Xiao-feng Yang, MD, PhD

The global incidence of overweight and obese individuals has skyrocketed in the past few decades resulting in a new health epidemic. In 1980, 5% of males and 8% of females were categorized as obese; by 2008 these values doubled equating to half a billion adults worldwide. This surge of overweight and obese individuals has driven a dramatic increase in people afflicted with metabolic disorders. As such, the term “metabolic syndrome” (MetS) has been coined to describe several interrelated metabolic risk factors which often present in concert. Specifically, metabolic syndrome refers to the presence of at least three of the following five conditions: central obesity, elevated triglycerides, diminished high density lipoprotein (HDL) cholesterol, hypertension, and insulin resistance (IR). MetS is a major health concern due to its ability to increase the likelihood of cardiovascular disease (CVD), diabetes, and other life-threatening ailments. In light of this growing medical epidemic, we have concentrated our efforts in evaluating the role of microRNA-155 (miR-155) in MetS development. MicroRNAs are a newly defined class of small, non-coding RNA which contain the unique ability to regulate gene expression through RNA interference. As a result of this ability, microRNAs can mediate a wide variety of cellular processes.

In order to evaluate the function of miR-155 in MetS, we established a novel miR-155^{-/-}/ApoE^{-/-} (DKO) mouse model. Coupling this model with the use of normal rodent or high fat diets allowed us to investigate how states of caloric balance and surplus affected the manifestation of the individual MetS components. We found that male and female DKO mice fed a high fat diet had significantly augmented body masses of 18% and 10% respectively, when compared to ApoE^{-/-} counterparts on the same diet. Evaluation of this phenotype with body composition analysis revealed an 18% and 46% increase in body fat percentage among the male DKO mice on normal and high fat diets, respectively. This trend was also observed in female DKO mice, albeit to a lesser extent. This phenotype was further substantiated by the observation of augmented gonadal white adipose tissue pad mass within male and female DKO mice fed either chow. This equated to a 43% and 112% increase in male mice and a 45% and 57% augmentation in female mice for normal and high fat chow diets, respectively.

In light of our findings, we also evaluated how miR-155 impacted glucose and insulin sensitivity. We found levels of insulin to be augmented by 181% and 148% in male DKO mice on normal and high fat diets, respectively. Furthermore, we found these mice to be euglycemic. These observations suggest that DKO mice are IR but capable of compensating for their insensitivity with elevated insulin production.

Due to the tight association between MetS and the development of non-alcoholic fatty liver disease (NAFLD) as well as CVD, we felt it prudent to investigate the manifestation of these conditions. We found elevated hepatic mass of 40% and 13% in male and female DKO mice on high fat chow. Furthermore, hepatic discoloration was seen in these mice prompting us to perform in-depth histological evaluation which

revealed widespread steatosis, a hallmark of NAFLD. Meanwhile, investigation of atherosclerosis, the key underlying cause of most CVDs, unexpectedly revealed diminished development. Due to the complex nature of atherosclerosis it is tough to explain the exact reason for this observation. Independent reports have shown that miR-155 plays a critical role in the development, maturation, or activation of B-cell, T-cells, macrophages, and dendritic cells. As a result, decreased immune cell infiltration may be the root cause for the observed decline in atherosclerosis.

Taking into account our observations of obesity, IR, and NAFLD in conjunction with independent findings of blood pressure mitigation by miR-155, we feel confident in reporting that miR-155 is a vital factor in preventing MetS and NAFLD development. Despite this, we surprisingly found atherosclerosis development to be diminished in these mice suggesting a pro-inflammatory role in atherogenesis. This duality highlights the complex and ambiguous nature of miRNAs. In light of this, further evaluations should be conducted to gain additional insight into these pathologies and hopefully the development of novel therapeutics.

ACKNOWLEDGEMENT

At this time I would like to first and foremost thank my supervisor, Dr. Xiao-feng Yang. His enthusiasm and dedication to the field of science has been an inspiration to me, motivating me throughout my graduate endeavors and driving me to succeed in my research. His extensive experience has made him an excellent mentor whose insight has proven invaluable. Dr. Yang has always treated me as a colleague, allowing me to vocalize my thoughts and opinions. In turn, this has allowed me to develop my critical thinking skills and mature as a scientist. I will be forever grateful for his critical suggestions, devotion of time, and guidance throughout this entire process.

I would also like to acknowledge and thank my co-supervisor, Dr. Hong Wang. She has generously provided her time and expertise to review my data and publications, providing valuable insight which has shaped my graduate project. Her passion for science, desire for excellence, and work ethic is a model to those around her. She has taught me to work with dedication, focus, and passion which I will not forget.

In addition to Dr. Yang and Dr. Wang, I am also appreciative of my other committee members Dr. Ashby, Dr. Autieri, Dr. Muniswamy, and Dr. Xiaolu Yang who have given their time and efforts. Their feedback and suggestions have been useful allowing me to carefully craft my thesis and graduate work. I am truly grateful for their guidance during this process.

Aside from my committee, I would like to express my gratitude to my colleagues within Dr. Yang's and Dr. Wang's laboratories. They have provided me with assistance throughout my time here at Temple. Specifically, I would like to thank our lab manager Xiaohua Jiang. She has graciously lent her scientific expertise and advice more times

than can be counted, while her professionalism and leadership has been a model for all others to aspire too. I would also like to personally acknowledge Ying Yin, Meghanna Pansuria, and Jietang Mai who have given me endless support. They have provided their time and expertise, personally teaching me most of the scientific skills which I have acquired at Temple. Most importantly, they have provided their friendships which have made this time more enjoyable and the completion of this program possible.

I would also like to acknowledge the National Institutes of Health, Temple University, and the American Heart Association for the funding and the financial support I have received. Without this, I would have been unable to enroll in this program and complete my doctorate.

Finally, I would like to thank my wife Shannon, who has provided an unfaltering support system which has instilled me with the resolve and wherewithal to complete my graduate work. Her understanding, patience, and sacrifice during this time have been endless and I am truly blessed to have her in my life. I love you and cannot thank you enough.

DEDICATION

This dissertation is dedicated to my wife, Dr. Shannon Myers Virtue, for her love and support.

TABLE OF CONTENTS

ABSTRACT	iii
ACKNOWLEDGEMENT	vi
DEDICATION	viii
LIST OF TABLES	xiii
LIST OF FIGURES	xiv
LIST OF ABBREVIATIONS.....	xvi
CHAPTER 1: GENERAL INTRODUCTION	1
Metabolic Syndrome Overview	1
Obesity	4
Body Fat Quantification.....	7
Physiological Role of Adipose Tissue	8
Adipogenesis.....	9
<i>Molecular Regulation of Adipogenesis</i>	9
Adipose Tissue as a Secretory Organ	13
Glucose Metabolism	13
Obesity and Insulin Resistance	14
<i>Adipokines in Insulin Resistance</i>	15
<i>Insulin Action in Adipocytes</i>	16
Non-Alcoholic Fatty Liver Disease	17
Cardiovascular Diseases	18
Atherosclerosis Overview.....	21
<i>The Pathological Progression of Atherosclerosis</i>	21

<i>Mouse Models of Atherosclerosis</i>	25
<i>Atherosclerosis Quantification</i>	27
MicroRNAs Overview	27
MicroRNAs Biogenesis	28
MicroRNAs Targeting	31
MicroRNAs-directed Endonucleic Cleavage.....	32
MicroRNAs-directed Translation Repression.....	33
MicroRNAs and Disease.....	37
Key Knowledge Gaps, Hypothesis, and Rationale of Thesis	40
CHAPTER 2: MATERIAL AND METHODS.....	43
Animal Care	43
Mouse Genotyping.....	43
Murine Age Development.....	44
Body Composition Analysis	45
Gonadal White Adipose Tissue (gWAT) Pad Analysis.....	45
Hepatic Tissue Analysis.....	46
Paraffin Embedding	46
Lipid, Lipoprotein, and Metabolic Parameter Analysis.....	47
Glucose Tolerance Test (GTT).....	47
Insulin Tolerance Test (ITT).....	48
RNA Extraction, Isolation, and Quantification.....	48
RNA Reverse Transcription.....	49
Quantitative Real-Time PCR	49

miFinder PCR Array	50
Atherosclerotic Lesion Analysis	50
Statistical Analysis	52
CHAPTER 3: RESULTS	53
Development of novel miR-155 ^{-/-} /ApoE ^{-/-} mice	53
DKO mice gain excessive body weight during periods of caloric surplus	55
DKO mice have augmented body fat % and reduced lean body mass %	57
DKO mice have larger gWAT deposits with hypertrophic adipocytes	60
DKO mice have augmented leptin and resistin when on a high fat diet	63
DKO mice are hyperinsulinemic amidst euglycemia	65
DKO mice are afflicted with NAFLD	71
DKO mice have no distinction in TG levels, elevated HDL on a high fat diet	74
DKO mice have greater hepatic and WAT C/EBP- α , C/EBP- β , and PPAR- γ	76
DKO mice have elevated gWAT levels of C/EBP- α , C/EBP- β , and PPAR- γ	79
Atherosclerosis development is reduced in DKO mice	80
CHAPTER 4: DISCUSSION	88
MiR-155 and Obesity	89
MiR-155 and Glucose/Insulin Expression	97
MiR-155 and NALFD	98
MiR-155 and Plasma Lipid Expression	100
MiR-155 and Hypertension	101
Molecular Mechanism and Working Model	104
MiR-155 and Atherosclerosis	108

Conclusion	112
Future Directions	113
REFERENCES CITED.....	115

LIST OF TABLES

Table 1: NCEP ATPIII and WHO clinical criteria for metabolic syndrome.....	3
Table 2: WHO defined BMI weight classes	7
Table 3: Association of miRNAs with common pathologies	39
Table 4: List of miR-155 experimentally verified targets	42
Table 5. List of primers used in qRT-PCR	50
Table 6: List of miRNAs which have a ≥ 4 -fold or greater expression change.....	84

LIST OF FIGURES

Figure 1: Prevalence of obesity in the United States by decade	5
Figure 2: Global prevalence of obesity in adults 20 years or older in 2008	6
Figure 3: Transcriptional regulation of adipogenesis.....	12
Figure 4: Leading causes of non-communicable mortality in the world	20
Figure 5: Multi-step development of atherosclerosis.....	24
Figure 6: MiRNAs biogenesis	30
Figure 7: Methods of miRNAs RNA interference.....	36
Figure 8: Breeding scheme for novel miR-155 ^{-/-} /ApoE ^{-/-} mice	54
Figure 9: Body weight development.....	56
Figure 10: NMR body composition assessment	59
Figure 11: Evaluation of murine gWAT mass and gross morphology	61
Figure 12: Histological evaluation of gWAT	62
Figure 13: Plasma adipokine levels	64
Figure 14: Plasma insulin levels	67
Figure 15: Blood glucose levels of fed and fasted mice	68
Figure 16: Glucose tolerance testing and quantification.....	69
Figure 17: Insulin tolerance testing and quantification.....	70
Figure 18: Evaluation of hepatic mass and gross morphology.....	72
Figure 19: Histological evaluation of hepatic tissue.....	73
Figure 20: Plasma triglyceride and HDL levels.....	75
Figure 21: Hepatic expression of C/EBP- α , C/EBP- β , and PPAR- γ	78
Figure 22: gWAT mRNAs expression of C/EBP- α , C/EBP- β , and PPAR- γ	79

Figure 23: Scatter plot of differentially expressed miRNAs in atherosclerosis....	83
Figure 24: Aortic miR-155 expression is increased during atherogenesis.....	85
Figure 25: <i>En face</i> atherosclerotic lesion quantification.....	86
Figure 26: Representative aortic sinus imagery.....	87
Figure 27: Molecular mechanism of miR-155 regulation of hypertension.....	103
Figure 28: Molecular mechanism for fat mass augmentation in the DKO mice	107
Figure 29: Molecular mechanism for IR in the DKO mice	107
Figure 30: Molecular mechanism for NALFD development in DKO mice	107

LIST OF ABBREVIATIONS

MetS	Metabolic syndrome
HDL	High density lipoprotein
IR	Insulin resistance
NCEP ATP III	National cholesterol education program – Adult treatment panel III
WHO	World health organization
CVD	Cardiovascular disease
DEXA	Dual energy x-ray absorptiometry
NMR	Nuclear magnetic resonance
BMI	Body mass index
FA	Fatty acids
PPARs	Peroxisome proliferator-activated receptors
C/EBPs	CCAT-enhancer-binding proteins
Acyl-CoA	Acyl-coenzyme A synthetase
aP2	Adipocyte lipid-binding protein
LPL	Lipoprotein lipase
PEPCK	Phosphoenolpyruvate carboxykinase
422aP2	422 adipose P2 protein
GLUT4	Flucose transporter 4
SCD1	Stearoyl-CoA desaturase 1
WAT	White adipose tissue
NAFLD	Non-alcoholic fatty liver disease

ECs	Endothelial cells
MCP-1	Monocyte chemoattractant protein-1
CCL5	C-C motif ligand 5
CXCL10	CXC-chemokine ligand 10
M-CSF	Macrophage colony-stimulating factor
TNF- α	Tumor necrosis factor- α
IL-1 β	Interleukin-1 β
VSMCs	Vascular smooth muscle cells
VLDL	Very-low-density lipoprotein
LDL	Low-density lipoprotein
ApoE	Apolipoprotein E
LDLR	Low-density lipoprotein receptor
TLR	Toll-like receptor
NF- κ B	Nuclear factor- κ B
AP-1	Activator protein-1
ICAM-1	Intracellular adhesion molecule-1
VCAM-1	Vascular adhesion molecule-1
GM-CSF	Granulocyte/macrophage colony stimulating factor
MiRNAs	MicroRNAs
3'UTR	3' untranslated region
RISC	RNA-induced silencing complex
Ago2	Argonaute 2
eIF4E	Eukaryote translation initiation factor 4E

SNP	Single-nucleotide polymorphisms
AT1R	Angiotension II type 1 receptor
BIC	B-cell integrated cluster
IACUC	International animal care and use committee
WT	Wildtype
DKO	miR-155 ^{-/-} /ApoE ^{-/-}
PCR	Polymerase chain reaction
NaCl	Sodium chloride
EDTA	Ethylenediaminetetraacetic acid
SDS	Sodium dodecyl sulfate
gWAT	Gonadal white adipose tissue
H&E	Hematoxylin and eosin
PFA	Paraformaldehyde
GTT	Glucose tolerance test
ITT	Insulin tolerance test
qRT-PCR	Quantitative real-time polymerase chain reaction
OCT	Optimal cutting temperature compound
PBS	Phosphate buffered saline
BCL6	B-cell CLL/Lymphoma 6

CHAPTER 1: GENERAL INTRODUCTION

Metabolic Syndrome Overview

Metabolic syndrome (MetS) is a recently coined clinical term which refers to several interrelated metabolic risk factors which often present in concert. Specifically, MetS refers to the presence of at least three of the following five conditions: central obesity, elevated triglycerides, diminished high density lipoprotein (HDL) cholesterol, hypertension, and insulin resistance (IR). Empirical values which indicate the presence of each of these conditions in humans have been established by the National Cholesterol Education Program – Adult Treatment Panel III (NCEP ATP III) and World Health Organization (WHO) which are summarized in Table 1(Grundy et al., 2004). Currently, it is predicted that MetS affects approximately 35% of adults or nearly 70 million Americans("American Heart Association: About Metabolic Syndrome," 2014). The rapid growth of individuals afflicted with MetS has put monumental stress on the health care system and has led to its categorization as a global epidemic.

MetS is a major health concern due to its ability to increase the likelihood of cardiovascular disease (CVD) and diabetes development. Each component of MetS is individually correlated with CVD; however, the presentation of several of these conditions in constellation, like seen in MetS, is a more comprehensive indicator of future cardiovascular risk than any of the markers alone. Individuals diagnosed with MetS have a 2-fold increased risk of suffering from stroke, myocardial infarction, atherosclerosis, or succumbing to CVD-associated mortality. Furthermore, those diagnosed with MetS are 5-fold more likely to develop type II diabetes(Hansson & Hermansson, 2011).

Due to the interdependent nature of the conditions which make up MetS, it is difficult to determine if one condition is primarily responsible for the manifestation of the other conditions. With that said, researchers within the field appear to be in agreement that obesity and IR are the cornerstones to MetS(Hansson et al., 2006; R. Kahn et al., 2005; Lann & LeRoith, 2007). Both conditions are tightly correlated to one another and capable of inducing the other components of MetS. The interrelated nature of obesity and IR will be discussed in greater detail as will their contributions to MetS and CVD development.

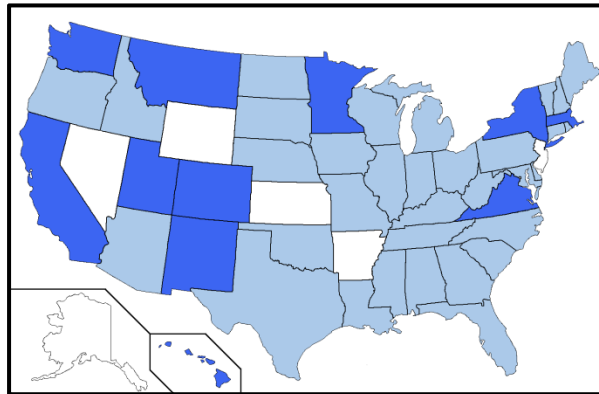
Table 1: NCEP ATPIII and WHO clinical criteria for metabolic syndrome

NCEP ATPIII	
Obesity (Waist Circumference)	>102 in males; >88 in females
Insulin Resistance	Fasted plasma glucose \geq 110mg/dL
Triglycerides	\geq 150 mg/dL
HDL	<40 mg/dL in males; <50 mg/dL in females
Blood Pressure	\geq 130/85 mm Hg
WHO	
Obesity (Waist/Hip Ratio)	>0.90 in males; >0.85 in females
Insulin Resistance	Fasted plasma glucose \geq 110mg/dL or impaired glucose tolerance or hyperinsulinemic or diabetes
Triglycerides	\geq 150 mg/dL
HDL	<35 mg/dL in males; <39 mg/dL in females
Blood Pressure	\geq 140/90 mm Hg

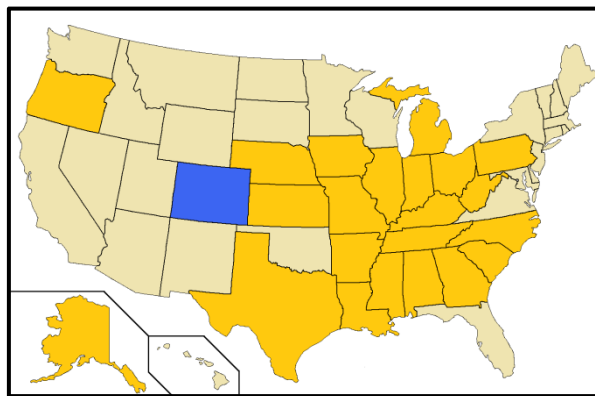
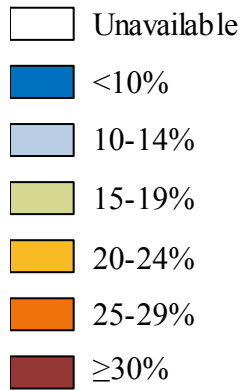
Obesity

Defined as excess body fat, obesity has skyrocketed over the past few decades (Figure 1). In 1980, 5% of males and 8% of females worldwide were obese. These values nearly doubled by 2008 with 10% of men and 14% of women being categorized as obese which staggeringly equated to half a billion adults worldwide. The majority of these cases are concentrated in developed countries (Figure 2)("World Health Organization: Obesity Fact Sheet," 2014). Specifically, in the U.S. alone, over 1/3 of adults are considered obese. This alarming number is placing substantial strain on the health care system and cost an estimated 147 billion dollars in 2008 alone("Centers for Disease Control and Prevention: Adult Obesity Facts," 2014). Physically, the detrimental effects of excess body fat cannot be stressed enough as it induces a pro-inflammatory state and adversely impacts several metabolic parameters including blood pressure, insulin sensitivity, cholesterol, and triglyceride levels. These physiological changes ultimately lead to an increased likelihood of a plethora of diseases like stroke, type 2 diabetes, heart disease, and several types of cancer("World Health Organization: Obesity Fact Sheet," 2014).

1990



2000



2010

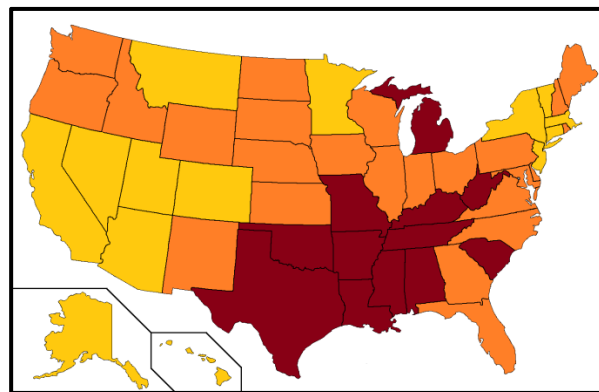


Figure 1: Prevalence of obesity in the United States by decade

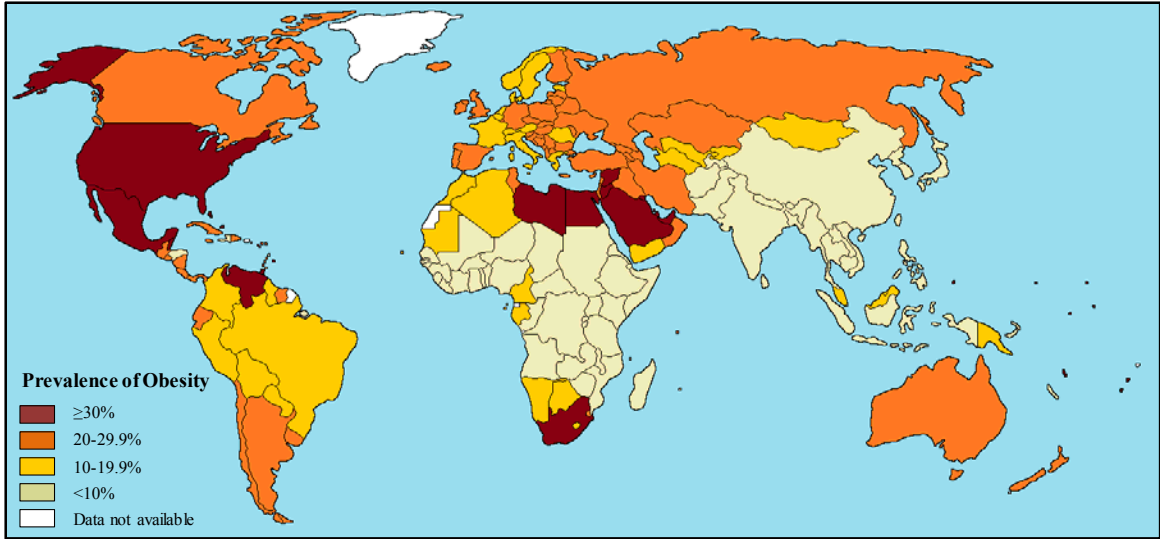


Figure 2: Global prevalence of obesity in adults 20 years or older in 2008

Body Fat Quantification

Body fat can be measured using several different methods including underwater weighing, dual-energy x-ray absorptiometry (DEXA), nuclear magnetic resonance (NMR), bioelectrical impedance, and skinfold thickness. However, due to expenses, availability, and difficulties associated with these techniques they are often not used clinically. Instead, the easily calculated surrogate measurement of body mass index (BMI) is commonly used. BMI is computed by dividing an individual's weight (kg) by their squared height (meters). The derived value is then determined to be within a particular range which represents a certain weight class. These weight classes and the corresponding numeric ranges can be found in Table 2 ("Centers for Disease Control and Prevention Website: About BMI for adults," 2014). Despite some shortcomings, BMI is a very useful tool for quickly assessing an individual's "adiposity" and gauging their health risk as a result of their weight.

Table 2: WHO defined BMI weight classes

BMI (kg/m ²)	Weight Class
Below 18.5	Underweight
18.5 – 24.9	Normal Weight
25.0 – 29.9	Overweight
30.0 – 34.9	Obese Class I
35.0 – 39.9	Obese Class II
40 and Up	Obese Class III

In spite of the advantages of using BMI, recently the measurement of waist circumference has become accepted as a more predictive value for health risk assessment. This is primarily due to the fact that abdominal fat or visceral fat is more tightly associated with metabolic risk than total body fat. This relationship is emphasized by the

fact that normal weight individuals with increased waist size are at elevated risk of CVD(Grundy, 2004). In fact, the WHO and NCEP ATPIII both emphasize abdominal girth and waist/hip ratio, respectively, as criteria for defining MetS(R. Kahn et al., 2005; Moller & Kaufman, 2005).

Physiological Role of Adipose Tissue

Physiologically adipose tissue functions as the primary energy storage site within the body. Adipocytes are uniquely capable of storing circulating triglycerides during periods of caloric surplus, producing reservoirs of metabolic energy for future use. In times of energy deprivation or during prolonged exercise, the stored triglycerides are hydrolyzed to glycerol and fatty acids (FA) and released into the blood stream where they are absorbed by tissue and oxidized to produce energy(Trayhurn & Beattie, 2001). Under physiological conditions, adipocytes adeptly balance the need for energy storage or release in order to maintain metabolic homeostasis.

The essential role of adipose tissue in metabolic homeostasis is highlighted in instances with abnormal adipose stores. As mentioned previously, excessive accumulation of adipose tissue results in the emergence of health complications including a heightened inflammatory state, IR, liver steatosis, and CVD-driven mortality. Interestingly, in lipoatrophic mouse models where there is almost complete loss of adipose tissue these medical complications also occur. Furthermore, these conditions can be reversed or offset with the implantation of adipose tissue. These findings highlight the necessity of adipose tissue in metabolic homeostasis(Gavrilova et al., 2000).

Adipogenesis

The expansion of adipose tissue mass can result from either adipocyte enlargement or *de novo* adipogenesis(P. Wang et al., 2008). The term adipogenesis encompasses the proliferation, differentiation, and transformation of cells within adipose tissue into cells capable of storing lipids. This process can be broken down into two key steps: determination and terminal differentiation. The first step, determination, involves the commitment of mesenchymal stem cells within adipose tissue to become pre-adipocytes. At this point, the cell is not distinct from its predecessor except that it can no longer differentiate into any other cell type. Pre-adipocytes can then undergo mitotic clonal expansion drastically increasing the pre-adipocyte population. In the second phase, terminal differentiation, the pre-adipocytes differentiate into mature adipocytes. This phase is hallmarked by a change in cell shape from fibroblastic to spherical. This alteration in appearance signals genetic expression modifications within the cell as the production of new cellular components and extracellular matrix would be required for this morphological transformation. It is hypothesized that these changes result from the activation of critical adipogenic transcription factors that are required for terminal adipocyte differentiation(Romao et al., 2011). At this point, the transforming cells become mature adipocytes gaining the ability to transport lipids, synthesize lipids, synthesize adipocyte-specific proteins, and become insulin sensitive(Rosen & MacDougald, 2006).

Molecular Regulation of Adipogenesis

The differentiation of cells from a primitive form to a terminal cell type requires a major genetic shift which is typically mediated by transcription factors. It has been

discovered that family members of the peroxisome proliferator-activated receptors (PPARs) and CCAT-enhancer-binding proteins (C/EBPs) are vital in adipogenesis (Romao et al., 2011). At the initiation of adipogenesis, the expression of C/EBP- β is rapidly induced. Sensibly, this transcription factor has been found to augment the expression of several genes which are important in early adipogenesis. Among its targets are the two critical adipogenic factors PPAR- γ and C/EBP- α (Rosen & Spiegelman, 2000). PPAR- γ is required for adipocyte differentiation and thus is considered the master regulator of adipogenesis. Abundant experimental evidence exists which shows that the deletion of PPAR- γ results in the loss of adipocyte maturation (Rosen et al., 2000). Furthermore, the independent over-expression of PPAR- γ within non-adipogenic mouse fibroblasts has been shown to instigate differentiation into mature fat cells (Rosen & MacDougald, 2006). Mechanistically, it has been reported that PPAR- γ activates several adipogenic genes such as acyl-coenzyme A synthetase (acyl-CoA), adipocyte lipid-binding protein (aP2), lipoprotein lipase (LPL), and phosphoenolpyruvate carboxykinase (PEPCK) (Romao et al., 2011). In fact, most pro-adipogenic factors gain their entitlement from augmenting PPAR- γ expression. Aside from adipocyte differentiation, PPAR- γ is also required for the maintenance of adipocyte terminal differentiation. The *in vitro* administration of PPAR- γ dominant negative adenoviruses in 3T3-L1 adipocytes results in the loss of lipid accumulation and adipocyte markers, while the inducible loss of PPAR- γ *in vivo* has been found to cause mature adipocyte cell death (Rosen & MacDougald, 2006).

Although C/EBP- α cannot individually induce adipocyte differentiation like PPAR- γ , it is still vital in adipogenesis. Its expression activates the transcription of

several adipogenic genes such as adiponectin, leptin, 422 adipose P2 protein (422aP2), glucose transporter 4 (GLUT4), and stearyl-CoA desaturase 1 (SCD1)(Lin & Lane, 1994; Lowe et al., 2011). Furthermore, its deletion results in significant hypoglycemia and perinatal lethality. Restoration of hepatic C/EBP- α permits viability but results in the virtual loss of all murine white adipose tissue (WAT). While PPAR- γ is believed to be the primary driver in adipocyte differentiation and maintenance, C/EBP- α has been indicated as the principle factor responsible for WAT insulin sensitivity(Rosen & MacDougald, 2006).

Both PPAR- γ and C/EBP- α are capable of inducing the expression of the other, forming a functional positive-feedback loop. In doing so, C/EBP- α and PPAR- γ work in a collaborative manner to promote an array of genes involved in the maturation and maintenance of mature adipocytes, encompassing genes involved in insulin sensitivity, lipogenesis, and lipolysis(Rosen et al., 2000). The timing of this highly regulated transcriptional cascade can be seen in Figure 3.

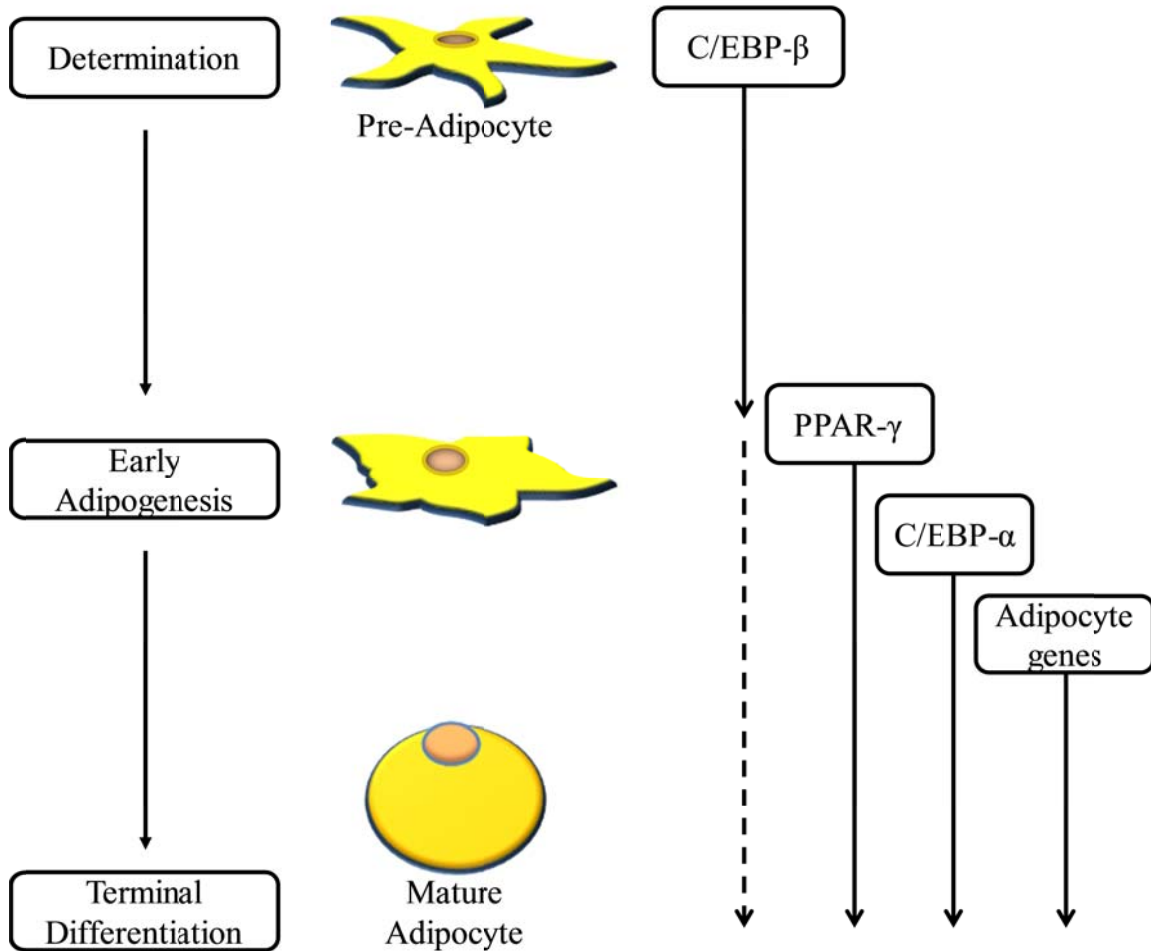


Figure 3: Transcriptional regulation of adipogenesis

The differentiation and maturation of fibroblasts into mature adipocytes is tightly controlled by the expression of key transcription factors. In brief, the expression of C/EBP- β is rapidly induced in early adipogenesis. As a result, numerous adipogenic genes are activated including PPAR- γ and C/EBP- α . These transcription factors further activate one another forming a positive feedback loop. As a consequence, the expression of genes vital to mature adipocytes are expressed like those associated with insulin sensitivity, lipogenesis, and lipolysis.

Adipose Tissue as a Secretory Organ

As the main energy reservoir, the secretion of FA by WAT has long been recognized. However, the ability of WAT to release proteins has only recently been discovered and has led to the characterization of WAT as a significant endocrine organ (P. Wang et al., 2008). These secreted factors, also termed adipokines, have a diverse physiological role impacting functions such as appetite satiety, insulin sensitivity, lipid metabolism, inflammation, blood pressure, and overall vascular homeostasis. The activity of these secreted proteins can be local in nature, either autocrine or paracrine, or be distant as endocrines (Trayhurn & Beattie, 2001). In obesity, the production of many of these factors like leptin and adiponectin becomes dysfunctional. As a result, high levels of these peptides are closely linked to diseases such as CVD, MetS, and IR (P. Wang et al., 2008).

Glucose Metabolism

Throughout the day, homeostatic glucose levels are dynamically challenged by shifts between fed and fasted states. Despite this, plasma glucose levels remain tightly controlled within a range of 4 and 7 mM in healthy adults. In order to maintain this narrow window, the body must balance intestinal glucose absorbance, hepatic glucose production, and peripheral glucose metabolism. In large part, this is accomplished through the actions of insulin. Although insulin is incapable of mediated intestinal glucose absorption, it can regulate hepatic glucose production and peripheral glucose metabolism. Specifically in the liver, insulin inhibits glycogenolysis and gluconeogenesis while activating glycogen synthesis. These actions allow insulin to modulate hepatic glucose production. Meanwhile, insulin also controls peripheral tissue

absorption and metabolism of glucose. This is possible by facilitating the cell membrane expression of GLUT4, the central glucose receptor. These abilities make insulin the primary regulator of glucose metabolism(Saltiel & Kahn, 2001).

The biological efficacy of insulin fluctuates throughout life in response to changes like puberty and pregnancy as well as lifestyle alterations such as physical exercise and diet(S. E. Kahn et al., 2006). Under certain pathological conditions like those seen in obesity, a significant biological loss of insulin activity can occur resulting in reduced glucose uptake, metabolism, or storage(S. E. Kahn, 2003). This condition is commonly referred to as insulin resistance (IR). In response IR, the production of additional insulin from existing β -cells occurs or β -cell mass is increased. Ultimately, this leads to elevated levels of circulating insulin termed hyperinsulinemia. In some cases this restores glucose levels to normal; however, it can also further instigate IR by reducing insulin receptor expression and desensitizing associated signaling pathways(B. B. Kahn & Flier, 2000). IR is a serious medical condition which disrupts metabolic homeostasis leading to the development of complications like type II diabetes, CVD, and MetS(S. E. Kahn et al., 2006).

Obesity and Insulin Resistance

There is substantial evidence demonstrating that fat is highly correlated with insulin sensitivity. Epidemiologic studies across all ethnic groups have shown that the risk of IR increases with body fat. Two murine models of obesity, ob/ob and db/db, result in gross weight gain due to the loss of leptin or its receptor. In these murine models, it is clear that excess fat precedes and contributes to the development of severe IR and hyperglycemia. This relationship is further supported by the finding that the surgical

removal of visceral fat pads from these mice results in improved hepatic insulin sensitivity(Moller & Kaufman, 2005). Mechanistically, the IR witnessed in obesity results from defects in glucose uptake, metabolism, and storage. Specifically, a decline in glucose metabolism within adipocytes and skeletal muscle, a reduction in GLUT4 receptor expression and activity, impaired glucose transport, and diminished inhibition of hepatic glucose production are observed(B. B. Kahn & Flier, 2000).

Adipokines in Insulin Resistance

With a clear causal relationship between obesity and IR, the possible role of adipokines in regulating insulin sensitivity has garnered interest. In particular, adiponectin, resistin, and leptin have risen to the forefront. Adiponectin levels have been found to be reduced in subjects afflicted with IR and MetS suggesting a possible mechanistic function. Thus far it has been determined that adiponectin can mediate glucose homeostasis and insulin sensitivity. The administration of recombinant adiponectin was found to reduce glucose levels in diabetic mice and enhance the biological action of insulin in hepatocytes. Furthermore, work conducted in adiponectin-deficient mice showed susceptibility to diet-induced insulin resistance. These experimental findings clearly demonstrate a connection between adiponectin and IR. It is hypothesized that the mechanistic effect of adiponectin is derived from actions on the activation of the AMP-activated protein kinase pathway. However, further investigation needs to be conducted to firmly cement this connection(Moller & Kaufman, 2005).

Resistin is another adipokine drawing major interest in regard to IR. Discovered in 2000, it was quickly determined to be capable of interfering with insulin action. In fact, plasma expression of resistin is elevated in obese and diabetic patients and

correlated with the development of CVDs and MetS. Similar elevations in plasma resistin levels are also reported in murine genetic and diet-induced obesity models. In rodents, the administration of resistin results in augmented hepatic glucose production and higher plasma glucose levels. Meanwhile, a reciprocal effect is witnessed in resistin-deficient mice which have diminished fasting glucose levels. Furthermore, the administration of an anti-resistin antibody in obese and IR mice was found to ameliorate insulin insensitivity. Aside from IR, resistin is also linked to atherosclerosis, non-alcoholic fatty liver disease (NAFLD), CVD, and several other inflammatory based diseases(Jamaluddin et al., 2012).

Leptin is also believed to be a key player in IR. This theory is primarily based on the fact that leptin replacement therapy in ob/ob mice dramatically alters glucose and insulin levels, an effect that is observed before alterations in food intake or weight are seen. Furthermore, experimental evidence obtained from normal rodents administered leptin acutely or chronically both demonstrate heightened insulin sensitivity(B. B. Kahn & Flier, 2000).

Insulin Action in Adipocytes

Adipocytes are one of the most highly responsive cells to insulin, which has been found to influence important facets of adipocyte biology(B. B. Kahn & Flier, 2000). In a fed state, elevated plasma insulin levels prompt fatty acid uptake, triglyceride storage, glucose uptake, and glycogen synthesis in adipose tissue while simultaneously impeding lipolysis. These functions are carried out by augmenting the activity of lipoprotein lipase which aids in the clearance of triglyceride-rich lipoproteins, facilitating the production of glycerol-3-phosphate which is integral to FA transformation to triglycerides, and by

inhibiting lipolysis(Ruan & Lodish, 2003). If adipose tissue becomes IR, the uptake and storage of triglycerides is reduced resulting in elevated levels of circulating FA. As a result, peripheral tissue like the liver and skeletal muscle will begin to store the excess triglycerides resulting in peripheral IR and the development of health complications(Ruan & Lodish, 2003).

Non-Alcoholic Fatty Liver Disease

NAFLD is a pathological condition encompassing an array of liver damage and hallmarked by steatosis, the abnormal accumulation of fat within cells(Fabbrini et al., 2010). Believed to afflict 1 in 4 American adults, NAFLD occurs when the rate of hepatic fatty acid uptake and *de novo* fatty acid synthesis outpaces the rate of fatty acid oxidation and export(Marchesini et al., 2003). This leads to the accumulation of intrahepatic triglycerides. As a result, altered metabolism of glucose, fatty acid, and lipoproteins occurs(Fabbrini et al., 2010). In most patients the intrahepatic triglyceride buildup does not lead to further disease progression, but in 20-30% of cases this results in inflammation and fibrosis. Ultimately, these individuals are at higher risk of liver failure, hepatic carcinoma, and cirrhosis(Marchesini et al., 2003).

The manifestation of NAFLD is tightly linked with the presence of MetS components and as such, NAFLD can be considered the hepatic manifestation of MetS. In fact, 90% of patients with NAFLD possess at least one component of MetS. For example, the onset of NAFLD is tightly linked to obesity with the prevalence of NAFLD increasing with BMI. The rate of hepatic steatosis is 15% in normal weight individuals while it is 65% in obese and 85% in the morbidly obese ($BMI \geq 40$)(Fabbrini et al., 2010). NAFLD has also been found to be tightly associated with abdominal obesity even

in patients with normal BMI, indicating that visceral fat is especially important in NAFLD development(Alba & Lindor, 2003). Aside from obesity, NAFLD is also closely affiliated with IR. Due to this, the presence of NAFLD can be used as an independent indicator of multi-organ IR as hepatic fat percentage has been shown to accurately predict peripheral insulin sensitivity(Fabbrini et al., 2010). The other MetS components, such as dyslipidaemia and hypertension, have also been long associated with liver dysfunction(Tarantino & Finelli, 2013).

Cardiovascular Diseases

The primary clinical concern of MetS is its increased risk of CVD development. This is extremely significant because CVDs and their related complications are the leading cause of non-communicable mortality in the world (Figure 4)("Global Status Report on Non-communicable Diseases 2010," 2011). As a class of diseases which afflict the heart or blood vessels, CVDs include coronary artery disease, cerebrovascular disease, peripheral arterial disease, myocardial infarction, angina pectoris, congenital heart disease, deep vein thrombosis, and stroke to name a few("Global atlas on cardiovascular disease prevention and control," 2011). Strikingly, CVDs afflict one third of the all American adults and was cited as the underlying cause for one third of the fatalities within the United States in 2008. To put those numbers into perspective, CVDs account for one death approximately every 40 seconds in America alone. Aside from the physical toll CVDs inflict, they also have a detrimental impact on the health care system. In 2005, CVDs were indicated as the reason for 1 in every 6 hospitalizations and accounted for nearly one fourth of all inpatient hospital costs. Both directly and indirectly, CVDs are believed to have cost 273 billion dollars in 2010 and these values

are projected to triple by 2030(Roger et al., 2012). These staggering numbers clearly demonstrate the need for additional medical research to reduce the loss of life as well as minimize the burden and financial stress CVDs place on the healthcare system.

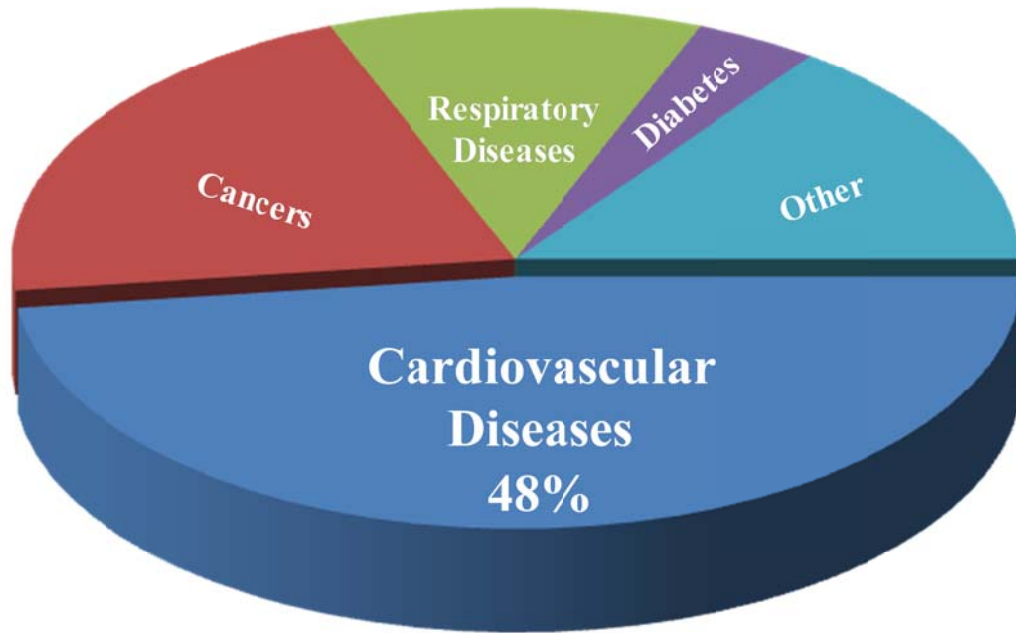


Figure 4: Leading causes of non-communicable mortality in the world

Atherosclerosis Overview

The major contributing factor of CVD is atherosclerosis, a disease affecting the large- and medium-sized arterioles("Global atlas on cardiovascular disease prevention and control," 2011). Atherosclerosis is characterized by the development of lesions within the intima of the vessel wall which are complex in nature containing lipids, several immunological cell types, smooth muscle cells, endothelial cells, fibrotic elements, and cellular debris. Clinically, the lesions themselves are fairly harmless unless they become large enough to cause vessel stenosis. Instead, the primary threat these lesions impose occurs after rupture which results in thrombosis or the release of clots causing downstream embolus(Hansson & Libby, 2006).

The Pathological Progression of Atherosclerosis

Originally thought to be a simple lipid storage disease, irrefutable evidence gathered over the past 25 years has proven atherosclerosis to be a chronic inflammatory disease which involves both the innate and adaptive immune system(Figure 5)(Galkina & Ley, 2009; Hansson & Hermansson, 2011; Hansson & Libby, 2006; Ross, 1999). Although the exact insult which initiates atherosclerosis development is unclear, several CVD risk factors such as hyperlipidemia and hypertension have been definitively correlated with atherosclerosis(Ross, 1999). The accumulation of lipids within the cell wall and the activation of endothelial cells (ECs) to a pro-inflammatory state begins the atherogenic process (Figure 5)(Hansson & Hermansson, 2011). The activation of ECs leads to the up-regulation of cellular adhesion molecules, increased endothelium permeability, and the secretion of pro-inflammatory cytokines and chemokines. The release of specific chemokines from the vessel wall results in the recruitment of particular

leukocyte cell types. The production of monocyte chemoattractant protein-1 (MCP-1) primarily lures monocytes, while the secretion of chemokines like C-C motif ligand 5 (CCL5), CXC-chemokine ligand 10 (CXCL10), and CXCL11 attract T-cells. Attracted leukocytes then adhere to the endothelium and transmigrate into the intima of the vessel. Monocytes, which are the predominately responding leukocyte, quickly differentiate into macrophages as a result of the presence of macrophage colony-stimulating factor (M-CSF) which is secreted by the inflamed vessel. The infiltrated macrophages perpetuate the pro-inflammatory environment through clonal expansion and the secretion of additional cytokines (Hansson et al., 2006). Specifically, tumor necrosis factor- α (TNF- α) and interleukin-1 β (IL-1 β) play an integral role in key pro-inflammatory signaling pathways involved in atherosclerosis development. The presence of M-CSF also induces macrophage expression of scavenger receptors. These receptors act to identify modified lipoproteins which accumulate within the intima. Once identified, the macrophages engulf the modified lipoproteins resulting in foam cell formation (Packard et al., 2009).

Simultaneous to the activation of ECs and the infiltration of leukocytes is the proliferation and activation of vascular smooth muscle cells (VSMCs). Once activated from a quiescent state, VSMCs migrate into the intima where they begin to synthesize collagen, elastin, proteoglycans, and growth factors. As the plaque matures, a necrotic core of apoptotic cells and cellular debris begins to form. In response, a fibrous cap envelops the plaque leading to the temporary stabilization of the area. However, over time the loss of VSMCs from apoptosis in conjunction with the production of proteases, coagulation factors, and radicals leads to cap destabilization as a result of collagen loss and matrix degradation. The plaque continues to weaken until it eventually ruptures as a

result of hemodynamic forces. As a result, pro-thrombotic material is then released from the plaque leading to thrombosis formation due to platelet activation and aggregation(Rudijanto, 2007).

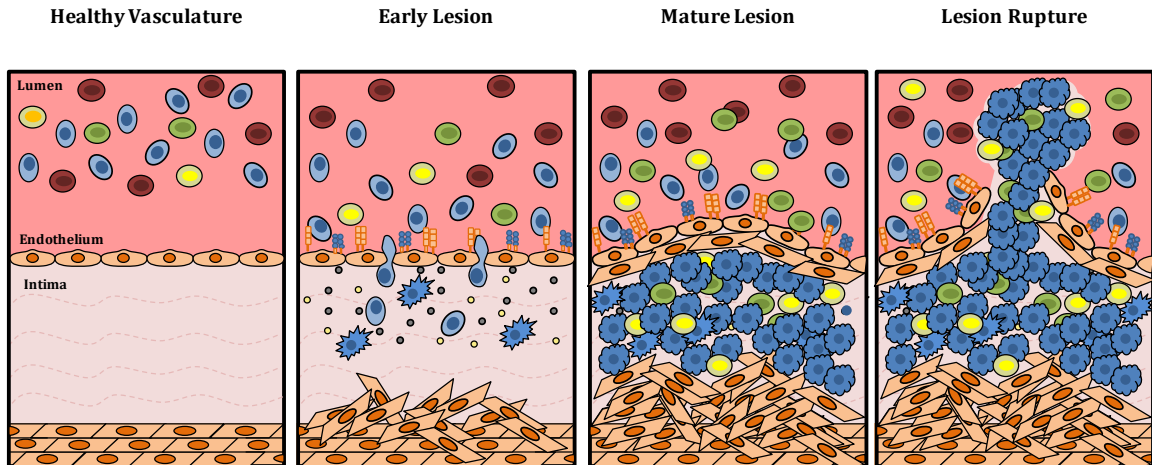


Figure 5: Multi-step development of atherosclerosis

Far Left: A healthy vessel with quiescent endothelium and no inflammation. **Middle Left:** Early lesion formation with endothelium activation resulting in the secretion of pro-inflammatory cytokines and chemokines as well as the up-regulation of cell adhesion molecules like intracellular adhesion molecule-1 and vascular adhesion molecule-1. This results in the attraction of leukocytes, their adherence, and transmigration into the intima. Predominately infiltrating monocytes quickly mature into macrophages, driven by the presence of M-CSF. Simultaneously, lipids begin to accumulate in the cell wall and VSMCs begin to proliferate. **Middle Right:** Advanced lesion formation is hallmarked by the accumulation of foam cells and the proliferation of VSMCs which aid in the formation of the fibrous cap over the growing necrotic core. **Far Right:** Eventually, atherosclerotic lesions destabilize and rupture leading to the release of pro-thrombotic factors and the aggregation of platelets.

Mouse Models of Atherosclerosis

The complex, chronic inflammatory nature of atherosclerosis makes the evaluation of its pathogenesis in humans difficult. In order to circumvent these issues several mouse models have been developed to examine the pathogenic progression of atherosclerosis. Universally, mice are an ideal species for conducted medical research for several reasons. First, the extensive genomic understanding of several mouse strains allows for specific genetic modifications such as precise gene knock-in, knock-out, and mutation. In addition, ease of housing, handling, and breeding make mice ideal candidates(Daugherty, 2002).

Wildtype mice are naturally very resistant to the development of atherosclerosis, most likely due to low levels of pro-atherogenic very-low-density lipoprotein (VLDL) and low-density lipoprotein (LDL) coupled with high levels of anti-atherogenic HDL(Zadelaar et al., 2007). Even the most susceptible strain, C57BL/6, only develops minor lesions restricted to the aortic root after prolonged high fat feeding. Furthermore, these lesions fail to replicate human lesions since they do not contain the cellular complexity seen in advanced human plaques(Daugherty, 2002; Paigen et al., 1985). In order to overcome these shortcomings, transgenic mouse models have been developed. The two most predominately used models to study atherosclerosis are apolipoprotein E-deficient mice (ApoE^{-/-}) and low-density lipoprotein receptor-deficient mice (LDLR^{-/-}).

Synthesized in the liver and by macrophages, ApoE serves as a critical ligand in the clearance of plasma lipoproteins(Mahley, 1988). As a consequence of its deletion, murine levels of VLDL and LDL dramatically increase(Zadelaar et al., 2007). As a result, spontaneous generation of atherosclerotic plaques occurs. Moreover, feeding with

high fat diet can further accelerate this process(Zhang et al., 1994). The development of plaques within ApoE^{-/-} mice is not merely restricted to the aortic root but also develops within the ascending arteries, aortic arch, descending aorta, renal junction, and iliac bifurcation. Furthermore, the content of these lesions resemble that of humans. Initially developing as fatty streaks, lesions progress and become more complex over time(Nakashima et al., 1994; Zadelaar et al., 2007). In fact, these plaques contain foam cells, T-cells, VSMC proliferation, and a fibrous cap, all the hallmarks of advanced human plaques. It should be noted though, spontaneous rupture has not been reported(Nakashima et al., 1994).

The other commonly utilized mouse model for atherosclerosis is LDLR^{-/-} mice. In humans, a genetic deficiency of LDLR causes pronounced hypercholesterolemia typically leading to morbidity in the twenties. However, the loss of LDLR protein in mice causes a less severe phenotype resulting in mildly elevated plasma cholesterol levels. As a result, developing lesions are simplistic in composition primarily containing lipid-laden macrophages(Daugherty, 2002). However, supplementation of LDL^{-/-} mice with a high fat diet dramatically elevates plasma cholesterol, specifically the LDL fraction, instigating the development of more complex lesions after prolonged feeding(Ishibashi et al., 1994).

It should be noted that lesions are reported to be larger in ApoE^{-/-} mice than LDLR^{-/-} after all time points. In addition, lesions within ApoE^{-/-} mice were more pronounced and contained more VSMC proliferation and banding when compared to LDLR^{-/-} mice, making it the preferred model in some instances(Roselaar et al., 1996). These atherogenic mouse models provide a critical vehicle for examining the

pathogenesis of atherosclerosis. Furthermore, crossing these standard atherogenic mouse models with mice containing genetic alterations permits the examination of specific gene contributions in atherosclerosis.

Atherosclerosis Quantification

There are two widely practiced techniques to quantify murine atherosclerotic lesions, cross-sectional analysis of the aortic sinus and *en face* analysis of the whole aorta. Both have distinct advantages and disadvantages. *En face* analysis permits the observation of atherosclerosis development throughout the entire length of the aorta. However, it does not afford an investigator the ability to further examine the thickness nor composition of the lesions. On the other hand, cross-sectional analysis addresses these shortcomings but solely inspects atherosclerosis lesion development within the aortic sinus(Daugherty & Whitman, 2003; Tangirala et al., 1995).

MicroRNAs Overview

The existence of miRNAs was first reported by Victor Ambrose in 1993 while working with *C. elegans*; however, it was almost a decade before the importance of this discovery was understood. In the early 2000s, the principle of RNA interference had just begun to take hold within the scientific community. Coupling this, with the fact that a second miRNAs with a highly conserved sequence was discovered and researchers began to realize they had identified a novel class of endogenous, non-coding RNAs which were capable of controlling complex biological functions through RNA interference(Naeem et al., 2010). It was later determined that this interference is carried out through Watson and Crick base-pairing within the 3'untranslated region (3'UTR) of messenger RNAs (mRNAs) resulting in mRNAs degradation or translation repression(Cordes et al., 2009;

Rasmussen et al., 2010). Thus far, over 2000 miRNAs have been identified which are predicted to regulate up to 30% of protein encoding genes. As such, miRNAs have been found to regulate almost all aspects of cellular function.

MicroRNAs Biogenesis

MiRNAs are unique in the fact that their genomic sequences can be found within the introns of other genes or be more traditionally located independently. As such, their transcription can be dependent on the transcription of other genes or be independent. In fact, a specific miRNA sequence can be found in multiple locations throughout the genome and therefore be generated from different chromosomes. Typically, miRNAs are transcribed into primary transcripts which are several hundred base-pairs in length (Figure 6). These transcripts then undergo post-transcriptional modification, receiving editing by adenosine deaminases and enzymatic cleavage by Drosha. After being truncated to a length of approximately 70 base-pairs, these precursor miRNAs are then exported from the nucleus to the cytoplasm by exportin 5 and Ran-GTP. Within the cytosol, the precursor miRNAs undergo further cleavage by a second enzyme Dicer, to a mature length of 18-23 base-pairs. These duplexes, formed by the initial hairpin structure of the primary miRNAs, are then unwound by RNA helicases. At this juncture, a single strand of the two enters the RNA-induced silencing complex (RISC), which then facilitates miRNAs-directed mRNAs translation repression or cleavage(V. N. Kim, 2005; Y. Lee et al., 2002; Winter et al., 2009). The ratio of which strand is loaded into the RISC can vary drastically and is dependent on the thermodynamic stability of the base-pairs at either end of the duplex. The strand that is loaded least frequently is often

designated with a “*” or the two strands can be labeled with 5p or 3p depending on its origin from the duplex(Winter et al., 2009).

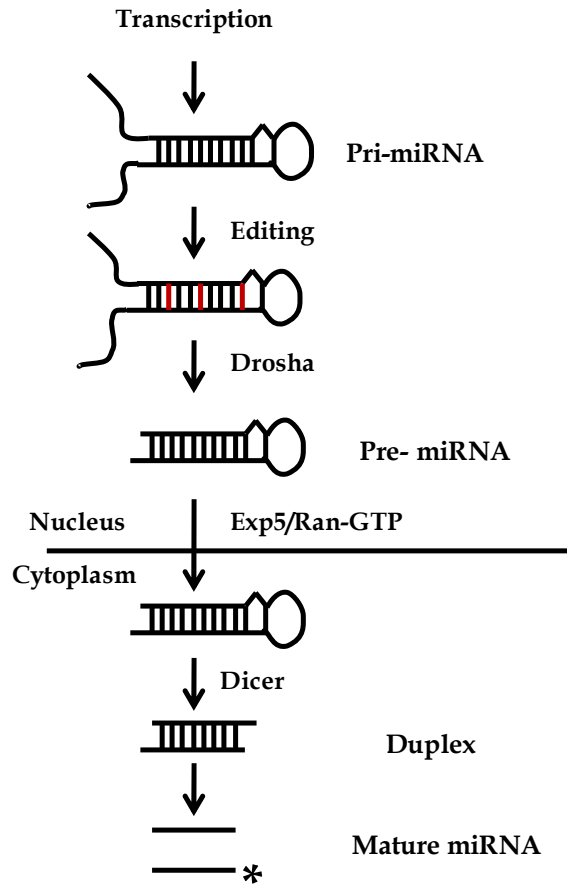


Figure 6: MiRNAs biogenesis

MiRNAs are transcribed into primary transcripts which are several hundred base-pairs in length. These primary transcripts then undergo editing by adenosine deaminases and are cleaved by Drosha. These precursor miRNAs are then exported from the nucleus by exportin 5 and Ran-GTP. Within the cytosol, further cleavage by Dicer occurs resulting in a duplex of 18-23 base-pairs in length. Unwound by RNA helicases two mature miRNAs are then formed termed miR-xxx-5p or miR-xxx-3p. The miRNAs from the lag strand may also be designated with a “*”.

MicroRNAs Targeting

MiRNAs target mRNAs within their 3'UTR through imperfect Watson and Crick base-pairing. This is noteworthy since imperfect base-pairing facilitates the possibility of multiple binding sites for a single miRNA with a particular mRNA. It also promotes promiscuity, allowing for multiple mRNA partners for a single miRNA. Although, the molecular details of how miRNAs specifically target mRNAs temporally and dynamically are still unknown, several structural features that promote miRNAs and mRNAs binding have been elucidated. It has been determined that a region of 6-8 nucleotides, at residues 2-7 on the 5' end of miRNAs, is critical in establishing miRNAs:mRNAs interactions and is commonly referred to as the "seed region"(Grimson et al., 2007). The significance of this region is supported by the fact that there is a high level of conservation at the 5' ends of related miRNAs(Brennecke et al., 2005; Krek et al., 2005; Lewis et al., 2005; Lewis et al., 2003). Meanwhile, the 3' ends of miRNAs have also been demonstrated to participate in base-pairing. It is postulated that while the 5' end is required for target identification, the 3' end contributes by modulating repression strength(Brennecke et al., 2005; Doench & Sharp, 2004; Grimson et al., 2007).

Other structural features have also been accredited with facilitating miRNAs interference. For example, AU richness proximally flanking the seed region binding site has been shown to contribute to miRNAs efficacy, although these contributions quickly diminish with distance(Corcoran et al.; Grimson et al., 2007; Nielsen et al., 2007). In addition, the location of the miRNAs binding site within the 3' UTR of mRNAs also plays a role in determining miRNAs functionality. Sites situated near either end of the 3'UTR of mRNAs have been reported to demonstrate greater activity compared to sites

that reside in the center of the 3'UTR region of mRNAs. Furthermore, it has been reported that this effect was more pronounced in longer 3'UTRs and that site-conservation in these areas was greater than centrally located sequences. It should be noted; however, that sites located very close to the open reading frame or within 15 nucleotides of the stop codon have been found to have low binding affinity(Farh et al., 2005; Grimson et al., 2007; Lewis et al., 2005; Lim et al., 2005). Aside from these structural features, it has also been revealed that proximal miRNAs binding sites tend to interact synergistically while multiple sites at distance behave independently with an additive affect(Brennecke et al., 2005; Doench & Sharp, 2004; Grimson et al., 2007; Lai et al., 2005; Saetrom et al., 2007). This synergistic affect potentially allows for efficient protein regulation with minimal increase in miRNAs cellular levels.

MicroRNAs-directed Endonucleic Cleavage

As mentioned previously, there are two methods by which miRNAs carry out RNAs interference. The first is miRNAs-directed endonucleic cleavage of mRNAs. Facilitated by members of the highly conserved Argonaute family, these proteins are basic in nature and contain a PAZ and PIWI domain (Cerutti et al., 2000; Song et al., 2004). The PAZ domain has affinity for single- and double-stranded RNAs allowing Argonaute proteins to bind to mature miRNAs loaded in the RISC complex(Lingel et al., 2003; Ma et al., 2004; Song et al., 2003; Yan et al., 2003). Meanwhile, the highly conserved PIWI domain contains an RNase H domain, which provides certain Argonaute proteins their splicing activity. In humans, four Argonaute family members exist, although only Argonaute 2 (Ago2) contains intrinsic enzymatic activity(Liu et al., 2004; Meister et al., 2004). The idea that Argonaute proteins carry out miRNAs-directed

splicing activity is supported by the fact that RNase H slicing results in a 3' overhang which is associated with miRNAs-directed cleavage(Ma et al., 2005; Parker & Song, 2004; Song et al., 2004; Yuan et al., 2005). Slicing typically occurs under conditions of perfect base-pairing between miRNAs and mRNAs although some mismatches can be tolerated(Guo et al., 2005; Mallory et al., 2004; Yekta et al., 2004). It should be noted though, that perfect base-pairing does not guarantee endonucleolytic cleavage(Chen, 2004). This suggests that additional RISC-associated molecules may be needed for the cleavage of certain mRNAs. Following cleavage, mRNA fragments undergo standard degradation through either conserved or eukaryotic specific pathways(Parker & Song, 2004; Valencia-Sanchez et al., 2006).

MicroRNAs-directed Translation Repression

Aside from endonucleic cleavage, translational repression is the other mechanism utilized by miRNAs to regulate gene expression. Several studies using various miRNAs have demonstrated a reduction in protein expression in the midst of unwavering or minimally altered mRNAs levels, suggesting some form of translation repression(Brennecke et al., 2003; Chen, 2004; Cimmino et al., 2005; R. C. Lee et al., 1993; Poy et al., 2004; Wightman et al., 1993). Although the exact mechanism of how the repression is facilitated is unknown, it can be postulated that this suppression occurs as a result of either a hindrance to translation initiation or some point thereafter. In fact, adequate amounts of data exist to support both mechanisms(Bhattacharyya et al., 2006; Chendrimada et al., 2007; X. C. Ding & Grosshans, 2009; Gu et al., 2009; Mathonnet et al., 2007; Nottrott et al., 2006; Petersen et al., 2006; Pillai et al., 2005). Thus far, it is known that miRNAs which employ translation initiation repression require the presence

of Ago-2(L. Ding & Han, 2007; Eulalio et al., 2007). It is believed that the cap binding-link motif of Ago-2 interferes with the association of the critical translation initiation protein, eukaryote translation initiation factor 4E (eIF4E), which has a similar motif(Cannell et al., 2008; Kiriakidou et al., 2007). This fact, along with additional experimental information, suggests that Ago-2 does in fact interact directly with the cap or indirectly through associated proteins(Cannell et al., 2008). It is reasonable to extrapolate that RISC association with the cap would dramatically affect translation initiation and thereby repress translation.

Evidence also exists that supports the notion of post-initiation translation repression. Sedimentation studies conducted with mRNAs under miRNAs repression revealed the association of polysomes. This provides evidence that particular miRNAs function through post-initiation translational interference(J. Kim et al., 2004; Kong et al., 2008; Maroney et al., 2006; Nottrott et al., 2006; Petersen et al., 2006; Thermann & Hentze, 2007). Furthermore, the activity of the associated polysomes in translation was verified through puromycin-sensitivity assays(Thermann & Hentze, 2007). It is postulated that two mechanisms may be involved in post-initiation suppression (Figure 7). First, miRNAs association could result in elongation interference leading to a dramatic reduction in elongation rate, or second, the presence of miRNAs may lead to premature ribosomal dissociation prior to the completion of translation as a consequence of mRNAs instability or physical impediment. Currently, the exact mechanism is unclear, which may indicate the possibility that different miRNAs may employ different methods. Whether initial or post-initial translation repression is utilized, both would

account for reductions in protein levels amidst unwavering mRNAs expression witnessed experimentally.

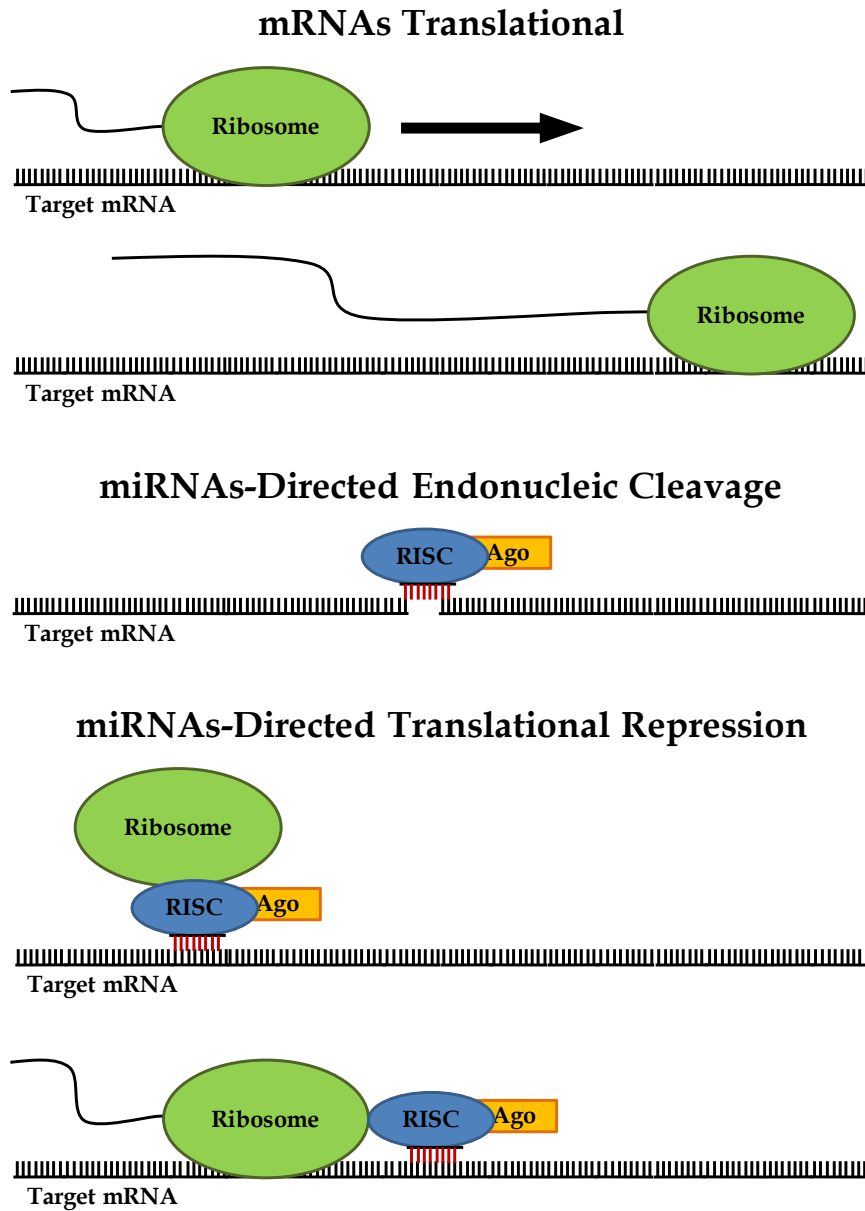


Figure 7: Methods of miRNAs RNA interference

Top: Typical ribosomal translation and elongation of mRNAs. **Middle:** MiRNAs-directed RISC association and endonucleic cleavage of target mRNAs. **Bottom:** MiRNAs-directed interference of ribosomal association with the mRNAs and miRNAs blockade of translation elongation.

MicroRNAs and Disease

The ability of miRNAs to modulate gene expression naturally makes them a target of interest when studying disease pathogenesis. In fact, there is substantial evidence demonstrating miRNAs expression shifts during disease progression. These changes could simply be a response to physiological changes spurred on by the disease or be the mechanism driving the ailment. In either case, the common occurrence of miRNAs deregulation and disease manifestation has led to the formation of databases such as the Human MicroRNAs Disease Database(Li et al., 2014). Table 3 provides a brief summary of the wide array of disease which are associated with miRNAs.

In addition to miRNAs expression deregulation, structural changes to target mRNAs can also lead to disease development. For example, a mutation in the 3'UTR of mRNAs might not affect protein functionality but may affect its expression. This mutation could either lead to gain or loss of miRNAs regulation, thereby dramatically altering protein expression. In fact, a single-nucleotide polymorphisms (SNP) within the 3'UTR of human angiotensin II type 1 receptor (AT1R) is known to cause hypertension. Significantly, this mutation occurs within a miRNAs binding site, negating this interaction(Hata, 2013).

Initially, the vast majority of research examining miRNAs in disease was conducted within the field of cancer due to the common occurrence of dramatic miRNAs expression changes. More recently, studies have also begun investigating the role of miRNAs in MetS and CVDs. Tellingly, miRNAs have been revealed to regulate an array of well-established metabolic and cardiovascular related functions such as lipid metabolism, glucose homeostasis, insulin expression, endothelial activation, VSMC

proliferation, and angiogenesis. These findings, along with data collected from murine disease models, have clearly demonstrated that miRNAs play an important role in MetS and CVD pathology(Rottiers & Naar, 2012; Zampetaki & Mayr, 2012).

Table 3: Association of miRNAs with common pathologies

Disease	MiRNA	Reference (Pubmed ID)
5q syndrome	miR-145 and miR-146a	22094949
Alzheimer's disease	miR-29, miR-9, miR-146, miR-107	23200134, 22094949
Amyotrophic lateral sclerosis	miR-206	22094949
Aneurysms	miR-29	23080337
Arrhythmia and hypertension	miR-1	22094949
Atherosclerosis	miR-10a, miR-145, miR-143 and miR-126, miR-33	22094949, 23080337
Cancer	miR-125b, miR-145, miR-21, miR-155, miR-210, miR-29b, let-7a	23200134
Cardiac hypertrophy	miR-21, miR-199b	22094949, 23080337
Crohn's disease	miR-196	22094949
Deafness	miR-96	22094949
Down's syndrome	miR-155, miR-802	22094949
Gastric cancer	miR-145	23200134
Hepatitis C	miR-122, miR-155	23200134
HIV-1	miR-28, miR-125b, miR-150, miR-223, miR-382	23200134
ICF syndrome	miR-34b, miR-34c, miR-99b, let-7e, miR-125a	22094949
Influenza	miR-21, miR-223	23200134
Metabolic disease	miR-208a	23080337
Multiple sclerosis	miR-145, miR-34a, miR-155, miR-326	23200134
NAFLD	miR-200a, miR-200b, miR-429, miR-122, miR-451, miR-27, miR-155	23200134
Parkinson's disease	miR-30b, miR-30c, miR-26a, miR-133b, miR-184, let-7, miR-7	23200134, 22094949
Pulmonary hypertension	miR-145	23080337
Rett's syndrome	miR-146a, miR-146b, miR-29, miR-382	22094949
Rheumatoid arthritis	miR-146a	22094949
Silver-Russell syndrome	miR-675	22094949
Spinal motor neuron disease	miR-9	22094949
Systemic lupus erythematosus	miR-146a	23200134
Type II diabetes	miR-144, miR-146a, miR-150, miR-182, miR-103, miR-107	23200134

Key Knowledge Gaps, Hypothesis, and Rationale of Thesis

As we have discussed, MetS and CVD are major health epidemics worldwide whose prevalence requires the development of novel therapeutics. In order to address this concern, we believe investigation of miRNAs expression within these pathologies could prove fruitful. One particular miRNA, miR-155, is of particular interest due to its multifunctional attributes. MiR-155 has been shown to mediate an array of cellular functions ranging from immunity, inflammation, haematopoieses, vascular homeostasis, and metabolism. This wide ranging cellular regulation is possible through the targeting of numerous genes, 140 of which have been experimentally verified as *bona fide* miR-155 targets (Table 4). Review of these targets reveals numerous genes which are pertinent to MetS and atherosclerosis development. However, comprehensive review of how miR-155 impacts these conditions has yet to be completed. We hypothesize that miR-155 plays a vital role in the development of MetS and atherosclerosis. As such, we feel the review of this particular miRNA within both conditions is prudent as it could provide novel insight into the mechanisms of these diseases. We will test this hypothesis through the use of the following two specific aims:

Specific Aim 1: Determine the role of miR-155 in MetS development.

Study 1: Evaluate the body mass of male and female ApoE^{-/-} and miR-155^{-/-}/ApoE^{-/-} mice on normal chow and when challenged with a high fat diet.

Study 2: Evaluate glucose and insulin levels and their responses to corresponding tolerance tests within male and female ApoE^{-/-} and miR-155^{-/-}/ApoE^{-/-} mice on normal and high fat chow.

Study 3: Evaluate blood pressure regulation in male and female ApoE^{-/-} and miR-155^{-/-}/ApoE^{-/-} mice on normal and high fat chow.

Study 4: Evaluate triglyceride and high density lipoprotein levels within male and female ApoE^{-/-} and miR-155^{-/-}/ApoE^{-/-} mice on normal and high fat chow.

Study 5: Evaluate the development of non-alcoholic fatty liver disease within male and female ApoE^{-/-} and miR-155^{-/-}/ApoE^{-/-} mice on normal and high fat chow.

Specific Aim 2: Determine the role of miR-155 on atherosclerosis development.

Study 1: Evaluate aortic miRNAs expression in atherosclerosis development in male ApoE^{-/-} mice.

Study 2: Evaluate atherosclerotic lesion development in male ApoE^{-/-} and miR-155^{-/-}/ApoE^{-/-} mice on high fat chow.

Table 4: List of miR-155 experimentally verified targets

APAF1	CUX1	INPP5F	MYST3	SMAD5
ARID2	CXorf39	INTS6	NARS	SMARCA4
ARL15	CYP2U1	IRAK3	PAK2	SOCS1
ARL6IP5	DCUN1D2	JARID2	PCDH9	SPI1
ARMC2	DET1	KBTD2	PDCD4	TAF5L
ARNT	DHX40	KIAA0430	PHC2	TBC1D14
AT1R	E2F2	KIAA1274	PHF14	TBCA
BACH1	EIF2C4	KLHL5	PHF17	TCF12
BC0RL1	ETS1	LCORL	PICALM	TLE4
C10orf104	EXOSC2	LNX2	PKN2	TOMM20
C10orf26	FADD	LRRC59	POLE3	TP53INP1
C16orf62	FAM135A	LSM14A	PRKAR1A	TRAK1
C1orf103	FAM177A1	MAP3K10	RAB11FIP2	TRIP13
C21orf66	FAM91A1	MAP3K14	RAC1	TSGA14
C3orf18	FGF7	MAP3K7IP2	RAPGEF2	TSPAN14
C5orf44	FOXO3	MASTL	RHEB	UBQLN1
CARD11	GABARAPL1	MBNL3	RHOA	VPS18
CARHSP1	GATM	MCM8	RIPK1	WEE1
CASP3	GNAS	MED13L	RNF123	WHSC1L1
CCDC41	GOLT1B	MEF2A	SAP30L	WWC1
CDC40	HBP1	MORC3	SDCBP	ZKSCAN5
CEBPB	HIF1A	MPP5	SECISBP2	ZNF248
CHD9	HIVEP2	MRPL18	SKI	ZNF254
CIAPIN1	IGJ	MRPS27	SLA	ZNF273
CLUAP1	IKBKE	MYBL1	SLC33A1	ZNF28
CSF1R	IL13RA1	MYD88	SLC35F2	ZNF611
CSNK1A1	IL17RB	MYO10	SMAD1	ZNF652
CTLA4	INPP5D	MYO1D	SMAD2	ZNF83

CHAPTER 2: MATERIAL AND METHODS

Animal Care

All animal use was authorized by, and performed in accordance with, Institutional Animal Care and Use Committee (IACUC) guidelines. In addition, all laboratory animal work was approved by the Experimental Animal Committee of Temple University School of Medicine. ApoE mutant mice (strain name: B6.129P2-Apoetm1Unc/J), miR-155 mutant mice (strain name: B6.Cg-Mir155tm1.1Rsky/J), and wild type (WT) mice were of a C57BL/6 background and purchased from The Jackson Laboratory (Bar Harbor, ME). Mice were housed in the Temple University Central Animal Facility under controlled conditions, given *ad libitum* access to standard chow diet and water, and put on a 12-hour light-dark cycle. Novel miR-155^{-/-}/ApoE^{-/-} (DKO) mice were generated by crossing miR-155^{-/-} mice with ApoE^{-/-} mice. In all experiments, mice were age-matched and gender-specified. At 8 weeks of age, mice were either maintained on their current normal chow diet (5% fat, Labdiet 5001) or switched to a diet supplemented with 0.2% (w/w) cholesterol and 21.2% (w/w) fat (high fat diet) (TD. 88137, Harlan Teklad, WI) for specified periods before being sacrificed for experimental use.

Mouse Genotyping

Mice were genotyped for a specific gene of interest with polymerase chain reaction (PCR) followed by agarose gel separation. First, mouse tail or ear tissue was collected and digested with 600µl of tissue lysis buffer [10mM tris (pH 8.0), 100mM sodium chloride (NaCl), 10mM ethylenediaminetetraacetic acid (EDTA, pH 8.0), and 0.5% sodium dodecyl sulfate (SDS)] containing 0.4mg/ml proteinase K (EMD Millipore, MA) at 55°C overnight. Tissue lysate was then centrifuged at 13,000rpm for 20 minutes.

Supernatant containing genomic DNA was then collected and DNA was precipitated in 700uL of 100% ethyl alcohol before being dissolved in 200uL of distilled deionized water at 37°C overnight.

Mouse genomic DNA was next amplified with the use of gene of interest-specific primer sets and PCR. The murine miR-155 allele was examined using the following primers: miR-155 common primer 5'-GTGCTGCAAACCAGGAAGG-3', miR-155 wild type primer 5'-CTGGTTGAATCATTGAAGATGG-3', and miR-155 knock-out primer 5'-CGGCAAACGACTGTCCTGGCCG-3'. Optimized miR-155 allele PCR was performed under conditions of 94°C for 30 seconds, 61.8°C for 60 seconds, and 72°C for 60 seconds for a total of 35 cycles. The PCR products were then separated by gel electrophoresis on a 1.5% agarose gel, with the wild type band resolving at 465bp and the knock-out band at 600bp. The murine ApoE allele was examined using the following primers: ApoE common primer 5'-GCCTAGCCGAGGGAGAGCCG-3', ApoE wild type primer 5'-TGTGACTTGGGAGCTCTGCAGC-3', and ApoE mutant primer 5'-GCCGCCCCGACTGCATCT-3'. Optimized ApoE allele PCR was performed under conditions of 94°C for 30 seconds, 68°C for 40 seconds, and 72°C for 60 seconds for 35 cycles. The PCR products were then separated on a 2% agarose gel by gel electrophoresis with the ApoE wild type band resolving at 155bp and the mutant band at 245bp. All gels were supplemented with 0.1mg/mL ethidium bromide and visualized using ultraviolet detection from a Foto® analyst image system (Fotodyne, WI).

Murine Age Development

Two weeks after birth, the development of male and female ApoE^{-/-} and DKO mice was determined by weighing their mass on a weekly basis with a ISO9001 scale

from Satorius®. At 4 weeks of age, mice were weaned into gender-specific cages with 2-5 mice per cage. Following maturation at 8 weeks of age, mice were then either kept on normal chow (5% fat, Labdiet 5001) or put on high fat feed (TD. 88137, Harlan Teklad, WI) until 20 weeks of age when they were sacrificed for experiment.

Body Composition Analysis

At 20 weeks of age, body composition analysis was performed on male and female ApoE^{-/-} and DKO mice fed either normal (5% fat, Labdiet 5001) or high fat chow (TD. 88137, Harlan Teklad, WI). In brief, mice were euthanized and frozen at -80°C until collection of the total experiment population. Mice were then thawed and NMR body composition analysis performed with a LF50 minispec from Bruker®. This analysis provided total body mass, fat mass, lean body mass, and free fluid mass measurements.

Gonadal White Adipose Tissue (gWAT) Pad Analysis

Male and female ApoE^{-/-} and DKO mice on normal or high fat chow were sacrificed at 20 weeks of age and the left gWAT pad was then excised, washed in PBS, and measured with an AB54-S scale from Mettler Toledo. The gWAT was then imaged with NIS Elements software on a radiograph copy stand from Ilex optical company with a Nikon® DS-Fi1 camera. A surgical ruler was used as a point of reference in all pictures.

The right gWAT was also excised and then fixed in 5 mL of Bouin Solution (75 mL of picric acid, 25 mL of 37-40% formaldehyde, and 5 mL glacial acetic acid) for 24 hours before paraffin embedded (described below). Paraffin blocks were then sent to AML Laboratories (Baltimore, MD) for sectioning and hematoxylin and eosin (H&E)

staining. Slides were then imaged using an Akioskop2 Plus microscope and Axiocam camera (Carl Zeiss Inc., NY). Adipocyte cell sizes within a 20x magnification field were then determined using Adobe® Photoshop CS5 software.

Hepatic Tissue Analysis

Livers from euthanized male and female ApoE^{-/-} and DKO mice on normal and high fat chow were excised, washed in PBS, and weighed with an AB54-S scale from Mettler Toledo®. Segments of liver were then fixed in 4% paraformaldehyde (PFA) (Sigma, Cat#P6148) for 24 hours before being embedded in paraffin (described below). Paraffin blocks were then sent to AML Laboratories (Baltimore, MD) for sectioning and H&E staining. Histological evaluation of the sections was then performed and images taken using an Akioskop2 Plus microscope and AxioCam camera. In addition to the livers used for histological purposes, other whole livers were imaged on a radiograph copy stand from Ilex optical company with NIS Elements software and a Nikon® DS-Fi1 camera. A surgical ruler was used as a point of reference in all pictures.

Paraffin Embedding

Tissue samples were fixed as previously described before paraffin embedding. After fixation, samples were dehydrated with various concentrations of isopropanol (Fisher Scientific, Cat#A522). In brief, samples were put in 50% isopropanol for 45 minutes and then 70% isopropanol for at least two hours. Following this, the tissues were submerged in 95% isopropanol for 45 minutes. Next, samples were soaked in 100% isopropanol for 30 minutes (twice) and then the tissue was dehydrated in xylene (Sigma, Cat#534056) for 45 minutes (twice). At this point, the samples were put in melted paraffin (Fisher Scientific, Cat#T565) which was then allowed to harden. The paraffin

was then melted in a 57°C incubator for 2-3 hours and the samples moved to fresh liquid paraffin and kept at 57°C for 1 hour. Finally, the tissue was moved to steel molds where fresh paraffin was poured on top and covered with a plastic mold (Fisher Scientific, Cat#15182701A). The liquid paraffin was then allowed to harden and the molds placed in a refrigerator at 4°C. After an hour, the steel molds were removed leaving the tissue containing paraffin block attached to the plastic mold.

Lipid, Lipoprotein, and Metabolic Parameter Analysis

Whole blood was collected from anesthetized animals via the inferior vena cava and deposited into mini-centrifuge tubes containing 25uL of 5% EDTA. Plasma was then isolated by centrifugation at 4°C for 15 minutes at 3000rpm and frozen at -80°C. The samples were then packed on dry ice and shipped overnight to either the National Mouse Metabolic Phenotyping Center in Yale Medical School (New Haven, CT) for measurement of low-density lipoprotein, high-density lipoprotein, total cholesterol, non-esterified fatty acids, and triglycerides or to the National Mouse Metabolic Phenotyping Center in the University of Massachusetts (Amherst, MA) for measurement of glucose, insulin, glucagon, leptin, adiponectin, and resistin.

Glucose Tolerance Test (GTT)

GTTs were performed on normal or high fat fed male and female ApoE^{-/-} and DKO mice at 20 weeks of age as previously described (Banerjee et al., 2004; Wu et al., 2011). In brief, following an overnight fast of 16 hours mice were restrained and their tail nicked for blood collection. Blood glucose levels were then determined by gently massaging a small drop of blood from the tail onto a glucometer strip. The strip was then analyzed with a Glucose 201 glucometer from HemoCue®. After determination of fasted

blood glucose levels, each mouse received a 1g/kg intraperitoneal (i.p.) injection of 10% D-Glucose (Sigma, Cat#158968). Blood glucose levels were then measured at 30, 60, 90, and 120 minutes post injection and recorded. In addition, each animal was weighed before and after fasting to ensure health before testing.

Insulin Tolerance Test (ITT)

ITTs were carried out on male and female ApoE^{-/-} and DKO mice in a similar fashion as described above. After baseline blood glucose levels were determined, each mouse received a 0.75 units/kg i.p injection of human insulin (Sigma, Cat#I2643). Blood glucose levels were then determined 30, 60, 90, and 120 minutes post injection.

RNA Extraction, Isolation, and Quantification

As described by the manufacturer, total RNAs including miRNAs were isolated from murine aorta, liver, and gWAT with the miRNeasy isolation kit (Qiagen, Cat#217004). In brief, RNA generated from murine tissue was isolated with homogenization with a Pro200 homogenizer from Scientific Pro® in 900uL of Qiazol® Reagent (Qiagen, Cat#79306). Next, 140ul of chloroform was added to each sample and the mixture shaken vigorously for 15 seconds before being allowed to stand for 2-3 minutes at room temperature. Following this, the samples were centrifugated at 13,000rpm for 15 minutes at 4°C. The upper aqueous phase was then collected and the RNA precipitated by the addition of 1.5 volumes of 100% ethyl alcohol (Pharmco-Aaper, Cat# 111000200). The solution was then added to Qiagen® mini spin columns and centrifuged at 12,000rpm for 60 seconds. Flow through was then discarded and the column washed with 700uL of Qiagen® RWT buffer. Again, the flow through was discarded and the column washed twice with Qiagen® RPE Buffer. After centrifugation,

the column was gently removed and placed into a clean microcentrifuge tube. The RNA was then solubilized in 30µl nuclease-free water and passed off the column. The quality and concentration of all RNA samples were then determined with a Nanodrop 2000 from Thermo Scientific®.

RNA Reverse Transcription

Total RNA was reverse transcribed to generate complementary DNA using the High Capacity cDNA Reverse Transcription Kit (Invitrogen, Cat#4368814) as per the manufacturer's instructions. Meanwhile, reverse transcription to generate complementary DNA for miRNAs was accomplished with the miScript II RT kit (Qiagen, Cat#218160) according to the manufacturer's instructions. All cDNA products were then stored at -80°C until further use.

Quantitative Real-Time PCR

The mRNA expression levels of protein coding genes as well as miRNA expression were determined by quantitative real-time PCR (qRT-PCR) performed with the StepOnePlus PCR system (Applied Biosystems, CA). SYBR-green dye (Invitrogen, CA) was used to quantify mRNA expression levels with transcripts being normalized to the constitutive mRNAs expression of GAPDH. The expression of miRNA was also detected by SYBR-green dye (Qiagen, Cat#218073) and transcripts normalized to the constitutively expressed ribosomal RNA, U6. The specific primers used are listed in (Table 5).

Table 5. List of primers used in qRT-PCR

Gene Name	Direction	Primer Sequences (5' – 3')
Murine GAPDH	Forward	GAGGCCGGTGCTGAGTATGTCGTGGA
	Reverse	CACACCCATCACAACTGGGGGCAT
Murine C/EBP β	Forward	CACCACGACTTCCTCTCCGACCTCT
	Reverse	GTACTCGTCGCTCAGCTTGTCCACCC
Murine C/EBP α	Forward	CGAGGAGGACGAGGCCGAAGCA
	Reverse	TGCGCAGGCGGTCATTGTCAC
Murine PPAR γ	Forward	TCCGTAGAAGCCGTGCAAGAGATCA
	Reverse	CAGCAGGTTGTCTTGGATGTCCTCG
Murine miR-155		Purchased from Qiagen
Murine/Human U6		Purchased from Qiagen

miFinder PCR Array

Total RNAs including miRNAs were isolated from the aortas of ApoE^{-/-} mice on 12 weeks of normal or high fat chow and reverse transcribed as previously described. The cDNA from 5 individual mice of the same experimental group was then equally mixed together and added to a miFinder PCR array (Qiagen, MIMM-001Z) and qRT-PCR performed. The data from each experimental array plate was then analyzed with software provided on the Qiagen website.

Atherosclerotic Lesion Analysis

Murine hearts and aortas were perfused with ice-cold PBS, harvested, and fixed overnight with 4% PFA. Fixed tissues were then kept in 20% (v/v) sucrose (Sigma,

Cat#S0389) for 24 hours. Following this, the lower ventricular portion of the mouse heart was removed with a scalpel and the upper cardiac portion embedded with Optimal Cutting Temperature compound (OCT) (Fischer Scientific, Cat#14-373-65) and frozen. Mouse aortas were transferred to mini-centrifuge tubes containing phosphate buffered saline (PBS) and stored at 4°C. The hearts were then cross-sectioned for observation of the aortic root with a Microme HM 560 cryostat (Thermo Scientific, MA). Mounted onto Superfrost® slides (Fisher Scientific, Cat#12-544-7), 10µm sections were taken from the point where the aortic valves first appeared until a total of 80 sections were collected serially across 10 slides. Slides were next stained with Oil red O (Sigma, Cat#O0625) and alum hematoxylin (Fischer Scientific, Cat#H345). Briefly, fixed sections were rinsed with 60% isopropanol and stained with freshly prepared Oil red O (0.3% Oil Red O in 60% isopropanol) for 18 minutes. Following this, slides were rinsed with 60% isopropanol, dipped in alum hematoxylin, and rinsed with distilled water. The stained sections were then mounted with aqueous mounting medium (Sigma, Cat#C9368) and stored at room temperature until imaging. Meanwhile, the aortas were used for *en face* staining. After fully removing all adipose and connective tissue, the aortas were stained with Sudan IV (5mg/mL in 70% isopropanol) (Sigma, Cat#S4261) for 40 minutes at 37°C. Following this, the aortas were incubated in 70% isopropanol for 5 minutes. Next, a longitudinal cut was made to expose the intimal surface of the vessel and pinned open on a black silicone tray for imaging.

Images of the aortic root were captured with an AxioCam camera mounted to a Axioskop 2 microscope, while images of the aorta were captured with the same camera mounted to a Stemi 2000-C microscope (Carl Zeiss Inc., NY). Atherosclerotic lesion

area within the aortic sinus was defined as the area stained with Oil red O and measured with ImageJ (NIH, MD). Evaluating all eight aortic sections per slide, the percentage of lesion area was calculated by dividing the lesion area by the total sinus area and averaging the values for the 8 sections. Meanwhile, the lesion area in the whole aorta was defined as red area stained with Sudan IV. The summated lesion area was then divided by the total aorta area to tabulate the atherosclerotic lesion area.

Statistical Analysis

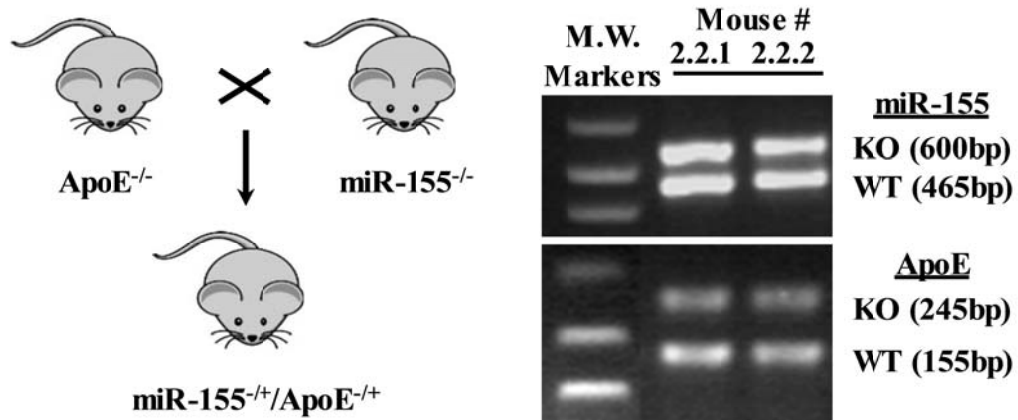
All statistical analyses were performed with the Graphpad Prism 5 software. For statistical comparison of single parameters between 2 groups, an independent t-test was used. Statistical significance was defined as $p < 0.05$.

CHAPTER 3: RESULTS

Development of novel miR-155^{-/-}/ApoE^{-/-} mice

In order to evaluate the role of miR-155 in MetS and atherosclerosis development, we bred a novel mouse model. Utilizing ApoE^{-/-} and miR-155^{-/-} mice purchased from The Jackson Laboratory, we were able to create an animal model which allowed us to explore the impact of miR-155 expression on MetS manifestation within a hyperlipidemic environment. Furthermore, the use of normal and high fat diets permitted us to investigate this relationship during conditions of normal and caloric surplus. In addition, the use of an ApoE^{-/-} background availed us the opportunity to investigate atherosclerosis development within a traditional and well-accepted atherosclerosis-susceptible model. We first crossed miR-155^{-/-} mice with ApoE^{-/-} mice to generate miR-155^{+/-}/ApoE^{+/-} mice (**Figure 8A**). These heterozygotes were then bred together to generate miR-155^{-/-}/ApoE^{-/-} mice (**Figure 8B**). The genotypes of all mice were verified with PCR.

A.



B.

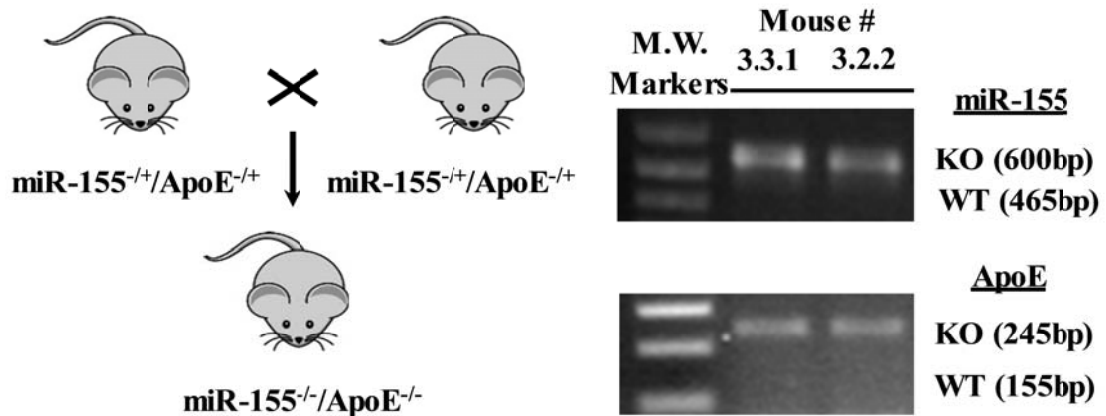


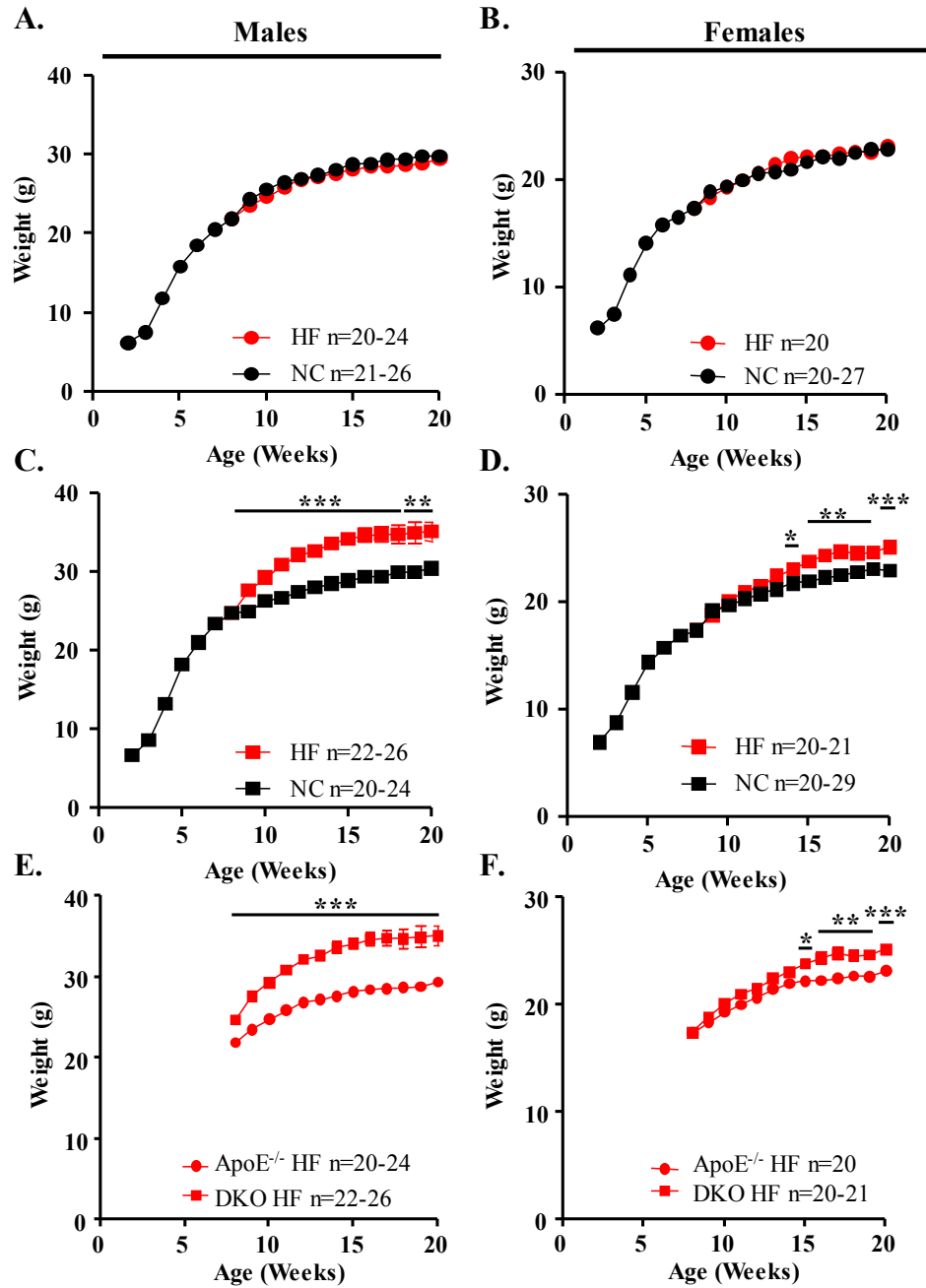
Figure 8: Breeding scheme for novel miR-155^{-/-}/ApoE^{-/-} mice

A. Single knockout ApoE and miR-155 mice were bred to develop novel miR-155^{+/-}/ApoE^{-/+} mice which were verified by genotypic PCR analysis.

B. Heterozygous mice were then bred to develop novel miR-155^{-/-}/ApoE^{-/-} mice.

DKO mice gain excessive body weight during periods of caloric surplus

Once we had generated the DKO mice, the first MetS parameter that we evaluated was body mass. The body weights of male and female ApoE^{-/-} and DKO mice were recorded 2 weeks following birth and weekly thereafter through 20 weeks of age. At 8 weeks of age, mice were either maintained on normal chow or given a high fat diet. We found that diet did not significantly affect male or female ApoE^{-/-} body weights at any time interval (**Figure 9A, B**). Furthermore, as expected, female ApoE^{-/-} mice weighed less than their male equivalents. Investigation of body weight in DKO mice on the other hand, yielded interesting results. Male DKO mice fed a high fat diet showed significant weight gain when compared to DKO mice on normal chow at all time points examined (**Figure 9C**). Furthermore, a similar phenotype was observed in the female DKO mice, albeit its onset was delayed and the distinction less (**Figure 9D**). In the female mice, a significant body weight difference was first observed at 13 weeks of age and continued through the end of the experiment. Again, male DKO mice were heavier than their female counterparts. A direct comparison of ApoE^{-/-} and DKO mice revealed that male DKO mice on high fat feed have significantly greater body mass than their ApoE^{-/-} counterparts at all time points (**Figure 9E**). In addition, like the males, female DKO mice on high fat feed had heavier body masses than their female ApoE^{-/-} equivalents (**Figure 9F**). This distinction did not reach statistical significance until week 15.



HF: High fat, NC: Normal chow, *P-value <0.05, **P-value <0.01, ***P-value <0.001

Figure 9: Body weight development

Body weight measurements of **A.** Male ApoE^{-/-}, **B.** Female ApoE^{-/-}, **C.** Male DKO, and **D.** Female DKO mice fed with normal and high fat chow. Gender-specific body weight comparisons of **E.** Male and **F.** Female ApoE^{-/-} and DKO mice on high fat feed.

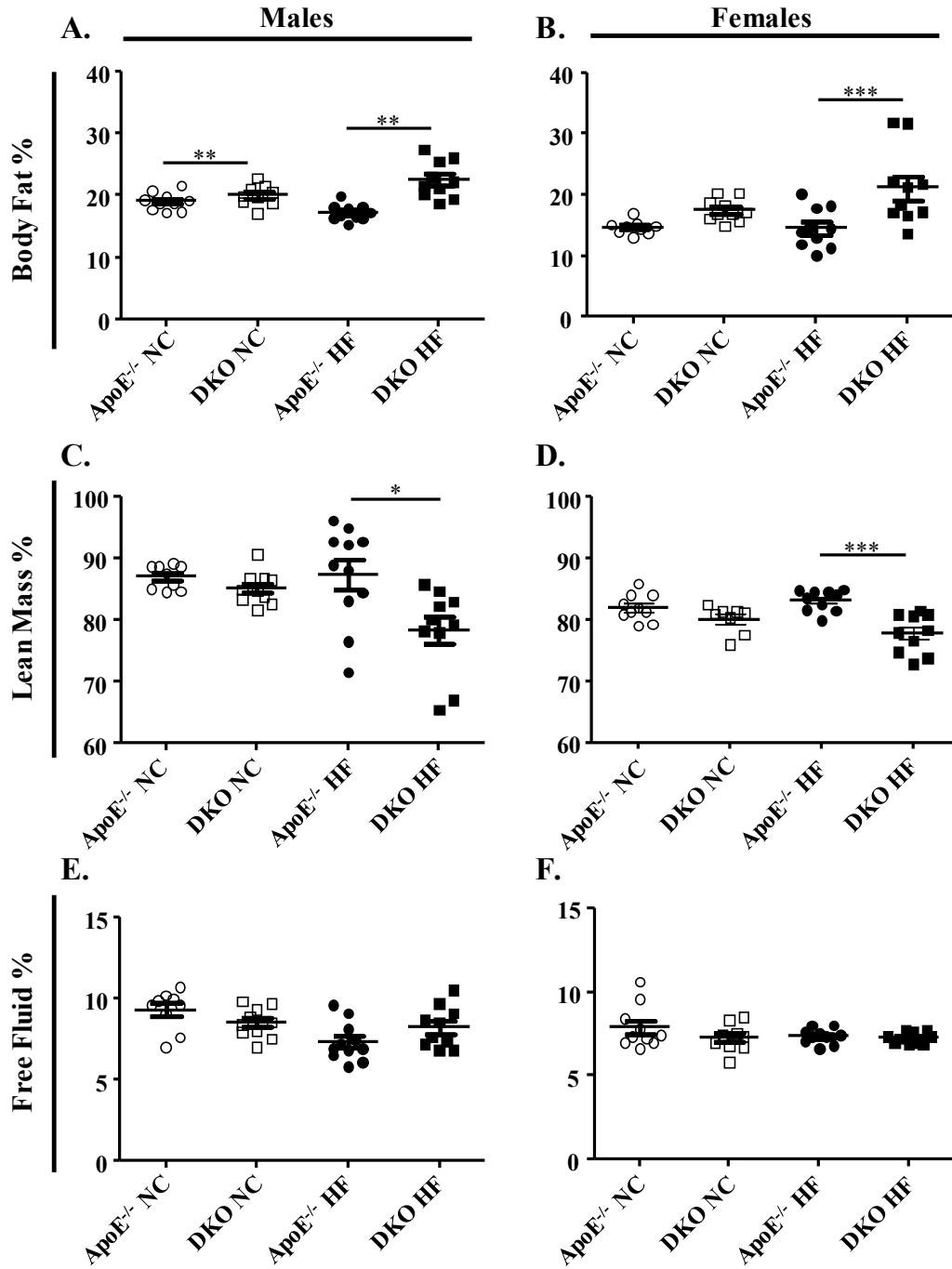
DKO mice have augmented body fat % and reduced lean body mass %

In light of the body mass discrepancies between ApoE^{-/-} and DKO mice on high fat feed, we felt an investigation of body composition may provide insight into this phenotype. Male and female ApoE^{-/-} and DKO mice were maintained on normal chow or placed on a high fat diet for 12 weeks after maturation. At 20 weeks of age, mice were subjected to NMR body composition analysis for body fat percentage, lean body mass percentage, and free fluid percentage. We found that male DKO mice on both normal or high fat chow had significantly elevated body fat percentage when compared to their male ApoE^{-/-} counterparts (**Figure 10A**). This corresponded to a body fat percentage increase of 19% and 46% in the normal and high fat chow groups, respectively. A similar phenotype was observed in the female mice. The female DKO mice on high fat feed had a 30% augmentation in body fat percentage when compared to equivalent ApoE^{-/-} mice, while female DKO mice on normal chow also had greater body fat percentage than equivalent ApoE^{-/-} mice but fell short of statistical significance (**Figure 10B**). In fact, male and female DKO mice on normal chow had even greater body fat percentages than ApoE^{-/-} gender counterparts on high fat.

Logically, when we investigated lean body mass percentage, we found an inverse relationship to the trends in body fat percentage. Specifically, lean body mass was reduced in male DKO mice when compared to male ApoE^{-/-} mice (**Figure 10C**). This reduction was significant and equated to a 10% decrease in lean body mass percentage between the high fat chow groups. We observed a similar trend in the normal chow groups, though it was not found to be significant. Lean body mass percentage in female DKO mice was also found to be significantly lower than their ApoE^{-/-} equivalents

(Figure 10D). This change was quantified as a 6.5% reduction in lean body mass percentage between the high fat chow groups. Like the males, a similar trend was witnessed in the female normal chow groups but was not found to be significant.

The final parameter evaluated with NMR was free body fluid percentage. We found no observable difference in any diet group for the males or females **(Figure 10E, F)**. This result was expected as free body fluid percentage serves as a baseline measurement and should be equal among groups.



HF: High fat, NC: Normal chow, *P-value <0.05, **P-value <0.01, ***P-value <0.001

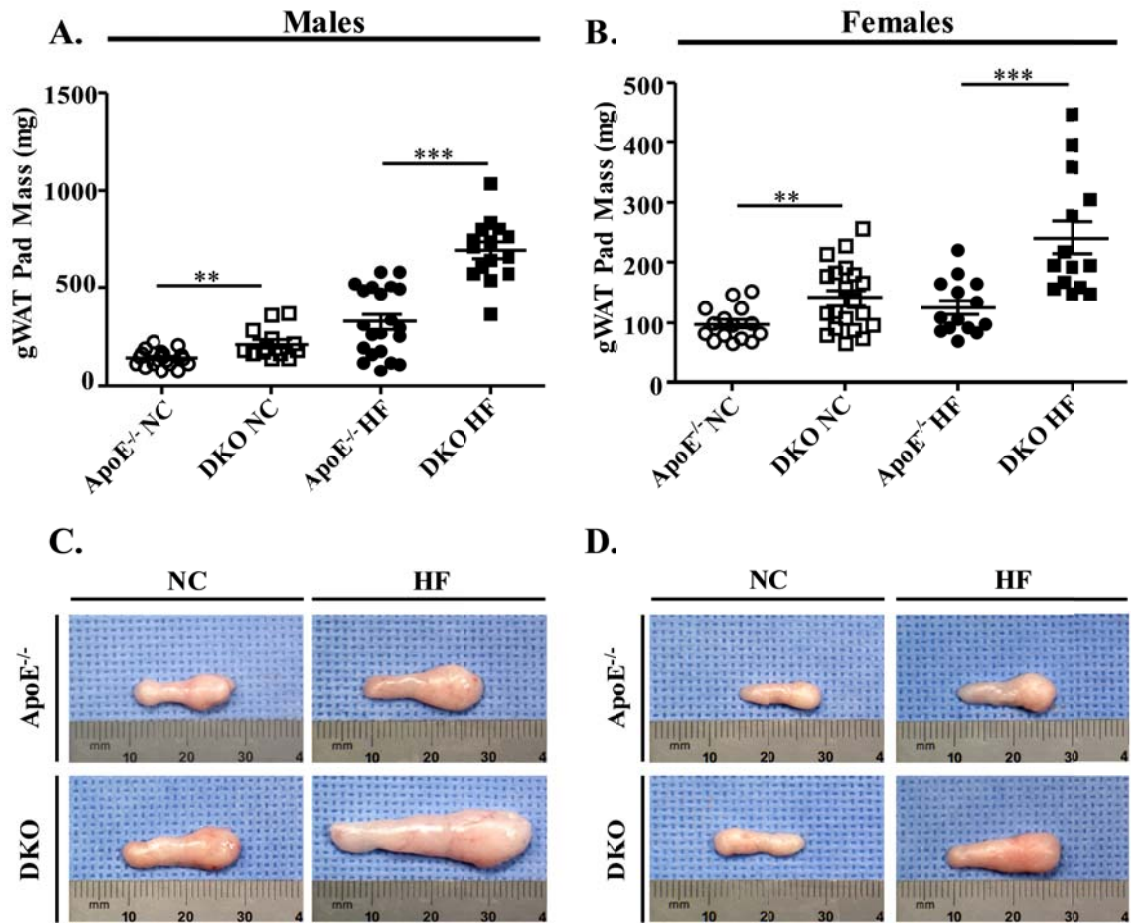
Figure 10: NMR body composition assessment

NMR body composition analysis was performed for **A, B**. Body fat percentage, **C, D**. Lean body mass percentage, and **E, F**. Free fluid percentage.

DKO mice have larger gWAT deposits with hypertrophic adipocytes

As a result of the increases in body fat percentage within DKO mice, we decided to determine if this augmentation pertained to visceral fat deposits as they are known to be highly correlated with MetS development(Grundy, 2004). Like in the previous two studies, male and female ApoE^{-/-} and DKO mice were fed normal chow or high fat diet for 12 weeks after maturation. At 20 weeks of age, left gonadal WAT pads (gWAT) were excised, weighed, and pictured. We found that gWAT mass was significantly increased in male DKO mice on both diets when compared to ApoE^{-/-} equivalents (**Figure 11A**). This augmentation equated to a 51% and 114% increase in gWAT pad mass in normal chow and high fat groups, respectively. In accordance with the male mice, female DKO mice also had larger gWAT deposits than their ApoE^{-/-} counterparts in both diet groups equaling a 45% and 92% increase in gWAT mass in the normal chow and high fat diet groups, respectively (**Figure 11B**). Furthermore, male gWAT deposits out-massed their female equivalents in all groups. The distinction in gWAT pad size was captured with a camera for visual comparison (**Figure 11C, D**).

Increases in adipose tissue mass typically occur as a result of adipocyte hypertrophy. To determine if this was the case for our augmented gWAT mass, we performed histological evaluation of gWAT from male and female ApoE^{-/-} and DKO on normal and high fat chow. We found male DKO adipocyte area to be greater in both normal and high fat fed mice than their corresponding ApoE^{-/-} counterparts (**Figure 12A**). In accordance with this finding, females also showed a similar phenotype with both female DKO feed groups having greater adipocyte cell size than their ApoE^{-/-} equivalents (**Figure 12B**).



gWAT: Gonadal white adipose tissue, HF: High fat, NC: Normal chow,
 *P-value <0.05, **P-value <0.01, ***P-value <0.001

Figure 11: Evaluation of murine gWAT mass and gross morphology

Gonadal WAT pads were excised, **A, B.** Weighed, and **C, D.** Pictured.

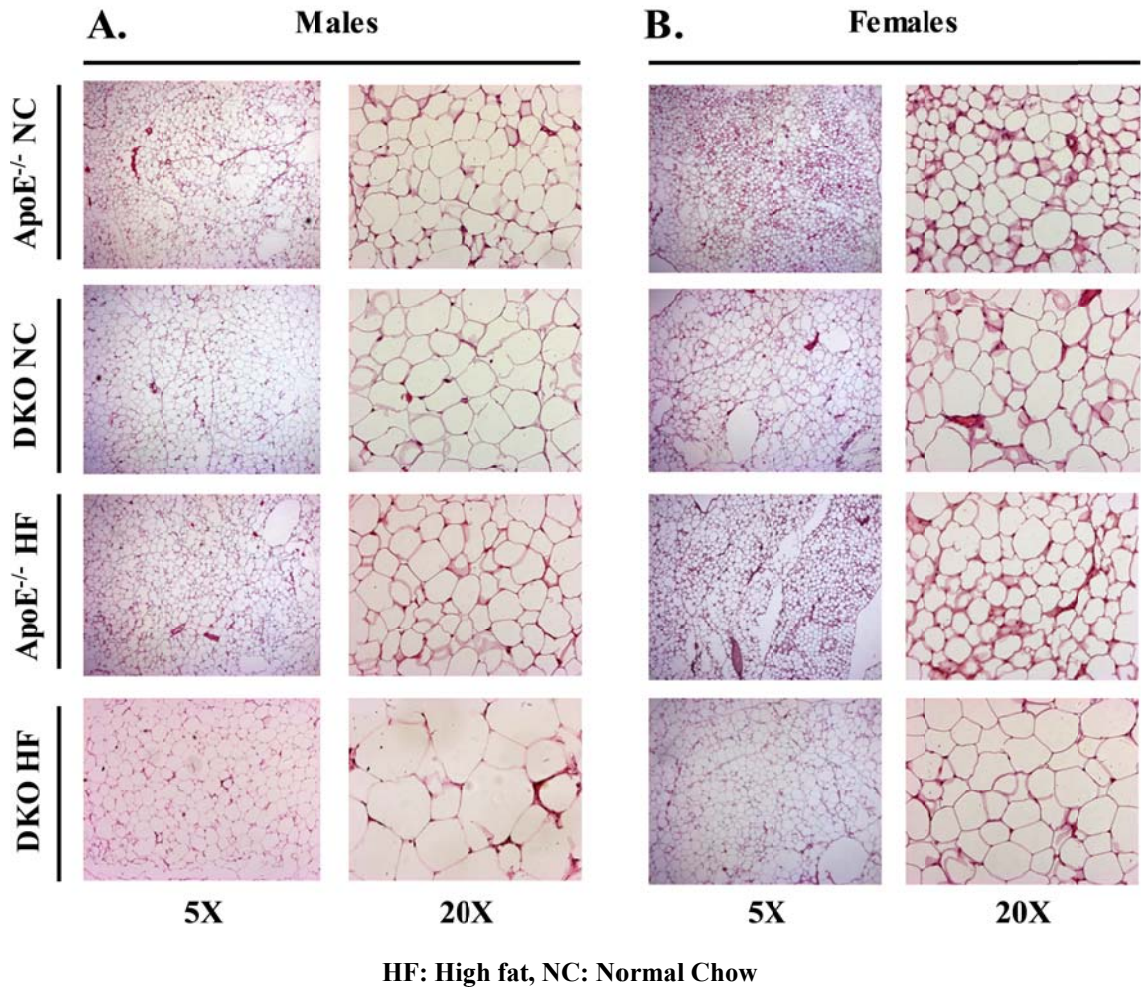


Figure 12: Histological evaluation of gWAT

A. Male and **B.** Female ApoE^{-/-} and DKO gWAT pads were fixed, sectioned, and subjected to H&E stain.

DKO mice have augmented leptin and resistin when on a high fat diet

Adipocytes from visceral fat are specifically reported to be tightly associated with the deregulation of adiponectin, resistin, and leptin in obese individuals (Bjorndal et al., 2011). Since we found augmented visceral mass in our DKO mice, we decided to investigate the plasma levels of these adipokines. Blood was drawn from male ApoE^{-/-} and DKO mice on normal or high fat chow and the plasma analyzed. We found that adiponectin levels were significantly augmented in ApoE^{-/-} and DKO mice on high fat diet when compared to normal chow equivalents (**Figure 13A**). However, there was no discernable difference between ApoE^{-/-} and DKO mice within chow groups. Like with adiponectin, there was a significant increase in leptin levels in the high fat diet groups when compared to normal chow counterparts (**Figure 13B**). However, this time there were distinctions among ApoE^{-/-} and DKO mice within chow groups. DKO mice showed an 86% and 101% increase in leptin over ApoE^{-/-} mice in normal and high fat chow groups, respectively. It should be noted that only the high fat group was statistically significant. Review of plasma resistin revealed that DKO mice on high fat chow had augmented levels by 70% when compared to ApoE^{-/-} mice, while no difference was seen in the normal chow groups (**Figure 13C**). The deregulated levels of adipokines further support the fact that the DKO mice are afflicted with obesity. Furthermore, they also suggest that the DKO mice may be suffering from IR since resistin directly functions to modulate insulin sensitivity.

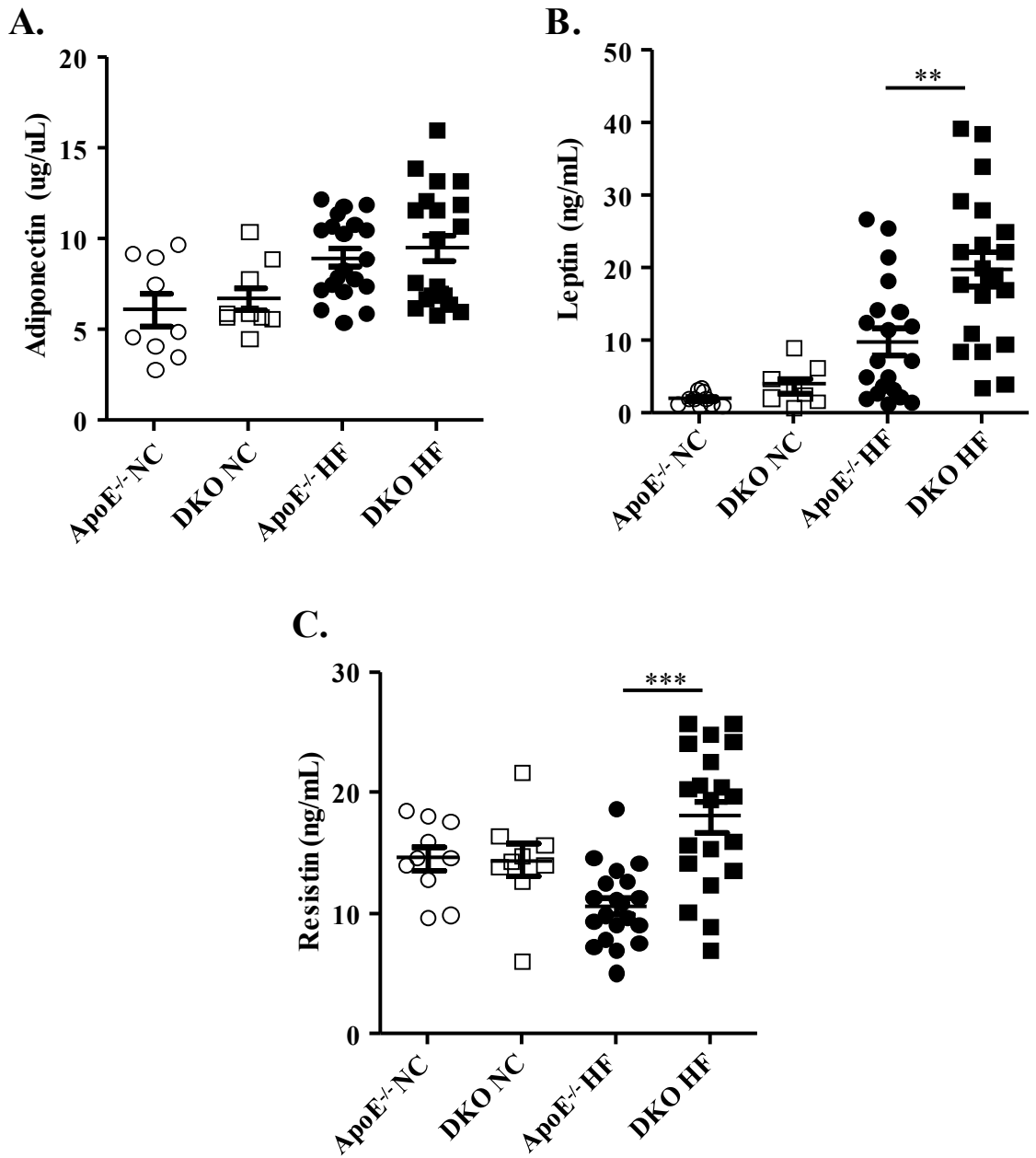


Figure 13: Plasma adipokine levels

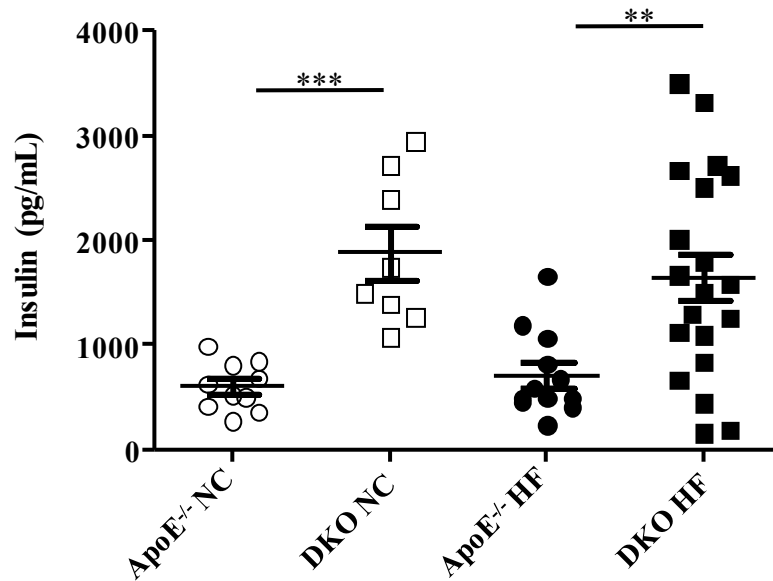
Plasma was isolated from male ApoE^{-/-} and DKO mice and analyzed for **A.** Adiponectin, **B.** Leptin, and **C.** Resistin.

DKO mice are hyperinsulinemic amidst euglycemia

The presence of excess visceral adipose tissue, like we witnessed in our DKO mice, is tightly correlated with and often an indicator of peripheral insulin resistance (Frayn, 2000). Furthermore, the deregulation of particular adipokines like resistin and leptin are frequently associated with glucose and insulin deregulation (Rabe et al., 2008). Due to this, we felt it was prudent to further investigate plasma insulin levels. Male ApoE^{-/-} and DKO mice were fed with normal chow or high fat diet for 12 weeks after maturation and then blood was drawn and plasma isolated for insulin level assessment. We found that DKO mice on both chows had significant increases in insulin levels when compared to ApoE^{-/-} equivalents (**Figure 14**). This distinction amounted to a 211% and 130% augmentation in insulin among normal chow and high fat diet groups, respectively. This data indicates that our DKO mice are insulin resistant, as hyperinsulinemia is a hallmark of insulin insensitivity.

In light of the hyperinsulinemia observed in our DKO mice, we felt it prudent to measure blood glucose levels in fed and fasted (16 hours) ApoE^{-/-} and DKO mice on normal and high fat diets. Murine tails were nicked, blood collected onto glucose strips, and measured with a Glucose201 meter from Hemocue®. Despite the hyperinsulinemia, we found no statistical differences between blood glucose levels of fed or fasted ApoE^{-/-} and DKO mice and their respective equivalents in either feed grouping (**Figure 15A-D**). To further confirm this matter, we performed glucose tolerance tests (GTT) and insulin tolerance tests (ITT). In brief, mice subjected to GTT received an injection of glucose (1g/kg) after an 16 hour fast. Glucose levels were then measured at 30, 60, 90, and 120 minutes after injection. Male and Female DKO mice on normal or high fat diets showed

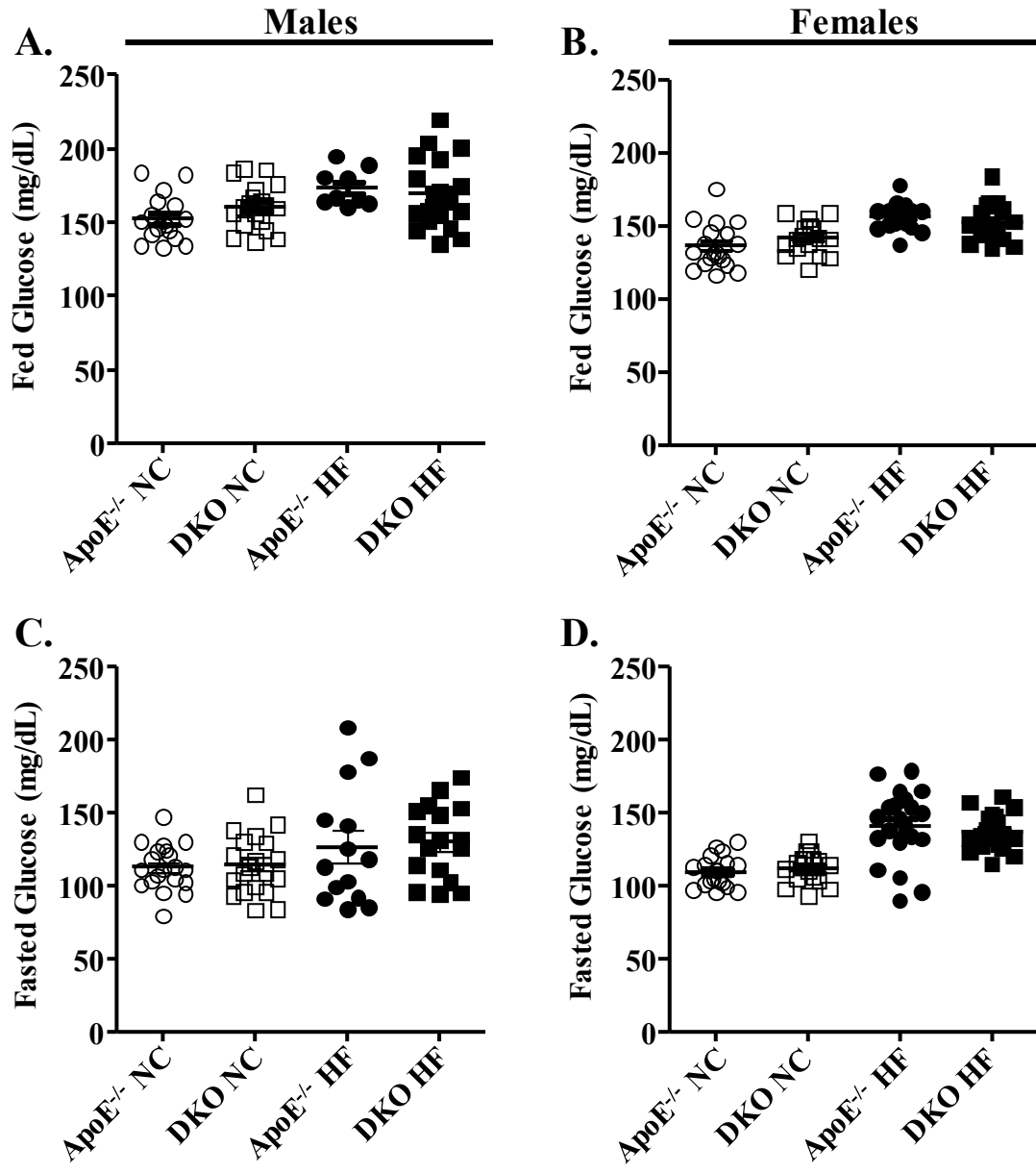
no observable difference in glucose tolerance profiling from their ApoE^{-/-} equivalents (**Figure 16A-F**). ITT were carried out in a similar fashion, albeit mice received an injection of human insulin (0.75units/kg) and were not fasted. Again, no discrepancies in either male or female DKO mice and their respective ApoE^{-/-} equivalents were seen with either diet (**Figure 17A-F**). This data indicates that despite IR in DKO mice, they are able to maintain euglycaemia.



HF: High fat, NC: Normal chow, **P-value <0.01, ***P-value <0.001

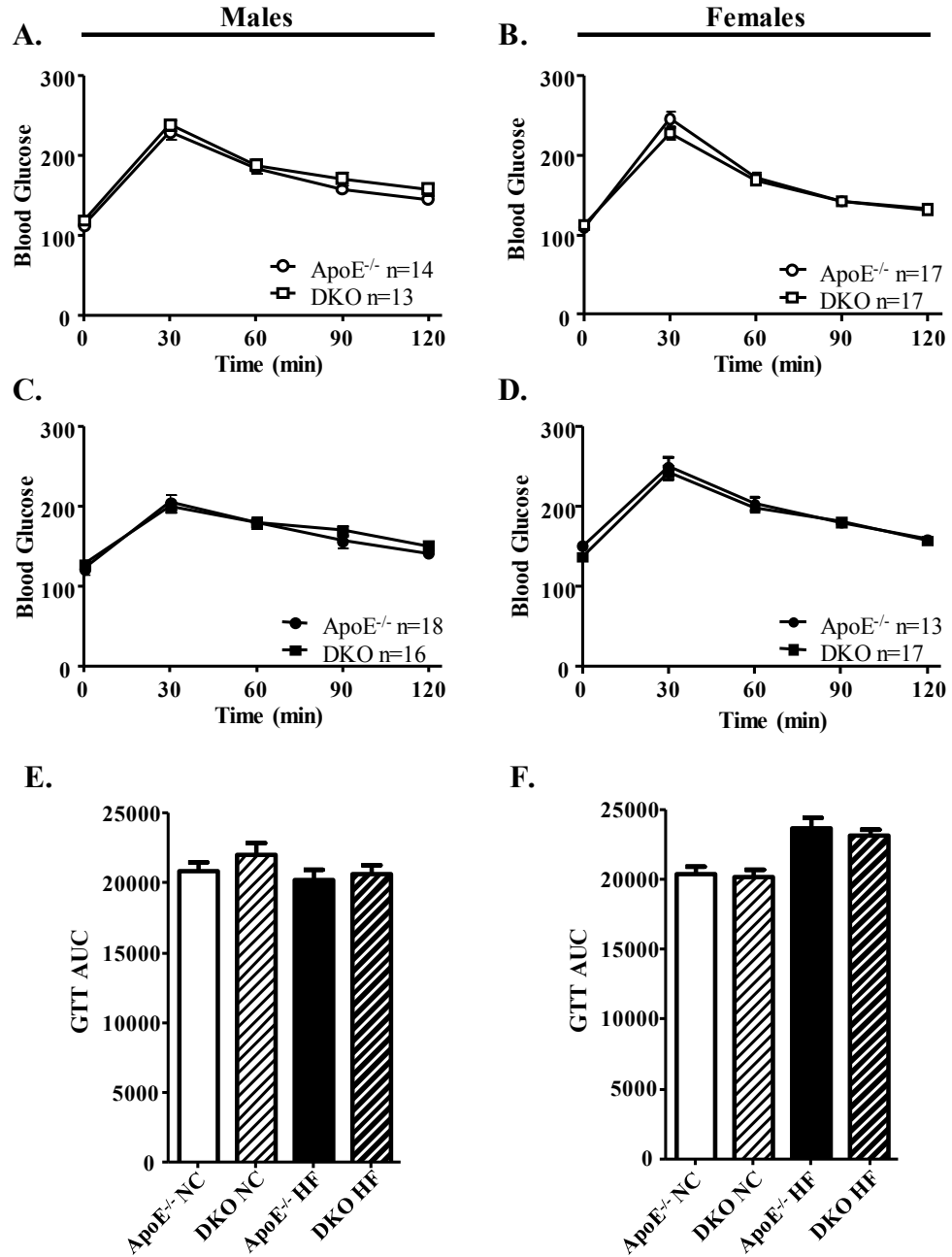
Figure 14: Plasma insulin levels

Blood was drawn from male ApoE^{-/-} and DKO mice, plasma isolated, and insulin levels assessed.



HF: High fat, NC: Normal chow

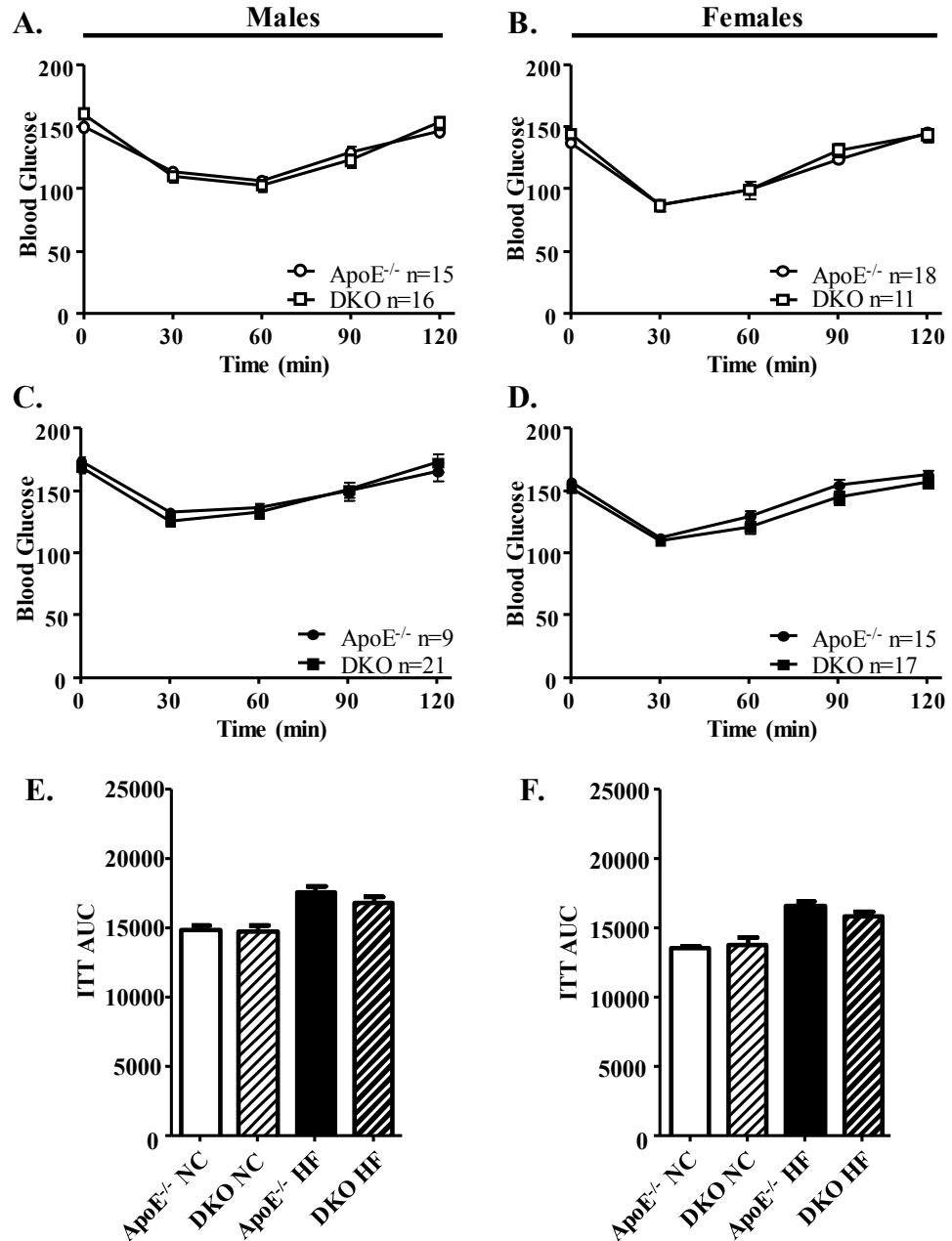
Figure 15: Blood glucose levels of fed and fasted mice
 Blood was drawn from **A, B.** Fed or **C, D.** Fasted ApoE^{-/-} and DKO mice for glucose level assessment.



GTT: Glucose tolerance test, AUC: Area under the curve HF: High fat, NC: Normal chow

Figure 16: Glucose tolerance testing and quantification

Mice were administered glucose (1g/kg) and blood drawn from ApoE^{-/-} and DKO mice fed with **A, B.** Normal chow and **C, D.** High fat chow for glucose levels and **E, F.** AUC calculated.



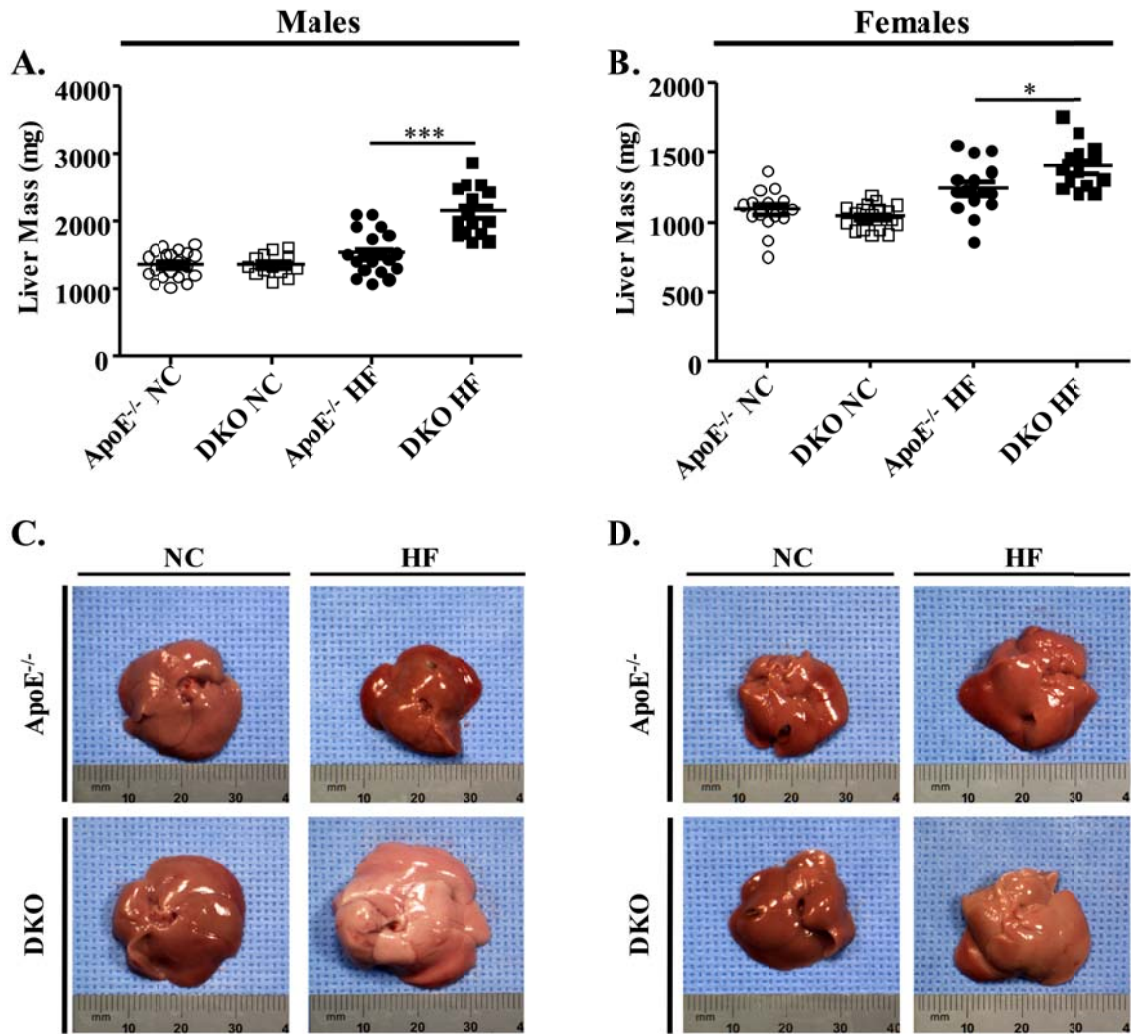
ITT: Insulin tolerance test, AUC: Area under the curve HF: High fat, NC: Normal chow

Figure 17: Insulin tolerance testing and quantification

Mice were administered insulin (0.75Units/kg) and blood drawn from ApoE^{-/-} and DKO mice fed with **A, B.** Normal chow and **C, D.** High fat chow for glucose levels and **E, F.** AUC calculated.

DKO mice are afflicted with NAFLD

NAFLD is a clinical condition hallmarked by the abnormal accumulation of triglycerides within the liver and is often considered a hepatic manifestation of MetS due to their tight affiliation (Fabbrini et al., 2010). As such, we felt it was sensible to evaluate the hepatic condition of our DKO mice. Male and female ApoE^{-/-} and DKO mice were fed a normal chow or high fat diet for 12 weeks after maturation and then livers were excised, weighed, and pictured. We found male hepatic mass to be significantly increased in DKO mice fed with high fat diet, a distinction that equated to a 40% increase from their ApoE^{-/-} counterparts (**Figure 18A**). Meanwhile, we found no discrepancy in hepatic weight among normal chow groups. In accordance with the males, female DKO mice on high fat diet also had greater hepatic mass (13%) when compared to ApoE^{-/-} equivalents (**Figure 18B**). Again, no discrepancy was seen in the normal chow groups. In addition, all male mice on either diet had greater hepatic mass than their female companions as expected. Visual inspection of livers revealed distinct pigmentation differences of male and female DKO mice on high fat feed when compared to the other mice (**Figure 18C, D**). This difference can be described as lighter and more whitish in appearance than the traditionally deep red pigment typically associated with healthy livers. To further investigate this matter we fixed, paraffin embedded, sectioned, and stained hepatic samples with H&E stain (**Figure 19A, B**). We found that male and female DKO mice on high fat chow had irregular hepatic tissue morphology. The hepatic sections from these mice showed signs of steatosis, a hallmark of NAFLD. All other hepatic sections had normal morphology. These findings suggest that our DKO mice are susceptible to NAFLD when exposed to a high caloric diet.



HF: High fat, NC: Normal chow, *P-value <0.05, ***P-value <0.001

Figure 18: Evaluation of hepatic mass and gross morphology

A. Male and **B.** Female ApoE^{-/-} and DKO livers were excised and weighed. **C, D.** Pictures were then taken so that size and pigmentation differences could be visualized.

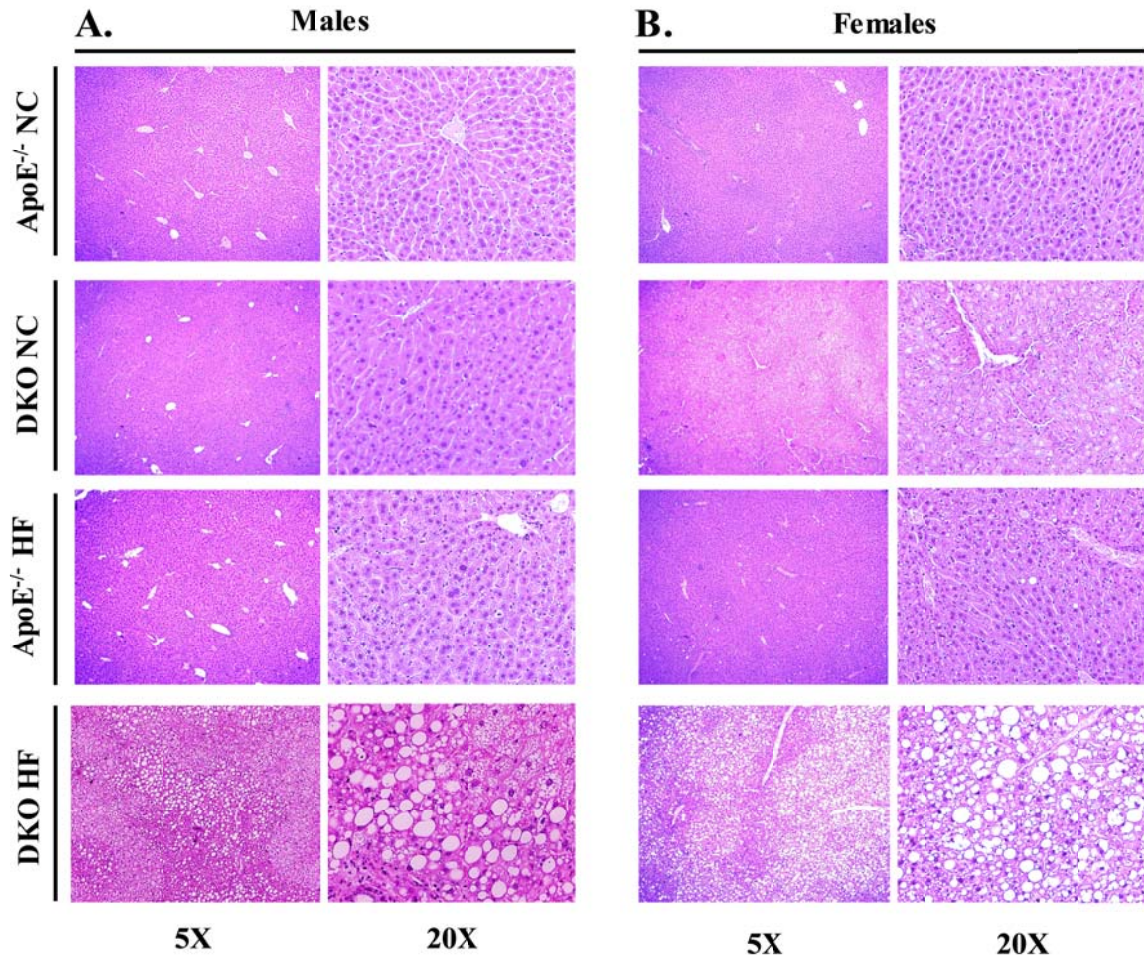
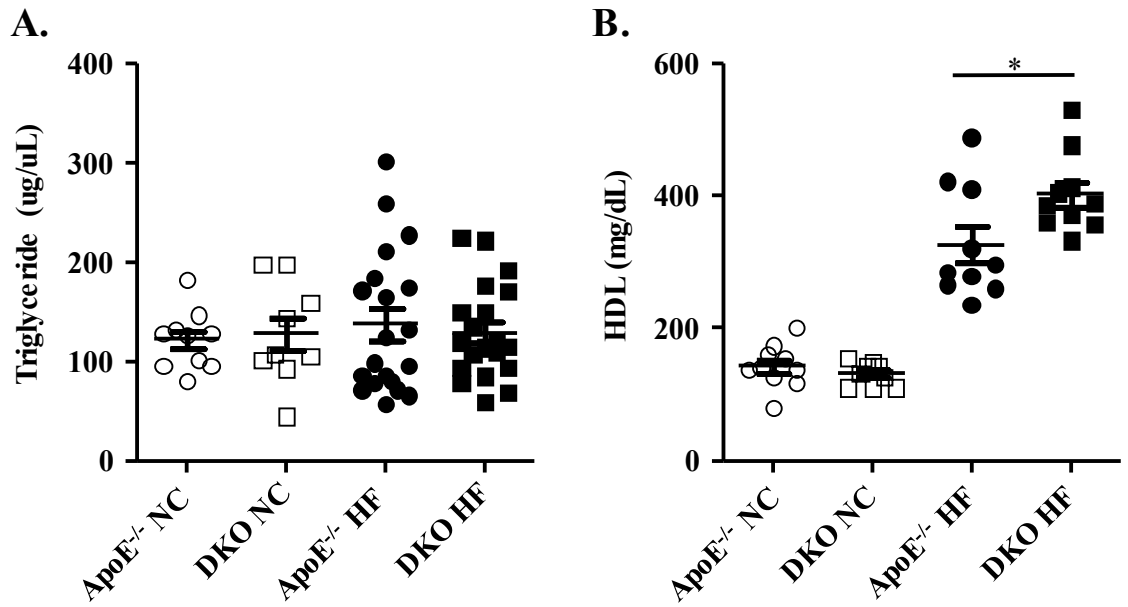


Figure 19: Histological evaluation of hepatic tissue

Livers from **A.** Male and **B.** Female ApoE^{-/-} and DKO mice were excised, fixed, embedded, sectioned, and subjected to H&E staining.

DKO mice have no distinction in TG levels, elevated HDL on a high fat diet

The two plasma lipid criteria of MetS are elevated plasma triglycerides and diminished HDL levels. To evaluate these parameters, blood was drawn from male mice and plasma isolated for triglyceride and HDL quantification. Male ApoE^{-/-} and DKO mice were fed with normal or high fat diet for 12 weeks after maturation and blood drawn for the specified plasma protein analysis. We found no distinction in triglyceride levels between any of the experimental groups (**Figure 20A**). When we looked at HDL levels we found a significant increase in ApoE^{-/-} and DKO mice fed with a high fat diet when compared to normal chow mice (**Figure 20B**). Furthermore, we saw augmented levels in the DKO mice on high fat feed when compared to ApoE^{-/-} equivalents.



HDL: High density lipoprotein, HF: High fat, NC: Normal chow, *P-value <0.05

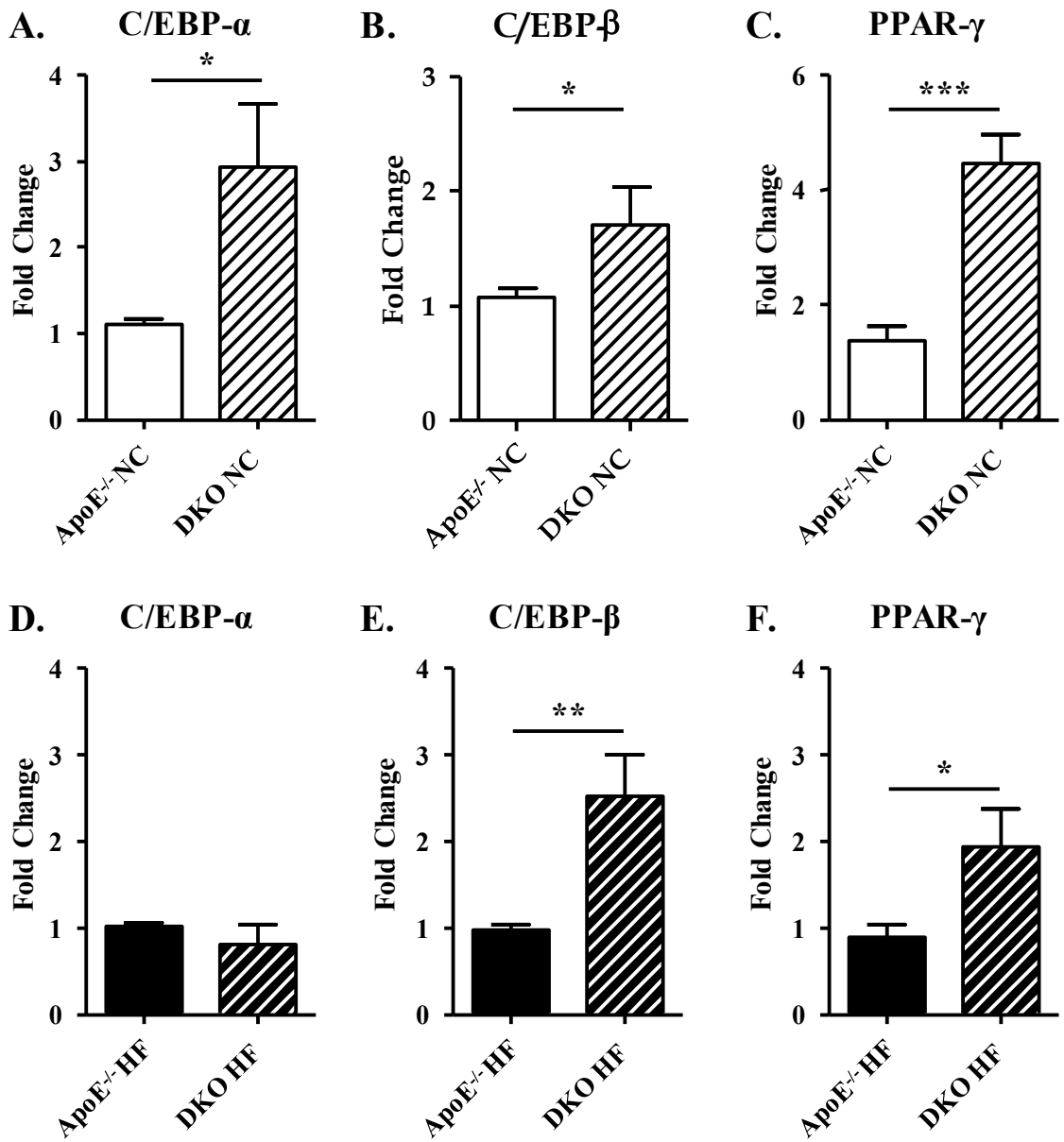
Figure 20: Plasma triglyceride and HDL levels

Male ApoE^{-/-} and DKO mice were fed with normal or high fat diet and blood drawn for the plasma analysis of **A.** Triglycerides and **B.** HDL.

DKO mice have greater hepatic and WAT C/EBP- α , C/EBP- β , and PPAR- γ

In order to determine the molecular reason for our DKO phenotype we reviewed the 140 experimentally verified targets of miR-155(Neilsen et al., 2013). Specifically, we focused on targets which played integral roles in adipogenesis, lipogenesis, inflammation, and NAFLD. One target in particular, C/EBP- β , was exceptionally well-fitting of our phenotype. As a transcription factor, C/EBP- β plays an important role in activating numerous genes involved in adipogenesis and lipid storage(Romao et al., 2011). Two particular targets, C/EBP- α and PPAR- γ , are the critical adipogenic transcription factors(Rosen & Spiegelman, 2000). As such, we decided to examine the hepatic and gWAT expression of C/EBP- β , C/EBP- α , and PPAR- γ . To do this, RNAs were isolated from the livers and gWAT and qRT-PCR run. We found that all three were significantly augmented in the livers of DKO mice on normal chow when normalized with ApoE^{-/-} equivalents (**Figure 21A-C**). Furthermore, a similar trend was witnessed in the high fat diet groups as well. The expressions of C/EBP- β and PPAR- γ were found to be significantly elevated in DKO mice when normalized by ApoE^{-/-} counterparts, while C/EBP- α showed no distinction in expression (**Figure 21D-F**). In the gWAT of male ApoE^{-/-} and DKO mice we found a similar trend. The expressions of C /EBP- α , C/EBP- β , and PPAR- γ were all augmented in DKO mice fed a normal chow; however, only PPAR- γ reached statistical significance (**Figure 22A-C**). The same trend was witnessed in the high fat chow groups where the expressions of C /EBP- α , C/EBP- β , and PPAR- γ were all found to be elevated in DKO mice; however, only C /EBP- α showed statistically significant distinction (**Figure 22D-F**). This hepatic and gWAT data show that the

expressions of C/EBP- α , C/EBP- β , and PPAR- γ are all augmented in our DKO mice providing a possible explanation for our observed phenotype.

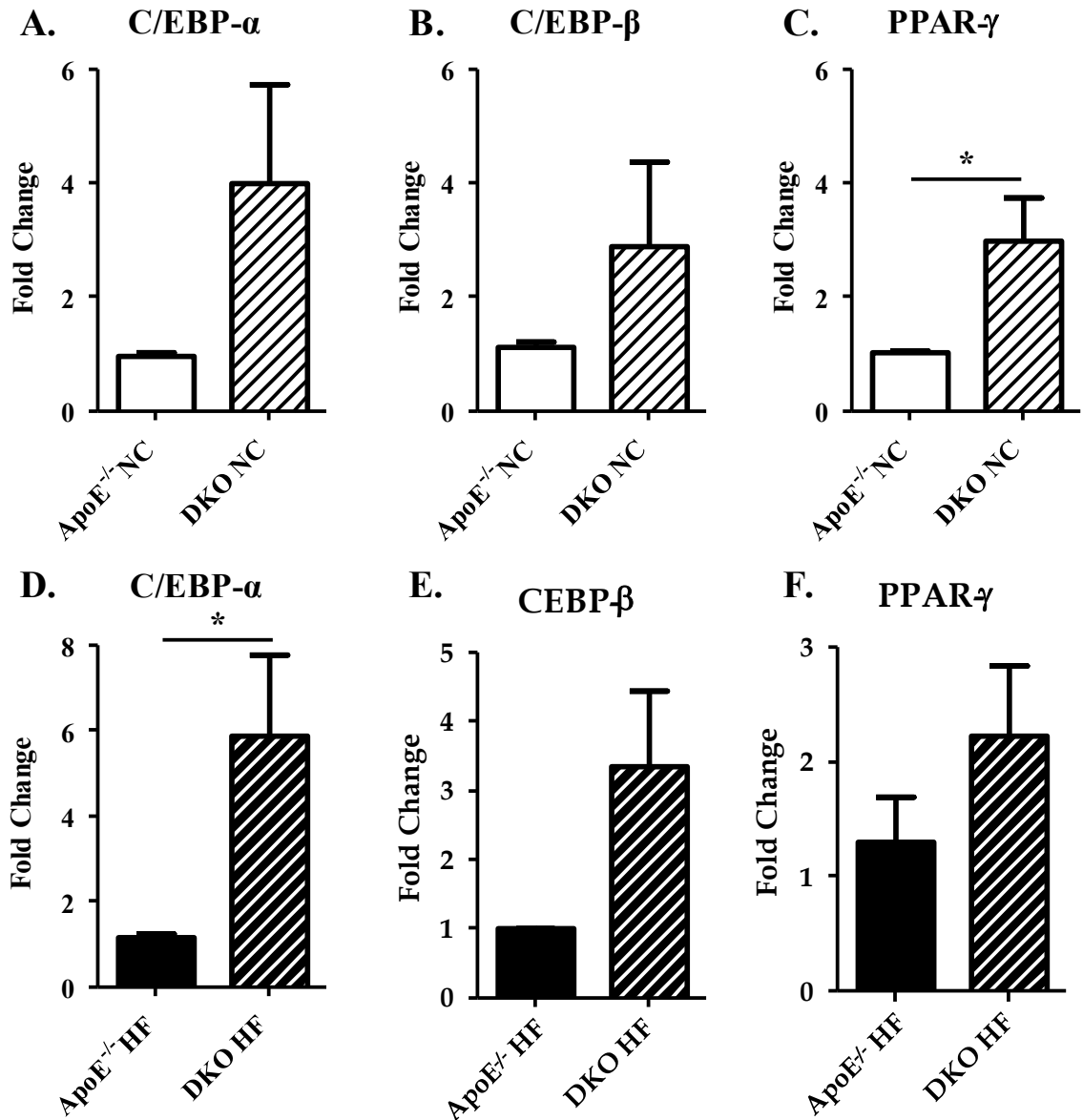


C/EBP- α : CCAAT/enhancer binding protein-alpha, C/EBP- β : CCAAT/enhancer binding protein-beta, PPAR- γ : Peroxisome proliferator-activated receptor-gamma, HF: High fat, NC: Normal chow, *P-value <0.05, **P-value <0.01, ***P-value <0.001

Figure 21: Hepatic expression of C/EBP- α , C/EBP- β , and PPAR- γ

RNAs were isolated from the livers of male ApoE^{-/-} and DKO mice and qRT-PCR run for A, C. C/EBP- α , B, D. C/EBP- β , and C, E. PPAR- γ .

DKO mice have elevated gWAT levels of C/EBP- α , C/EBP- β , and PPAR- γ



C/EBP- α : CCAAT/enhancer binding protein-alpha, C/EBP- β : CCAAT/enhancer binding protein-beta, PPAR- γ : Peroxisome proliferator-activated receptor-gamma, HF: High fat, NC: Normal chow, *P-value <0.05, **P-value <0.01, ***P-value <0.001

Figure 22: gWAT mRNAs expression of C/EBP- α , C/EBP- β , and PPAR- γ

RNAs were isolated from the livers of male ApoE^{-/-} and DKO mice and qRT-PCR run for

A, C. C/EBP- α , B, D. C/EBP- β , and C, E. PPAR- γ .

Atherosclerosis development is reduced in DKO mice

One of the reasons MetS is a major health concern is its ability to increase the likelihood of CVD. Individuals diagnosed with MetS have a 2-fold increased risk of suffering from stroke, myocardial infarction, and succumbing to CVD-associated mortality (Hansson & Hermansson, 2011). As such, we decided to evaluate if our DKO mice, which are afflicted with metabolic syndrome, were also susceptible to atherosclerosis development.

We first wanted to determine if miR-155 expression was altered in atherosclerosis development and measure its relevancy against other miRNAs. To do this, we decided to perform a PCR array designed to screen 84 of the most abundant and well-characterized miRNAs in miRBase. We isolated aortic RNA from ApoE^{-/-} mice fed with normal or high fat chow for 12 weeks. The RNAs from 5 mice per feed group were then pooled together and used with the miFinder PCR array from Qiagen® to evaluate miRNAs expression change (**Figure 23**). We found that 7 miRNAs were up-regulated by at least 4-folds and 9 miRNAs that were down-regulated by at least 4-folds during atherogenesis. The identities of these vastly differentiated miRNAs are listed in **Table 6**. Of these miRNAs, miR-155 was found to be augmented by 16.7-fold. This finding suggests that miR-155 is an important factor during atherosclerosis development. To verify this finding and determine at what point this augmentation occurs, we performed qRT-PCR with aortic RNA collected from ApoE^{-/-} mice fed with high fat for 0 weeks, 3 weeks, 6 weeks, and 12 weeks. After normalization to the 0 weeks groups, we found that miR-155 expression was in fact augmented during atherosclerosis development (**Figure 24**). Furthermore, we found significant elevation in miR-155 expression as early as 3 weeks

after high fat feed. This qRT-PCR data verifies our screening results and suggests that miR-155 plays an important role in atherosclerosis development.

Now that we knew miR-155 expression was drastically altered with atherogenesis, we decided to determine what its impact was on atherosclerosis development. We fed male ApoE^{-/-} and DKO mice with high fat diet for various durations including 0 weeks, 3 weeks, 6 weeks, and 12 weeks. Full length aortas were then excised from mice, cleaned of perivascular fat, splayed open, and stained with Sudan IV which stains regions of lipid accumulation. Individual lesion areas within an aorta were then quantified using Adobe Photoshop®, summated, and presented as a percentage of total aortic area (**Figure 25B**). As expected, we found no staining in the 0 weeks groups and minimal staining in the 3 weeks high fat feed groups (**Figure 25A**). However, after 6 weeks of high fat feeding obvious amounts of staining could be visualized. Interestingly, we found a noticeable 32% reduction in lesion area in DKO mice, albeit this distinction did not reach statistical significance. This trend was also witnessed after 12 weeks of high fat feed, where statistical significance was achieved in DKO mice which had a 45% reduction in atherosclerotic plaque area. These results suggest that the DKO mice are protected from atherosclerosis development.

We decided to further confirm the 12 weeks high fat feed results with aortic root evaluation. To complete this, hearts from male ApoE^{-/-} and DKO mice were excised, embedded in OCT, and cross-sectioned. The aortic root was then stained with Oil Red O for atherosclerotic plaque visualization and quantified as described above. We expectantly found that the aortic roots of ApoE^{-/-} and DKO mice not fed with high fat had no atherosclerotic lesion development (**Figure 26A**). However, following 12 weeks of

high fat feed, both ApoE^{-/-} and DKO mice had definitive atherosclerosis development. Of these, DKO mice possessed a significant reduction of 9.5% in plaque area when compared to ApoE^{-/-} (**Figure 26B**). These aortic root results confirmed are previous finds with the full-length aortas, indicating that the DKO mice are in fact protected from atherosclerosis development.

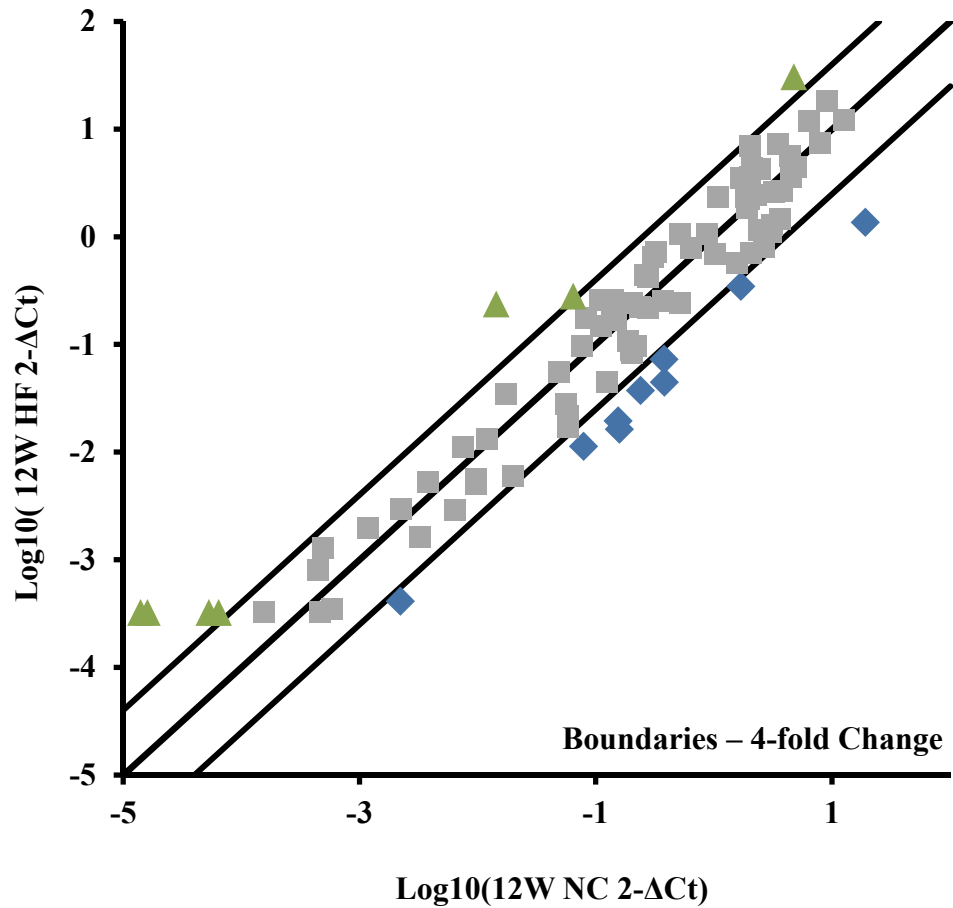
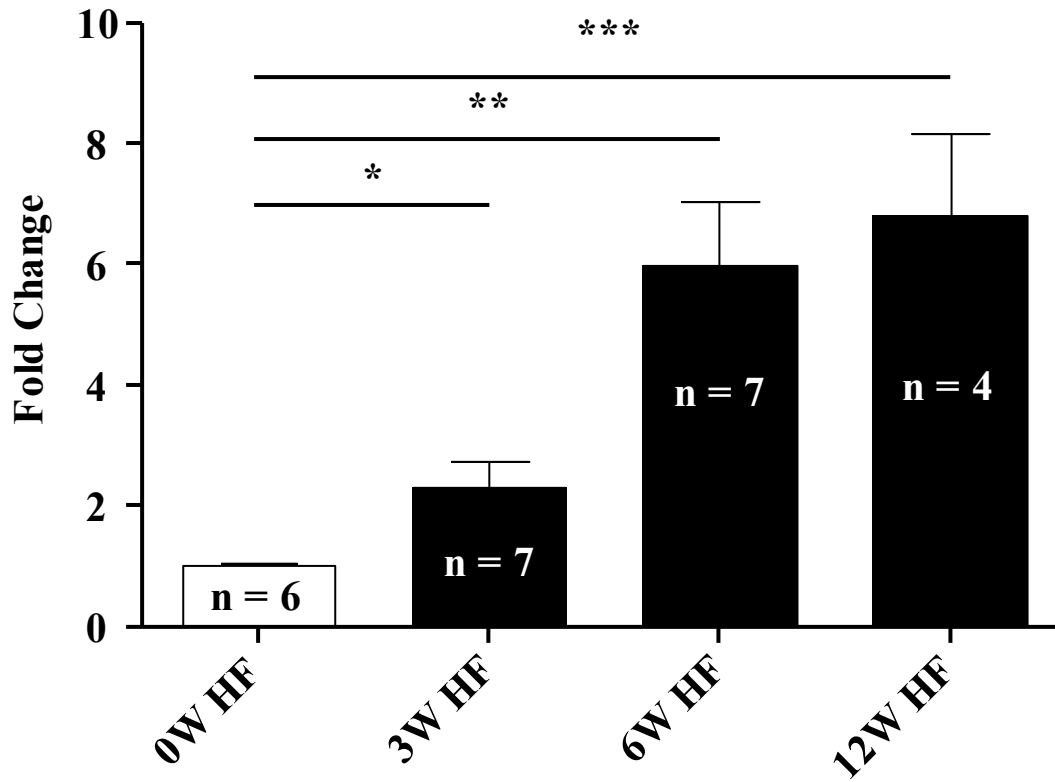


Figure 23: Scatter plot of differentially expressed miRNAs in atherosclerosis

Outer plot boundaries represent a 4-fold change with those miRNAs with ≥ 4 -fold positive change represented by green triangles, those with a ≥ 4 -fold negative change symbolized with blue diamonds, and those with less than a 4-fold change depicted by gray squares.

Table 6: List of miRNAs which have a ≥ 4 -fold or greater expression change

miRNAs	Fold Change
miR-880-3p	23.1
miR-295-3p	20.2
miR-155-5p	16.7
miR-21a-5p	6.5
miR-302d-3p	6.2
miR-291a-3p	5.1
miR-744-5p	4.4
miR-99a-5p	-4.8
miR-199a-5p	-5.2
miR-335-5p	-5.4
miR-142-3p	-6.4
miR-142-5p	-6.9
miR-19b-3p	-7.9
miR-101a-3p	-8.5
miR-19a-3p	-9.7
miR-22-3p	-14.0



W: Week(s), HF: High fat, *P-value <0.05, **P-value <0.01, ***P-value <0.001

Figure 24: Aortic miR-155 expression is increased during atherogenesis

Aortic RNA was subjected to qRT-PCR for miR-155 expression.

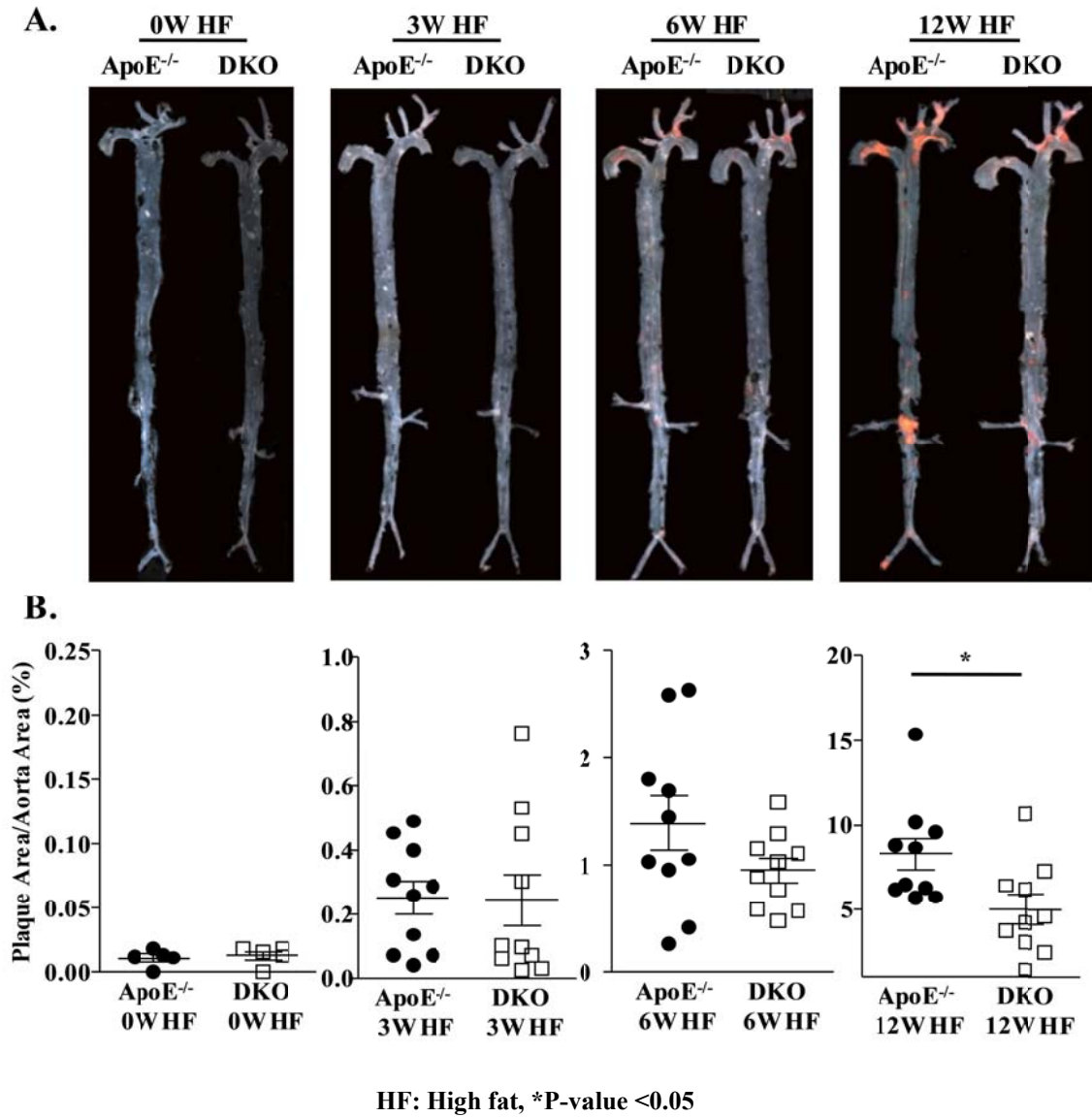


Figure 25: *En face* atherosclerotic lesion quantification

Full length aortas from male ApoE^{-/-} and DKO mice were **A.** Stained with Sudan IV for atherosclerotic plaque identification and **B.** Quantified.

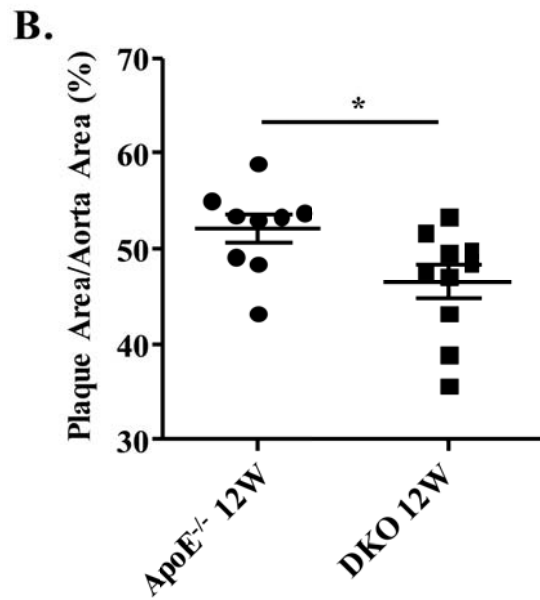
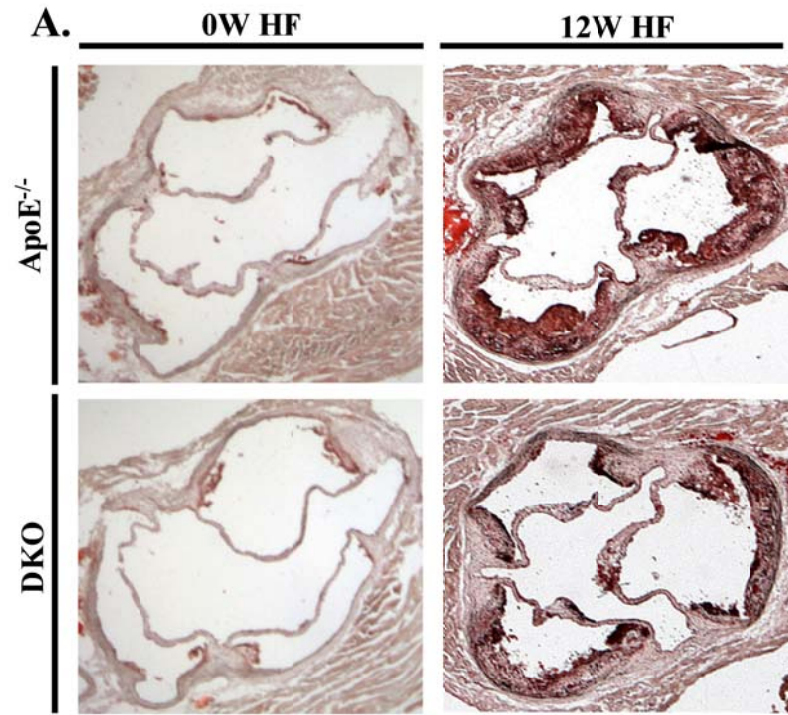


Figure 26: Representative aortic sinus imagery

A. Oil Red O staining of hearts from male ApoE^{-/-} and DKO mice for atherosclerotic plaque visualization and **B.** Quantification.

CHAPTER 4: DISCUSSION

The incidence of overweight and obese individuals is a growing epidemic worldwide. As a result, individuals afflicted with MetS and CVD have simultaneously skyrocketed posing a major health problem. To combat this problem, the role of miRNAs in these medical complications is under evaluation. Thus far, miR-155 has been indicated as a mediator of several cellular processes related to these pathologies. In light of this, we set out to determine the role of miR-155 in obesity, MetS, and atherosclerosis development. In doing so, we have illustrated for the first time that miR-155 plays an integral role in mediating metabolic homeostasis and provided further evidence of its role in atherosclerosis development. We found 4 major findings in our novel DKO mouse model: first, DKO mice had augmented body mass and excessive fat accumulation when challenged with a high fat diet; second, DKO mice were hyperinsulinemic; third, DKO mice are susceptible to NAFLD; and fourth, DKO mice were protected from atherosclerosis development.

To examine the effect of miR-155 in obesity, MetS, and atherosclerosis we devised a novel mouse model. We accomplished this, by crossing miR-155-deficient mice with hyperlipidemic and atherosclerosis-prone ApoE knockout mice. Breeding schemes and verification of this novel mouse strain can be found in **Figure 8**. In conjunction with these mice, we used normal or high fat feed which allowed us to examine the effects of miR-155 deficiency in caloric balance and in times of surplus like that seen in obesity, MetS, and atherosclerosis.

MiR-155 and Obesity

The first thing we investigated was the development of ApoE^{-/-} and DKO mice. We accomplished this by weighing male and female mice on a weekly basis from 2 to 20 weeks of age. At maturity, or 8 weeks of age, mice were either kept on normal chow or put on a high fat diet. After recording the body masses of male and female ApoE^{-/-} mice we found no gender-specific differences in body weight when fed either normal or high fat chow (**Figure 9**). Like ApoE^{-/-} mice, mature male and female DKO mice on normal chow showed no difference in body weight; however, when challenged with high fat diet male and female DKO mice exhibited a clear phenotype with body mass augmentation. This difference rapidly manifested in male DKO mice showing statistical difference after only one week with high fat feed and persisting throughout the duration of the study. The greatest difference in body mass was observed in weeks 14, 15, and 17 corresponding to an 18.0% increase in DKO mice. Female DKO mice also demonstrated significant distinction from ApoE^{-/-} counterparts on high fat feed, although this phenotype was delayed in onset until 13 weeks and was not as dramatic as in the males. The largest augmentation in body mass was witnessed in weeks 17 and 20 at 9.6%. Direct comparison of ApoE^{-/-} and DKO mice on high fat feed revealed a clear distinction between the two. We found male DKO to have at least a 17.8% increase in body mass, seen in week 9, which increased up to 22% in week 17. In females, the augmented body mass ranged from 2.5% - 10.1%. These findings are novel to the scientific community as previous publications examining the effects of miR-155^{-/-} within mice have not reported differences in body weight from wildtype mice (Miller et al., 2013). This most likely can be attributed to the fact that our miR-155^{-/-} mice are within an ApoE^{-/-} background while

the other miR-155 mouse models were not. Our data suggests that miR-155 plays an integral part in maintaining metabolic homeostasis during times of caloric surplus.

We believed that the augmentation in body weight within our DKO mice was due to an increase in body fat mass so we decided to perform body composition analysis to confirm this hypothesis. Using NMR we were able to evaluate body fat mass, lean body mass, and free fluid mass. We found that male DKO mice on normal or high fat chow had significantly elevated body fat percentage when compared to ApoE^{-/-} counterparts. This difference equated to a 19% and 46% increase within the normal and high fat chow groups, respectively. This trend was also observed in the female DKO mice where the high fat group had a statistically significant 30% augmentation over female ApoE^{-/-} equivalents. Meanwhile, the same trend was observed in the normal chow groups though it did not reach statistical significance. This data definitively shows that the elevated body mass in the DKO mice is a direct result of augmented body fat mass. Furthermore, the smaller distinction in body fat percentage among females was in accordance with the smaller body weight observations showing continuity among our data.

We next analyzed lean body mass with NMR and expectantly found an inverse relationship with body fat percentage. This is logical since an increase in body fat percentage must result in a reduction in lean mass percentage. Specifically, we saw that lean body mass percentage was significantly reduced in male DKO mice by ~10% in comparison to male ApoE^{-/-} mice on high fat diet. Furthermore, the same trend was observed in normal chow groups although statistical significance was not achieved. When we investigated female DKO mice on high fat chow we also found a significant reduction of 6.5% when compared to ApoE^{-/-} equivalents. Like the males, a statistically

significant distinction between female mice on normal chow could not be established even though DKO mice again had lower lean body mass percentage. From this data we can conclude that the DKO mice have diminished lean body mass percentage. Furthermore, we can definitively say that this reduction in lean body mass percentage is due to an increase in body mass as a result of increased body fat and not a reduction in lean body mass. This can be stated since we saw no distinction in lean body mass between ApoE^{-/-} and DKO mice on either diet. Finally, this data provides additional support and confidence in our body fat percentage data.

The final measurement we calculated from the NMR data was free body fluid percentage. In this case, we observed no difference between or within diet groups for males or females. This uniformity among ApoE^{-/-} and DKO mice was expected since free body fluid serves as a baseline parameter between groups.

The lack of previous publications in regard to our findings on body mass and body fat percentage prompted us to further confirm these novel findings through fat pad examination. While there are several sites where adipose tissue resides, the gWAT deposit was chosen for further analysis. This site was selected for its size, comprising of up to 50% of murine adipose tissue, and because it is the primary murine visceral fat deposit(Casteilla et al., 2008). Visceral fat is of particular interest to us since it is highly correlated with MetS and CVD. This tight affiliation is why the WHO and NCEP ATP III use waist circumference and waist/hip ratio when diagnosing MetS, respectively. Investigation of the left gWAT pad revealed a significant increase in mass among male DKO mice on either chow when compared to ApoE^{-/-} equivalents. This observation equated to a 43% and 112% increase in gWAT pad mass in normal and high fat fed mice,

respectively. In accordance with these male findings, female DKO mice also had larger gWAT deposits amounting to a 45% and 57% increase in the normal and high fat chow groups, respectively. Our finding of augmented gWAT mass supports our previous body composition data, and is significant due to the classification of gWAT as visceral fat. This suggests that the DKO mice are obese and are susceptible to CVD and MetS.

Expansion of adipose tissue mass can occur by two processes: hyperplasia, the increase of mature adipocyte cell number, or by adipose hypertrophy, the enlargement of adipocyte cellular volume. During periods of positive caloric imbalance, adipocyte hypertrophy is believed to be the main contributor of augmented adipose tissue mass. In fact, for some time it was believed that adipocyte cell number in adults was fixed. However, recent publications have proven this theory wrong. Using C¹⁴ tracing, Spalding et al. were able to demonstrate that 50% of adipocytes turnover every 8 years. As a result, the generation of new adipocytes is constantly occurring to replace this loss (Spalding et al., 2008). Primarily carried out as a means of cell replacement, this process can be accelerated during times of increased adipocyte turnover and is believed to be highly regulated (Sun et al., 2011).

Meanwhile, the role of adipocyte hypertrophy in metabolic and cardiovascular complications has recently garnered interest as it has been independently correlated with hypertension, dyslipidemia, serum insulin levels, IR, and type 2 diabetes (Arner et al., 2010; Bays et al., 2008). In fact, obese individuals with enlarged adipocytes have been reported to be more hyperinsulinemic and glucose intolerant than similarly obese patients with normal adipocyte size (Arner et al., 2010). It has also been reported that excessive

hypertrophy can cause adipocyte dysfunction which contributes to MetS and CVD(Bays et al., 2008).

To determine if adipocyte hypertrophy was the source for the increased adipocyte mass within our DKO mice, histological evaluation of adipocyte area within gWAT was performed. Our investigation revealed a clear and significant phenotype. As depicted in **Figure 12**, male and female DKO adipocyte cell area is drastically larger than adipocytes from ApoE^{-/-} equivalents. This data supports our earlier observations of increased gWAT mass and provides evidence that the increased visceral fat mass can at least partially be explained by adipocyte hypertrophy. This is noteworthy since hypertrophy is tightly correlated with CVD and MetS as previously discussed. Therefore, it can be concluded that the DKO mice are at greater risk of developing MetS and CVD because of their hypertrophic adipocytes.

Adipocytes from visceral fat have been reported to be more lipolytically active than adipocytes from other fat pads and are closely linked with the deregulation of adiponectin, resistin, and leptin in obese individuals(Bjorndal et al., 2011). In light of this, we decided to examine the plasma levels of these adipokines (**Figure 13**). Analysis of plasma leptin levels within male DKO mice revealed a statistically significant distinction in the male high fat groups and a similar albeit non-significant trend in the normal chow groups (p-value=0.0665). Quantification of this phenotype revealed an 86% and 101% increase in DKO leptin levels among the normal and high fat chow groups, respectively, when compared to ApoE^{-/-} counterparts. These findings are noteworthy for several reasons. Leptin is a powerful long-term appetite suppressant whose circulating levels are directly correlated with WAT mass. In fact, two of the most

widely used murine models of obesity contain a mutation to the leptin gene (ob/ob mice) or its receptor (db/db mice) demonstrating the importance of leptin in metabolic homeostasis(Ahima & Flier, 2000). Logically, because of its therapeutic potential, independent researchers have examined leptin treatment in mice. Two seminal papers were published in Science in 1995; both reporting that daily intraperitoneal administration of recombinant leptin led to reduced body weight and food consumption and improved murine energetics. Furthermore, the treatment of wildtype mice with leptin resulted in sustained weight loss(Maffei et al., 1995; Pelleymounter et al., 1995). Possibly the most significant finding from these papers was that leptin administration in mice resulted in a loss of adipose tissue mass independent of lean muscle mass loss. This was critical since it opened the door for researchers to begin examining leptin as a potential therapeutic in human obesity(Halaas et al., 1997; Harris et al., 1998). When researchers began work in humans, they found that while the administration of leptin to obese individuals who suffer from rare mutations in the leptin gene proved fruitful, the treatment of generally obese individuals with leptin was ineffective(Farooqi et al., 1999; Heymsfield et al., 1999). Researchers determined that this lack of efficacy can primarily be attributed to the development of leptin resistance or the biological loss of leptin's efficacy. This idea explains why several studies have shown that leptin levels are augmented in obesity, a seemingly contradictory finding(Considine et al., 1996; Mahabir et al., 2007; Monteleone et al., 2002). Leptin resistance is believed to develop after prolonged elevation like that seen in obesity, which eventually results in downstream desensitization to the signal. These scientific findings taken in conjunction with the elevated leptin levels in the DKO mice amidst increases in body weight suggest that the

DKO mice are leptin resistant. Furthermore, it has been reported that circulating levels of leptin are directly correlated to WAT mass(Ahima & Flier, 2000). Due to this, the finding of elevated leptin levels within the DKO mice further supports our previous finding that the DKO mice contain greater WAT mass.

Aside from the correlation between leptin and adiposity, leptin has also been linked to IR. Four autonomous studies across varying human populations have shown that elevated leptin levels positively correspond with IR independent of adiposity(Esteghamati et al., 2009; Huang et al., 2004; Mente et al., 2010; Zuo et al., 2013). This suggests that further evaluation of glucose and insulin levels is warranted and the results from this investigation will be discussed later.

Next, we reviewed plasma resistin levels and found a statistically significant 70% increase among male DKO mice on high fat feed when compared to ApoE^{-/-} equivalents. Meanwhile, no difference was seen in the normal chow groups. This finding of elevated resistin within the DKO mice on high fat chow potentially has major implications on insulin-sensitivity in these animals. Discovered a little over a decade ago, resistin was first described by Stepan et al. in 2001. This seminal publication yielded several important findings: first, circulating resistin levels were augmented in both genetic- and diet-induced murine obesity models; second, the treatment of obese or insulin-resistant mouse models with anti-resistin antibodies resulted in improved insulin action; third, the administration of recombinant resistin in healthy animals leads to diminished glucose tolerance and insulin sensitivity; and finally, resistin reduces insulin-induced glucose uptake in adipocytes(Stepan et al., 2001). Taken together, these findings clearly show that resistin is integral in mediating the actions of insulin. In addition to these murine

results, studies in humans have cited increased circulating levels of resistin in diabetic and obese patients. Furthermore, these studies have shown that resistin levels are correlated with CVD in patients with MetS(Gerber et al., 2005; Reilly et al., 2005; Steppan et al., 2001). Taking into account these findings, as well as the augmented plasma resistin levels within the DKO model, suggests that the DKO mice are in fact obese and are predisposed to IR and MetS.

The final adipokine we reviewed was adiponectin. First reported in 1995, adiponectin is exclusively produced by white adipose tissue and secreted into the circulation at abundant levels (mg/mL)(Chandran et al., 2003; Lihn et al., 2005). The primary function of adiponectin appears to be the inhibition of hepatic glucose production and the augmentation of peripheral insulin sensitivity. As such, the murine administration of adiponectin has been found to lower glucose levels. Importantly, this reduction in blood glucose was independent of circulating insulin levels and also observed in mice incapable of insulin secretion, thus suggesting that that the primary action of adiponectin is facilitating insulin sensitivity and not its secretion(Lihn et al., 2005). Due to this, it can be concluded that adiponectin most likely plays a critical role in the development of metabolic diseases. In fact, its levels have been shown to be reduced in metabolic diseases associated with IR in obesity, type 2 diabetes, fatty liver disease, and MetS. Furthermore, BMI and visceral adiposity have been shown to be inversely related to adiponectin expression. In accordance with this, adiponectin mRNA levels have been found to be lower in the adipocytes of obese people in comparison to lean individuals. It is also worth noting that adiponectin levels appear to be reduced prior to the development of IR indicating that it may be a root cause and not simply a symptom of IR. In review

of these findings by the scientific community we anticipated lower levels of adiponectin in the DKO mice. However, we did not find any significant discrepancy in adiponectin levels among the mice.

MiR-155 and Glucose/Insulin Expression

Since we witnessed the presence of excess visceral adipose tissue and the deregulation of particular adipokines like resistin and leptin, we felt it prudent to further investigate plasma glucose and insulin levels. One of the hallmarks of IR is the presence of elevated insulin levels like that typically seen in obese, diabetic, and MetS afflicted individuals. In fact, we also found significantly augmented levels of insulin in the overweight DKO mice accounting for a 181% and 148% increase in normal and high fat chow groups, respectively, when compared to ApoE^{-/-} counterparts. Observing hyperinsulinemia within fed mice is significant since its manifestation is typically only seen in fasted mice demonstrating the robustness of this phenotype. Also noteworthy is the fact that hyperinsulinemia is seen in both diet groups. In fact, insulin levels between dietary groups were comparable for both ApoE^{-/-} and DKO mice. This implies that added dietary stress is not required for, nor does it augment hyperinsulinemia in these mice. These findings indicate that our DKO mice are insulin-resistant and may be susceptible to glucose deregulation and diabetes development.

Since we found hyperinsulinemia, we next decided to assess fed and fasted glucose levels in male and female mice. In general and as expected, we found elevated blood glucose levels in the high fat feed groups when compared to normal chow groups for both fed and fasted male and female mice. Furthermore, as anticipated, we observed reduced blood glucose levels in the fasted mice in comparison to the fed mice. However,

we found no significant differences in blood glucose levels between ApoE^{-/-} and DKO mice despite the hyperinsulinemia (**Figure 15**). For more in depth analysis, we performed glucose and insulin tolerance tests in hopes of seeing a phenotype. However, again we found no discernible difference between ApoE^{-/-} and DKO mice in either gender or diet group (**Figure 16 and Figure 17**). Even though we did not see a difference in blood glucose levels this is not a contradictory result to the hyperinsulinemia. As peripheral insulin insensitivity develops, a robust and persistent response from β -cells occurs resulting in augmented hepatic insulin secretion. This elevated output compensates for the IR and results in hyperinsulinemia. In particular instances, this augmented β -cell function is able to fully compensate for the IR resulting in euglycaemia amidst hyperinsulinemia(Rees & Alcolado, 2005). We believe that this is the case in our murine model.

MiR-155 and NAFLD

As discussed in the introduction, NAFLD is a clinical condition hallmarked by the abnormal accumulation of triglycerides within the liver and is often considered a hepatic manifestation of MetS due to their tight affiliation. As such, we felt it was prudent to evaluate the hepatic condition of the DKO mice. The data we collected clearly demonstrates that miR-155 plays a role in the development of NAFLD. As depicted in **Figure 19**, the morphology of hepatic tissue from male and female DKO mice fed with high fat chow is different than their ApoE^{-/-} equivalents. Specifically, widespread hepatic accumulation of triglycerides is seen in the DKO mice. We believe that this steatosis may be the cause for the distinction in hepatic pigmentation between ApoE^{-/-} and DKO mice. Livers excised from DKO mice on high fat diets were more pale and whitish in

color than their deeply crimson-pigmented counterparts from ApoE^{-/-} mice. Furthermore, when we evaluated hepatic weight we found a statistically significant 40% increase in hepatic mass in DKO mice on high fat diet when compared to ApoE^{-/-} equivalents, while no difference in normal chow groups was noted. The same trend was witnessed in female mice where a 16% increase in hepatic weight within DKO mice on high fat chow was detected and no difference in normal chow groups was seen. This liver mass data is in accordance with our reports of triglyceride accumulation within the livers of high fat fed DKO mice.

Review of recently published data by the scientific community provided further evidence which substantiates our findings. Hepatic miRNAs profiling studies have reported shifted miRNAs expressions in murine and human steatohepatitis suggesting a critical role of miRNAs in the disease pathogenesis. Among these differentially expressed miRNAs was miR-155(Pogribny et al., 2010; B. Wang et al., 2009). The hepatic expression of miR-155 has been reported to be modest in 8 week old wildtype mice when measured against other tissue such as WAT, lung, kidney, muscle, heart, and spleen. However, this hepatic expression could be dramatically augmented when wildtype mice were put on a high fat diet for 24 weeks. It has also been reported that hepatic miR-155 expression is elevated in ob/ob mice on normal chow when evaluated against wildtype mice suggesting that hepatic miR-155 expression is elevated during conditions of obesity and hyperlipidemia which would be the case in an ApoE-deficient background like in the DKO mice(Miller et al., 2013).

Our other hepatic findings in regard to weight augmentation and color distinction have similarly been reported elsewhere. Miller et al. reported an increase in hepatic

weight in miR-155^{-/-} mice on normal or high fat chow when compared to wildtype equivalents as well as a change in liver coloration (Miller et al., 2013). It should be noted that we did not see these effects in our normal chow groups like Miller et al. Overall, our data and that of the scientific community indicate a critical role of miR-155 in NAFLD development.

MiR-155 and Plasma Lipid Expression

The two lipid criteria of MetS are elevated plasma triglycerides and diminished HDL levels. To address this, blood was drawn from male mice and plasma isolated for triglyceride and HDL quantification. We found no distinction in triglyceride levels between ApoE^{-/-} and DKO mice and no discrepancies between the normal and high fat chow groups (**Figure 20**). This result was somewhat surprising in light of the accumulated triglycerides within the liver as well as the adipocyte hypertrophy. It is plausible that the ectopic accumulation of triglycerides within peripheral tissue, the liver, and WAT has resulted in normal circulating triglyceride levels. Furthermore, the observation of unwavering triglyceride levels has also been reported by other members of the scientific community. Donners et al. reported no discernable difference in triglyceride levels between wildtype and hematopoietic miR-155-deficient mice on high cholesterol diet (Donners et al., 2012).

The assessment of HDL levels also revealed no significant difference among ApoE^{-/-} and DKO mice on normal chow but an elevation in HDL levels among DKO mice on high fat diet. Again, this result was unanticipated as we hypothesized that HDL levels may be diminished in the DKO mice. To further understand this result we reviewed published data for relevant findings. We found that no difference in HDL levels

between hematopoietic miR-155-deficient and wildtype mice following 10 weeks of high cholesterol diet had been previously reported (Donners et al., 2012). This finding was also substantiated by another group among ApoE^{-/-} mice and ApoE^{-/-} mice with miR-155 hematopoietic deficiency (Nazari-Jahantigh et al., 2012).

In response to these findings we selectively investigated LDL, total cholesterol, and non-esterified fatty acids within the high fat groups to observe if miR-155 had any effect on other common plasma lipids (Data not shown). Again, we found no distinction between ApoE^{-/-} and DKO mice for any of these parameters. These findings were partially confirmed by published results from both Donners and Nazari-Jahantigh using the murine models described above. Both manuscripts found no statistical difference in LDL and total cholesterol (Donners et al., 2012; Nazari-Jahantigh et al., 2012). In addition, these groups also reported no disparity in VLDL levels which we did not investigate. Overall, our data and that of independently published groups suggest that miR-155 has little to no effect on the plasma lipid expression.

MiR-155 and Hypertension

Hypertension is a multifaceted disease which arises from a combination of genetic and environment factors. Angiotensin II is a particular important factor in regulating blood pressure, acting as a potent vasoconstrictor. The majority of the physiological effects associated with angiotensin II are mediated through its receptor, angiotensin II type 1 receptor (AT1R). A polymorphism involving an A to C transversion at position 1166 in human AT1R has long been associated with cardiovascular complications and hypertension. Investigations into why this polymorphism leads to hypertension had previously been fruitless as the polymorphism occurred in the 3'UTR and not the protein

coding region of the AT1R gene. With the discovery of miRNAs and their known targeting within the 3'UTR, researchers began to examine the possibility that this polymorphism was either positively or negatively impacting a miRNAs binding site. *In silico* evaluation of the proximal region to the polymorphism revealed a miR-155 binding site. When the 1166 position contains the A-allele, miR-155 is capable of interacting with the 3'UTR of AT1R and suppressing its expression; however, if the C-allele is present this interaction is compromised and miR-155 can no longer mitigate AT1R protein expression. As a result AT1R expression is augmented, leading to higher blood pressure. Since AT1R expression is positively correlated with blood pressure, it is believed that the loss of miR-155 binding is the root cause for the hypertension associated with the A1166C polymorphism(Ceolotto et al., 2011). These molecular interactions and there effects on blood pressure are summarized in **Figure 27**.

Aside from the A1166C polymorphism, it has also been reported by several independent sources that miR-155 expression is diminished in hypertensive patients and mice, further strengthening the argument of miR-155 in blood pressure regulation(Blanco et al., 2012; Ceolotto et al., 2011; Xu et al., 2008). Moreover, evidence of miR-155 in blood pressure regulation has been gathered from twins discordant for chromosome 21 trisomy. In these cases, the twin afflicted with this trisomy typically has lower blood pressure than their counterpart. Since the BIC gene which encodes for miR-155 is located on chromosome 21, it was hypothesized that trisomy of chromosome 21 results in overproduction of miR-155 which leads to diminished blood pressure. In fact, miR-155 expression has been found to be significantly elevated in the trisomic twin and AT1R protein levels were found to be diminished by approximately 30%. Taken together, this

data provides strong evidence that miR-155 plays a vital role in blood pressure regulation within humans. However, further verification of miR-155's ability to mitigate AT1R expression in mice has yet to be completed. This is due to the lack of conservation of the miR-155 binding site within the 3'UTR of the AT1R gene in mice(Sethupathy et al., 2007). For this reason, we did not evaluate blood pressure within the DKO mouse model. However, we feel that it is reasonable to extrapolate that the DKO mice would show signs of elevated blood pressure if the miR-155 site was conserved.

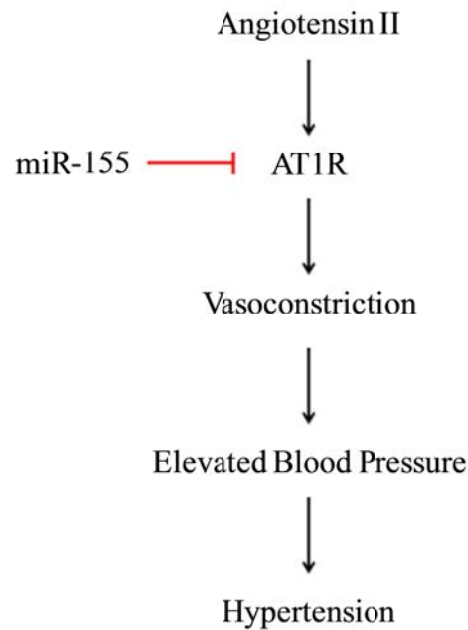


Figure 27: Molecular mechanism of miR-155 regulation of hypertension

Molecular Mechanism and Working Model

Thus far, we have seen several phenotypic distinctions in the DKO mice. However, we have not identified a specific molecular target of miR-155 which explains these findings. To do this, we reviewed the 140 experimentally verified targets of miR-155 and identified several possible prospects. Specifically, we focused on targets which played integral roles in adipogenesis, adipocyte hypertrophy, IR, and NALFD. One target was of particular interest. As discussed in the introduction, C/EBP- β is a member of the C/EBP family which are transcription factors that are critical in energy metabolism, adipogenesis, inflammation, immunity, cell differentiation and proliferation (Tsukada et al., 2011). As such, we felt further investigation of C/EBP- β was warranted so we evaluated the hepatic and WAT mRNAs expression of C/EBP- β . Within the livers of DKO mice fed normal or high fat chow, we found significantly increased levels of C/EBP- β mRNAs (**Figure 21B, E**). This difference equated to an approximate 3.5-fold increase in both diet groups when normalized by ApoE^{-/-} equivalents. A similar trend was observed in gWAT with the same 3.5-fold increase in both fed groups (**Figure 22B, E**). However, due to higher variability among samples this distinction did not reach statistical significance.

Due to the changes in C/EBP- β expression, we felt it prudent to also examine the two critical adipogenic transcription factors, C/EBP- α and PPAR- γ , which are activated by C/EBP- β . We found significantly elevated levels of C/EBP- α in the livers of DKO mice receiving a normal chow diet, while no difference was seen in the high fat chow groups (**Figure 21A, D**). Further evaluation of C/EBP- α within gWAT revealed an approximate 4-fold and 6-fold increase in normal and high fat diet mice, respectively

(Figure 22A, D). Meanwhile, we witnessed statistically significant augmentation in PPAR- γ within DKO livers equating to an approximate 4.5-fold and 2-fold increase among normal and high fat diet groups, respectively **(Figure 21C, F)**. This same trend was witnessed in gWAT where an approximate 3-fold and 2-fold increase was witnessed **(Figure 22C, F)**.

These findings are significant as it explains the WAT expansion in the DKO mice. As outlined in the introduction, C/EBP- α , C/EBP- β , and PPAR- γ are transcription factors which are known to be integral in adipogenesis, promoting adipocyte fatty acid uptake, and adipocyte differentiation. Therefore, their elevated expression would be pertinent to our observation of augmented DKO mouse mass. A summary of these molecular interactions and how they contribute to the DKO mouse obesity phenotype is summarized in **Figure 28**. Furthermore, we believe that the augmentation in WAT as a result of these factors also explains the manifestation of hyperinsulinemia in the DKO mice. With an increase adipose mass a corresponding augmentation in adipokine production occurs. As such, elevated adipokine secretion like with resistin would result in peripheral insulin insensitivity and the development of IR. Again, we summarized these interactions and how they lead to hyperinsulinemia in **Figure 29**.

The augmented hepatic expressions of C/EBP- α , C/EBP- β , and PPAR- γ can also explain the development of NAFLD in the DKO mice. The hepatic expressions of both C/EBP- α and C/EBP- β have been reported to be increased in aged mice which are susceptible to NAFLD. Mechanistically, the promoters of several important triglyceride synthetic enzymes contain high affinity C/EBP binding elements. Specifically, two of these enzymes, DGAT1 and DGAT2, are important modulators of energy metabolism and

have been shown to be key signaling molecules in hepatic steatosis development. Experiments carried out in transgenic mice with over-expression of either DGAT enzyme led to TG accumulation of cytosolic lipid droplets in the liver. Furthermore, knockdown of DGAT2 with oligonucleotides was shown to mitigate hepatic steatosis in obese mice(Jin et al., 2013). Meanwhile, PPAR- γ hepatic expression has been found to be induced in mice fed a high fat diet (Ables, 2012; Kallwitz et al., 2008). Reported independently by two groups, the liver-specific deletion of PPAR- γ results in protection from steatosis and thus is involved in liver triglyceride accumulation(Gavrilova et al., 2003; Matsusue et al., 2003). In agreement with this, it has also been reported that PPAR- γ over-expression within the liver results in susceptibility to steatosis(Ables, 2012). Based on these results, our witnessed increase in hepatic C/EBP- α , C/EBP- β , and PPAR- γ would be a driving force for the DKO liver steatosis. A working model summarizing these molecular interactions and how they affect NALFD development is shown in **Figure 30**.

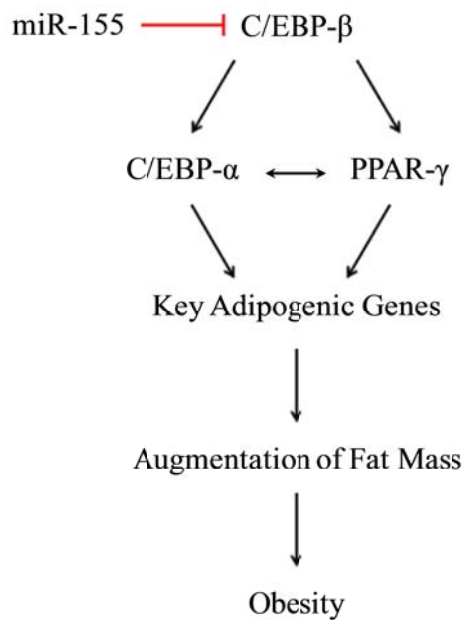


Figure 28: Molecular mechanism for fat mass augmentation in the DKO mice

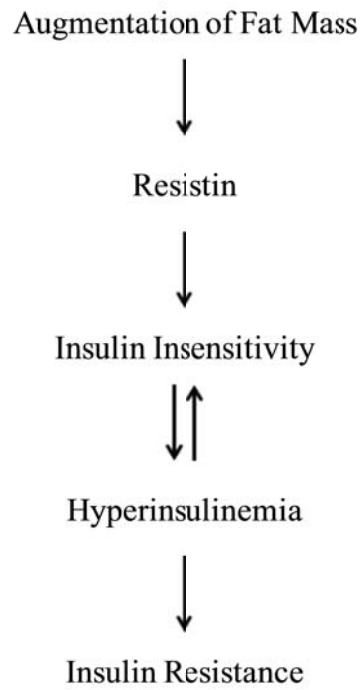


Figure 29: Molecular mechanism for IR in the DKO mice

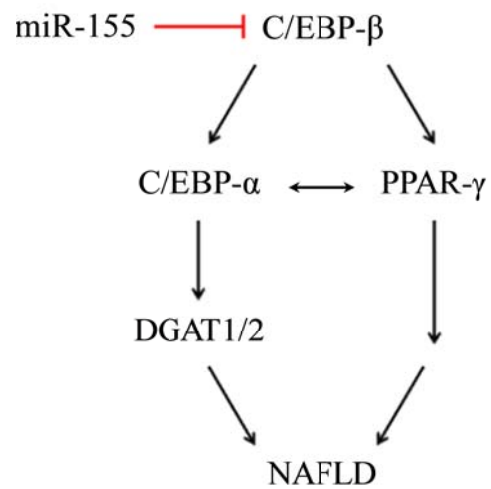


Figure 30: Molecular mechanism for NAFLD development in DKO mice

MiR-155 and Atherosclerosis

Even though we had finished gauging the role of miR-155 in the development of MetS components, we wanted to examine if the impact of miR-155 on MetS development also translated to an increase in CVD. Specifically, we evaluated atherosclerosis development. As discussed in the introduction, atherosclerosis is a complex inflammatory disease of the vasculature and is the underlying cause for most CVD events. In order to determine the role of miR-155 in atherosclerosis development as well as measure its relevancy against other miRNAs, we utilized a PCR array to screen 84 of the most abundant and well-characterized miRNAs in miRBase. We compared the aortic miRNAs expression profiles of ApoE^{-/-} mice fed with normal chow vs ApoE^{-/-} mice fed with high fat diet for 12 weeks after maturation. Analysis of the array data revealed several miRNAs that were differentially regulated including 7 miRNAs that were up-regulated by at least 4-fold and 9 miRNAs down-regulated by at least 4-fold (**Figure 23**). Among the up-regulated miRNAs was miRNA-155. In fact, miR-155 was one of 4 miRNAs with a 10-fold or greater change in expression. This dramatic shift in miR-155 gave us confidence that it played a critical function in atherosclerosis and is one of the most important contributing miRNAs. We next confirmed our miR-155 screening results with qRT-PCR. We fed ApoE^{-/-} mice with high fat for 0 weeks, 3 weeks, 6 weeks, and 12 weeks to examine when this augmentation in expression occurred. We found that the aortic expression of miR-155 was indeed increased in ApoE^{-/-} mice on high fat chow compared to the mice with 0 weeks high fat feeding (**Figure 24**). A statistically significant 2-fold increase in miR-155 expression was observed after 3 weeks of high fat

diet which continued to increase with duration of feeding to approximately 6-fold at 12 weeks.

Our findings of elevated aortic miR-155 expression during atherogenesis were substantiated by independently published data. Nazari-Jahantigh et al. reported augmented aortic miR-155 expression in ApoE^{-/-} mice following 12 and 40 weeks of high fat diet. In addition, they reported elevated miR-155 expression within the carotid artery of mice with partial ligation and subjected to 6 weeks high fat diet (Nazari-Jahantigh et al., 2012). Our and Nazari-Jahantigh's murine findings also appear to translate to humans as well. Raitoharju et al. completed human miRNAs expression profiling with various arterial beds and found the expressions of several miRNAs to be modulated. Specifically, miR-155 expression was up-regulated in the femoral artery and aorta of patients with atherosclerosis when compared to health patients (Raitoharju et al., 2011). In a second study, the levels of miR-155 were found to be elevated in human carotid artery plaques when compared with non-plaque areas of the vessel wall (Nazari-Jahantigh et al., 2012). These data and our findings definitively demonstrate that miR-155 expression is increased in mice and humans during atherogenesis, indicating a pertinent role of miR-155 in atherosclerosis.

Thus far, the scientific community has provided two conflicting reports on the role of miR-155 in atherosclerosis, one citing miR-155 as pro-atherogenic and the other anti-atherogenic. The first paper, authored by Donners et al., reported that hematopoietic miR-155-deficiency in LDL^{-/-} mice resulted in larger aortic root lesion areas than in LDL^{-/-} mice receiving wildtype bone marrow. Furthermore, the plaques in the hematopoietic miR-155^{-/-} mice were characterized as more advanced in composition than in the control

mice. The authors of this manuscript mainly attributed this augmentation in atherosclerosis development to an increase in pro-inflammatory cell infiltration into atherosclerotic plaques (Donners et al., 2012).

The second paper examining the effects of miR-155 in atherosclerosis, published by Nazari-Jahantigh et al., reported a pro-atherogenic effect of miR-155. In this study, wildtype and miR-155^{-/-} bone marrow was transplanted into ApoE^{-/-} mice to examine hematopoietic contributions in atherosclerosis. Mechanistically, it was reported that miR-155 played an important role in promoting pro-inflammatory macrophage response through direct repression of B-cell lymphoma 6 (BCL6), a transcription factor known to repress NF-κB signaling. It was proposed that the loss of miR-155 expression led to the witnessed elevation in BCL6 expression and as a result led to the observed reduction in MCP-1. In turn, the diminished MCP-1 expression was cited as the cause for the observed reduction in macrophage recruitment to atherosclerosis lesions and the reduction in lesion size (Nazari-Jahantigh et al., 2012).

Even though the studies conducted by Donners and Nazari-Jahantigh both utilized bone marrow transplant techniques to examine the role of hematopoietic contributions to atherosclerosis, they both reported conflicting effects of miR-155 on atherosclerosis development. We can speculate that this discrepancy might be the result of transplantations into two different murine backgrounds, ApoE^{-/-} versus LDL^{-/-}. Furthermore, Donners et al. observed differences in neutrophil recruitment which is more significant in early lesion development while Nazari-Jahantigh's group focused on monocyte recruitment which is more important in advanced atherosclerosis development. Due to the conflicting reports within the scientific community, we felt that atherosclerosis

assessment within our model would provide useful and significant insight into the topic. In addition, we felt that our global knockout model would provide novel perspective as it would take into account contributions by the vasculature as well.

Investigation of atherosclerosis within the DKO model yielded some interesting results. At 8 weeks of age male mice were fed with high fat diet for 0 weeks, 3 weeks, 6 weeks, or 12 weeks at which point aortas were excised for *en face* analysis (**Figure 25**). Expectantly, we observed virtually no plaque formation in the 0 week mice and very minimal plaque development after 3 weeks with no discernible difference between ApoE^{-/-} and DKO mice. However, after 6 weeks of high fat feeding plaque formation was noticeable and a phenotype began to develop. We found DKO mice had 32% less aortic lesions, though this distinction was not statistically significant. Observation after 12 weeks of high fat diet resulted in statistically significant findings, translating to a 45% decrease in lesion area in DKO mice in comparison to their ApoE^{-/-} equivalents. We then confirmed this 12 week high fat data by examining atherosclerotic plaque development within the aortic root. Again, we observed a significant statistical difference in plaque area between ApoE^{-/-} and DKO mice. These findings strongly indicate that miR-155 is pro-atherogenic in nature, aligning our data with that published by Nazari-Jahatigh et al.

The atherosclerosis protection afforded the DKO mice was surprising in light of their obese nature. In-depth examination of literature focusing on miR-155 regulation of immune physiology provides further insight into its pro-atherogenic role. Several papers have been published which show that miR-155 expression is dramatically induced within activated B-cells, T-cells, macrophages, and dendritic cells indicating a functional role in these cells(Faraoni et al., 2009). In fact, miR-155 has been reported to be critical in

lymphocyte development and the inflammatory responses of B- and T-cells(O'Connell et al., 2010; Vigorito et al., 2007). Furthermore, the dendritic cells from miR-155^{-/-} mice have been reported to have impaired differentiation and antigen-presentation(Lu et al., 2011; Martinez-Nunez et al., 2009; Turner et al., 2011). In light of these findings, one can surmise that the reduction in atherosclerosis that we observed in the DKO mice might be due to these immune complications. If the DKO mice are unable to generate a typical inflammatory response then a decrease in atherosclerosis would be logical.

Conclusion

As we outlined in the introduction, MetS is a constellation of several metabolic conditions and is defined by the presence of 3 of the following 5 conditions: obesity, insulin resistance, hypertension, diminished HDL, or elevated triglycerides. The majority (61%) of individuals afflicted with MetS possess 3 of these components while 29% present with 4 conditions and 10% with all 5 components(Paschos & Paletas, 2009). We have for the first time comprehensively evaluated the pertinence of miR-155 in the development of MetS. In review of our results and those by independent researchers, we feel that miR-155 should be considered a critical factor in mitigating the development of MetS. While the root cause for MetS has yet to be determined, obesity and IR are considered the cornerstones to MetS pathology(R. Kahn et al., 2005; Lann & LeRoith, 2007). Our data has shown that miR-155 impacts both of these components. Specifically, we found excessive weight gain in our DKO mice when put on a high caloric diet as a result of enlarged visceral adipose tissue deposits. We also observed elevated plasma insulin levels in the DKO mice, a hallmark of IR. Furthermore, the use of NAFLD as an identifier of MetS has recently been discussed. In light of this, we also

evaluated the impact of miR-155 on NAFLD and found hepatic steatosis leading to augmented hepatic weight and altered pigmentation. Our experimental observations in regard to obesity, IR, and NAFLD, along with the published data on hypertension, strongly support a role of miR-155 in the prevention of MetS. Finally, our investigation of atherosclerosis development in the DKO model revealed a pro-atherogenic role of miR-155. This phenotype can most likely be attributed to the multiple roles miR-155 plays in the development and activation of traditional immune cells like B-cells, T-cells, macrophages, and dendritic cells.

Future Directions

In response to our findings, further investigation into the role of miR-155 and MetS should be conducted. We suggest this be done in 3 ways: MetS component-specific mouse models, in-depth *in vitro* mechanism assessment, and *in vivo* therapy. The development of novel murine models would allow for further elucidation of the impact of miR-155 on individual MetS components. For example, the creation of a human transgenic AT1R mouse deficient for miR-155 would be extremely useful in confirming the role of miR-155 in blood pressure regulation. Also the development of a novel db/db mouse also deficient for miR-155 would allow for more in-depth observation of how miR-155 impacts glucose and insulin regulation within a traditional type II diabetic model which is susceptible to glucose deregulation unlike our ApoE^{-/-} background. This model would also be useful in assessing the impact of miR-155 on fat accumulation within a genetic obesity model opposed to our diet-induced obesity model. Aside from these mouse models, *in vitro* assessment of adipocytes in the presence of miR-155 mimics and inhibitors would allow us to confirm our findings and possibly provide a

more detailed understanding of the mechanisms associated with our phenotype. Finally, attempts at phenotypic rescue through the administration of miR-155 mimics and inhibitors would be helpful in assessing the therapeutic potential of miR-155.

REFERENCES CITED

- Ables, G. P. (2012). Update on ppargamma and nonalcoholic Fatty liver disease. *PPAR Res*, 2012, 912351. doi: 10.1155/2012/912351
- Ahima, R. S., & Flier, J. S. (2000). Leptin. [Research Support, Non-U.S. Gov't Research Support, U.S. Gov't, P.H.S. Review]. *Annu Rev Physiol*, 62, 413-437. doi: 10.1146/annurev.physiol.62.1.413
- Alba, L. M., & Lindor, K. (2003). Review article: Non-alcoholic fatty liver disease. [Review]. *Aliment Pharmacol Ther*, 17(8), 977-986.
- American Heart Association: About Metabolic Syndrome. (2014) Retrieved January 5th, 2014
- Arner, E., Westermark, P. O., Spalding, K. L., Britton, T., Ryden, M., Frisen, J., . . . Arner, P. (2010). Adipocyte turnover: relevance to human adipose tissue morphology. [Research Support, Non-U.S. Gov't]. *Diabetes*, 59(1), 105-109. doi: 10.2337/db09-0942
- Banerjee, R. R., Rangwala, S. M., Shapiro, J. S., Rich, A. S., Rhoades, B., Qi, Y., . . . Lazar, M. A. (2004). Regulation of fasted blood glucose by resistin. [Research Support, Non-U.S. Gov't Research Support, U.S. Gov't, P.H.S.]. *Science*, 303(5661), 1195-1198. doi: 10.1126/science.1092341
- Bays, H. E., Gonzalez-Campoy, J. M., Bray, G. A., Kitabchi, A. E., Bergman, D. A., Schorr, A. B., . . . Henry, R. R. (2008). Pathogenic potential of adipose tissue and metabolic consequences of adipocyte hypertrophy and increased visceral adiposity. [Review]. *Expert Rev Cardiovasc Ther*, 6(3), 343-368. doi: 10.1586/14779072.6.3.343
- Bhattacharyya, S. N., Habermacher, R., Martine, U., Closs, E. I., & Filipowicz, W. (2006). Relief of microRNA-mediated translational repression in human cells subjected to stress. *Cell*, 125(6), 1111-1124.
- Bjorndal, B., Burri, L., Staalesen, V., Skorve, J., & Berge, R. K. (2011). Different adipose depots: their role in the development of metabolic syndrome and mitochondrial response to hypolipidemic agents. *J Obes*, 2011, 490650. doi: 10.1155/2011/490650

- Blanco, R. R., Austin, H., Vest, R. N., 3rd, Valadri, R., Li, W., Lassegue, B., . . . Zafari, A. M. (2012). Angiotensin receptor type 1 single nucleotide polymorphism 1166A/C is associated with malignant arrhythmias and altered circulating miR-155 levels in patients with chronic heart failure. [Research Support, N.I.H., Extramural Research Support, Non-U.S. Gov't Research Support, U.S. Gov't, Non-P.H.S.]. *J Card Fail*, 18(9), 717-723. doi: 10.1016/j.cardfail.2012.06.531
- Brennecke, J., Hipfner, D. R., Stark, A., Russell, R. B., & Cohen, S. M. (2003). bantam encodes a developmentally regulated microRNA that controls cell proliferation and regulates the proapoptotic gene hid in *Drosophila*. *Cell*, 113(1), 25-36.
- Brennecke, J., Stark, A., Russell, R. B., & Cohen, S. M. (2005). Principles of microRNA-target recognition. *PLoS Biol*, 3(3), e85.
- Cannell, I. G., Kong, Y. W., & Bushell, M. (2008). How do microRNAs regulate gene expression? *Biochem Soc Trans*, 36(Pt 6), 1224-1231.
- Casteilla, L., Penicaud, L., Cousin, B., & Calise, D. (2008). Choosing an adipose tissue depot for sampling: factors in selection and depot specificity. *Methods Mol Biol*, 456, 23-38. doi: 10.1007/978-1-59745-245-8_2
- Centers for Disease Control and Prevention Website: About BMI for adults. (2014) Retrieved January 12th, 2014
- Centers for Disease Control and Prevention: Adult Obesity Facts. (2014) Retrieved January 8th, 2014
- Ceolotto, G., Papparella, I., Bortoluzzi, A., Strapazon, G., Ragazzo, F., Bratti, P., . . . Semplicini, A. (2011). Interplay between miR-155, AT1R A1166C polymorphism, and AT1R expression in young untreated hypertensives. [Multicenter Study]. *Am J Hypertens*, 24(2), 241-246. doi: 10.1038/ajh.2010.211
- Cerutti, L., Mian, N., & Bateman, A. (2000). Domains in gene silencing and cell differentiation proteins: the novel PAZ domain and redefinition of the Piwi domain. *Trends Biochem Sci*, 25(10), 481-482.
- Chandran, M., Phillips, S. A., Ciaraldi, T., & Henry, R. R. (2003). Adiponectin: more than just another fat cell hormone? [Research Support, Non-U.S. Gov't Research

Support, U.S. Gov't, Non-P.H.S. Research Support, U.S. Gov't, P.H.S. Review].
Diabetes Care, 26(8), 2442-2450.

Chen, X. (2004). A microRNA as a translational repressor of APETALA2 in Arabidopsis flower development. *Science*, 303(5666), 2022-2025.

Chendrimada, T. P., Finn, K. J., Ji, X., Baillat, D., Gregory, R. I., Liebhaber, S. A., . . . Shiekhattar, R. (2007). MicroRNA silencing through RISC recruitment of eIF6. *Nature*, 447(7146), 823-828.

Cimmino, A., Calin, G. A., Fabbri, M., Iorio, M. V., Ferracin, M., Shimizu, M., . . . Croce, C. M. (2005). miR-15 and miR-16 induce apoptosis by targeting BCL2. *Proc Natl Acad Sci U S A*, 102(39), 13944-13949.

Considine, R. V., Sinha, M. K., Heiman, M. L., Kriauciunas, A., Stephens, T. W., Nyce, M. R., . . . et al. (1996). Serum immunoreactive-leptin concentrations in normal-weight and obese humans. [Research Support, Non-U.S. Gov't Research Support, U.S. Gov't, P.H.S.]. *N Engl J Med*, 334(5), 292-295. doi: 10.1056/NEJM199602013340503

Corcoran, D. L., Georgiev, S., Mukherjee, N., Gottwein, E., Skalsky, R. L., Keene, J. D., & Ohler, U. PARalyzer: definition of RNA binding sites from PAR-CLIP short-read sequence data. *Genome Biol*, 12(8), R79.

Cordes, K. R., Sheehy, N. T., White, M. P., Berry, E. C., Morton, S. U., Muth, A. N., . . . Srivastava, D. (2009). miR-145 and miR-143 regulate smooth muscle cell fate and plasticity. *Nature*, 460(7256), 705-710.

Daugherty, A. (2002). Mouse models of atherosclerosis. [Review]. *Am J Med Sci*, 323(1), 3-10.

Daugherty, A., & Whitman, S. C. (2003). Quantification of atherosclerosis in mice. [Research Support, Non-U.S. Gov't Research Support, U.S. Gov't, P.H.S.]. *Methods Mol Biol*, 209, 293-309.

Ding, L., & Han, M. (2007). GW182 family proteins are crucial for microRNA-mediated gene silencing. *Trends Cell Biol*, 17(8), 411-416.

- Ding, X. C., & Grosshans, H. (2009). Repression of *C. elegans* microRNA targets at the initiation level of translation requires GW182 proteins. *Embo J*, 28(3), 213-222.
- Doench, J. G., & Sharp, P. A. (2004). Specificity of microRNA target selection in translational repression. *Genes Dev*, 18(5), 504-511.
- Donners, M. M., Wolfs, I. M., Stoger, L. J., van der Vorst, E. P., Pottgens, C. C., Heymans, S., . . . de Winther, M. P. (2012). Hematopoietic miR155 deficiency enhances atherosclerosis and decreases plaque stability in hyperlipidemic mice. [Research Support, Non-U.S. Gov't]. *PLoS One*, 7(4), e35877. doi: 10.1371/journal.pone.0035877
- Esteghamati, A., Khalilzadeh, O., Anvari, M., Rashidi, A., Mokhtari, M., & Nakhjavani, M. (2009). Association of serum leptin levels with homeostasis model assessment-estimated insulin resistance and metabolic syndrome: the key role of central obesity. *Metab Syndr Relat Disord*, 7(5), 447-452. doi: 10.1089/met.2008.0100
- Eulalio, A., Behm-Ansmant, I., Schweizer, D., & Izaurralde, E. (2007). P-body formation is a consequence, not the cause, of RNA-mediated gene silencing. *Mol Cell Biol*, 27(11), 3970-3981.
- Fabbrini, E., Sullivan, S., & Klein, S. (2010). Obesity and nonalcoholic fatty liver disease: biochemical, metabolic, and clinical implications. [Research Support, N.I.H., Extramural Review]. *Hepatology*, 51(2), 679-689. doi: 10.1002/hep.23280
- Faraoni, I., Antonetti, F. R., Cardone, J., & Bonmassar, E. (2009). miR-155 gene: a typical multifunctional microRNA. [Research Support, Non-U.S. Gov't Review]. *Biochim Biophys Acta*, 1792(6), 497-505. doi: 10.1016/j.bbadis.2009.02.013
- Farh, K. K., Grimson, A., Jan, C., Lewis, B. P., Johnston, W. K., Lim, L. P., . . . Bartel, D. P. (2005). The widespread impact of mammalian MicroRNAs on mRNA repression and evolution. *Science*, 310(5755), 1817-1821.
- Farooqi, I. S., Jebb, S. A., Langmack, G., Lawrence, E., Cheetham, C. H., Prentice, A. M., . . . O'Rahilly, S. (1999). Effects of recombinant leptin therapy in a child with congenital leptin deficiency. [Case Reports Research Support, Non-U.S. Gov't]. *N Engl J Med*, 341(12), 879-884. doi: 10.1056/NEJM199909163411204

- Frayn, K. N. (2000). Visceral fat and insulin resistance--causative or correlative? [Review]. *Br J Nutr*, 83 Suppl 1, S71-77.
- Galkina, E., & Ley, K. (2009). Immune and inflammatory mechanisms of atherosclerosis (*). [Research Support, N.I.H., Extramural Research Support, Non-U.S. Gov't Review]. *Annu Rev Immunol*, 27, 165-197. doi: 10.1146/annurev.immunol.021908.132620
- Gavrilova, O., Haluzik, M., Matsusue, K., Cutson, J. J., Johnson, L., Dietz, K. R., . . . Reitman, M. L. (2003). Liver peroxisome proliferator-activated receptor gamma contributes to hepatic steatosis, triglyceride clearance, and regulation of body fat mass. *J Biol Chem*, 278(36), 34268-34276. doi: 10.1074/jbc.M300043200
- Gavrilova, O., Marcus-Samuels, B., Graham, D., Kim, J. K., Shulman, G. I., Castle, A. L., . . . Reitman, M. L. (2000). Surgical implantation of adipose tissue reverses diabetes in lipoatrophic mice. *J Clin Invest*, 105(3), 271-278. doi: 10.1172/JCI7901
- Gerber, M., Boettner, A., Seidel, B., Lammert, A., Bar, J., Schuster, E., . . . Kratzsch, J. (2005). Serum resistin levels of obese and lean children and adolescents: biochemical analysis and clinical relevance. [Research Support, Non-U.S. Gov't]. *J Clin Endocrinol Metab*, 90(8), 4503-4509. doi: 10.1210/jc.2005-0437
- Global atlas on cardiovascular disease prevention and control. (2011). Geneva: World Health Organization.
- Global Status Report on Non-communicable Diseases 2010. (2011). Geneva: World Health Organization.
- Grimson, A., Farh, K. K., Johnston, W. K., Garrett-Engle, P., Lim, L. P., & Bartel, D. P. (2007). MicroRNA targeting specificity in mammals: determinants beyond seed pairing. *Mol Cell*, 27(1), 91-105.
- Grundy, S. M. (2004). Obesity, metabolic syndrome, and cardiovascular disease. [Review]. *J Clin Endocrinol Metab*, 89(6), 2595-2600. doi: 10.1210/jc.2004-0372
- Grundy, S. M., Brewer, H. B., Jr., Cleeman, J. I., Smith, S. C., Jr., & Lenfant, C. (2004). Definition of metabolic syndrome: Report of the National Heart, Lung, and Blood Institute/American Heart Association conference on scientific issues related to

definition. [Consensus Development Conference Review]. *Circulation*, 109(3), 433-438. doi: 10.1161/01.CIR.0000111245.75752.C6

Gu, S., Jin, L., Zhang, F., Sarnow, P., & Kay, M. A. (2009). Biological basis for restriction of microRNA targets to the 3' untranslated region in mammalian mRNAs. *Nat Struct Mol Biol*, 16(2), 144-150.

Guo, H. S., Xie, Q., Fei, J. F., & Chua, N. H. (2005). MicroRNA directs mRNA cleavage of the transcription factor NAC1 to downregulate auxin signals for arabidopsis lateral root development. *Plant Cell*, 17(5), 1376-1386.

Halaas, J. L., Boozer, C., Blair-West, J., Fidahusein, N., Denton, D. A., & Friedman, J. M. (1997). Physiological response to long-term peripheral and central leptin infusion in lean and obese mice. [Research Support, Non-U.S. Gov't Research Support, U.S. Gov't, P.H.S.]. *Proc Natl Acad Sci U S A*, 94(16), 8878-8883.

Hansson, G. K., & Hermansson, A. (2011). The immune system in atherosclerosis. [Research Support, Non-U.S. Gov't Review]. *Nat Immunol*, 12(3), 204-212. doi: 10.1038/ni.2001

Hansson, G. K., & Libby, P. (2006). The immune response in atherosclerosis: a double-edged sword. [Research Support, N.I.H., Extramural Research Support, Non-U.S. Gov't Review]. *Nat Rev Immunol*, 6(7), 508-519. doi: 10.1038/nri1882

Hansson, G. K., Robertson, A. K., & Soderberg-Naucler, C. (2006). Inflammation and atherosclerosis. [Research Support, N.I.H., Extramural Research Support, Non-U.S. Gov't Review]. *Annu Rev Pathol*, 1, 297-329. doi: 10.1146/annurev.pathol.1.110304.100100

Harris, R. B., Zhou, J., Redmann, S. M., Jr., Smagin, G. N., Smith, S. R., Rodgers, E., & Zachwieja, J. J. (1998). A leptin dose-response study in obese (ob/ob) and lean (+/?) mice. *Endocrinology*, 139(1), 8-19. doi: 10.1210/endo.139.1.5675

Hata, A. (2013). Functions of microRNAs in cardiovascular biology and disease. [Research Support, N.I.H., Extramural Research Support, Non-U.S. Gov't Review]. *Annu Rev Physiol*, 75, 69-93. doi: 10.1146/annurev-physiol-030212-183737

- Heymsfield, S. B., Greenberg, A. S., Fujioka, K., Dixon, R. M., Kushner, R., Hunt, T., . . . McCamish, M. (1999). Recombinant leptin for weight loss in obese and lean adults: a randomized, controlled, dose-escalation trial. [Clinical Trial Multicenter Study Randomized Controlled Trial Research Support, Non-U.S. Gov't Research Support, U.S. Gov't, P.H.S.]. *JAMA*, 282(16), 1568-1575.
- Huang, K. C., Lin, R. C., Kormas, N., Lee, L. T., Chen, C. Y., Gill, T. P., & Caterson, I. D. (2004). Plasma leptin is associated with insulin resistance independent of age, body mass index, fat mass, lipids, and pubertal development in nondiabetic adolescents. [Research Support, Non-U.S. Gov't]. *Int J Obes Relat Metab Disord*, 28(4), 470-475. doi: 10.1038/sj.ijo.0802531
- Ishibashi, S., Goldstein, J. L., Brown, M. S., Herz, J., & Burns, D. K. (1994). Massive xanthomatosis and atherosclerosis in cholesterol-fed low density lipoprotein receptor-negative mice. [Research Support, Non-U.S. Gov't Research Support, U.S. Gov't, P.H.S.]. *J Clin Invest*, 93(5), 1885-1893. doi: 10.1172/JCI117179
- Jamaluddin, M. S., Weakley, S. M., Yao, Q., & Chen, C. (2012). Resistin: functional roles and therapeutic considerations for cardiovascular disease. [Research Support, N.I.H., Extramural Review]. *Br J Pharmacol*, 165(3), 622-632. doi: 10.1111/j.1476-5381.2011.01369.x
- Jin, J., Iakova, P., Breaux, M., Sullivan, E., Jawanmardi, N., Chen, D., . . . Timchenko, N. A. (2013). Increased expression of enzymes of triglyceride synthesis is essential for the development of hepatic steatosis. [Research Support, N.I.H., Extramural]. *Cell Rep*, 3(3), 831-843. doi: 10.1016/j.celrep.2013.02.009
- Kahn, B. B., & Flier, J. S. (2000). Obesity and insulin resistance. [Research Support, Non-U.S. Gov't Research Support, U.S. Gov't, P.H.S. Review]. *J Clin Invest*, 106(4), 473-481. doi: 10.1172/JCI10842
- Kahn, R., Buse, J., Ferrannini, E., & Stern, M. (2005). The metabolic syndrome: time for a critical appraisal: joint statement from the American Diabetes Association and the European Association for the Study of Diabetes. [Review]. *Diabetes Care*, 28(9), 2289-2304.
- Kahn, S. E. (2003). The relative contributions of insulin resistance and beta-cell dysfunction to the pathophysiology of Type 2 diabetes. [Research Support, U.S. Gov't, Non-P.H.S. Research Support, U.S. Gov't, P.H.S. Review]. *Diabetologia*, 46(1), 3-19. doi: 10.1007/s00125-002-1009-0

- Kahn, S. E., Hull, R. L., & Utzschneider, K. M. (2006). Mechanisms linking obesity to insulin resistance and type 2 diabetes. [Research Support, N.I.H., Extramural Research Support, Non-U.S. Gov't Research Support, U.S. Gov't, Non-P.H.S. Review]. *Nature*, *444*(7121), 840-846. doi: 10.1038/nature05482
- Kallwitz, E. R., McLachlan, A., & Cotler, S. J. (2008). Role of peroxisome proliferators-activated receptors in the pathogenesis and treatment of nonalcoholic fatty liver disease. [Review]. *World J Gastroenterol*, *14*(1), 22-28.
- Kim, J., Krichevsky, A., Grad, Y., Hayes, G. D., Kosik, K. S., Church, G. M., & Ruvkun, G. (2004). Identification of many microRNAs that copurify with polyribosomes in mammalian neurons. *Proc Natl Acad Sci U S A*, *101*(1), 360-365.
- Kim, V. N. (2005). MicroRNA biogenesis: coordinated cropping and dicing. *Nat Rev Mol Cell Biol*, *6*(5), 376-385.
- Kiriakidou, M., Tan, G. S., Lamprinaki, S., De Planell-Saguer, M., Nelson, P. T., & Mourelatos, Z. (2007). An mRNA m7G cap binding-like motif within human Ago2 represses translation. *Cell*, *129*(6), 1141-1151.
- Kong, Y. W., Cannell, I. G., de Moor, C. H., Hill, K., Garside, P. G., Hamilton, T. L., . . . Bushell, M. (2008). The mechanism of micro-RNA-mediated translation repression is determined by the promoter of the target gene. *Proc Natl Acad Sci U S A*, *105*(26), 8866-8871.
- Krek, A., Grun, D., Poy, M. N., Wolf, R., Rosenberg, L., Epstein, E. J., . . . Rajewsky, N. (2005). Combinatorial microRNA target predictions. *Nat Genet*, *37*(5), 495-500.
- Lai, E. C., Tam, B., & Rubin, G. M. (2005). Pervasive regulation of Drosophila Notch target genes by GY-box-, Brd-box-, and K-box-class microRNAs. *Genes Dev*, *19*(9), 1067-1080.
- Lann, D., & LeRoith, D. (2007). Insulin resistance as the underlying cause for the metabolic syndrome. [Review]. *Med Clin North Am*, *91*(6), 1063-1077, viii. doi: 10.1016/j.mcna.2007.06.012
- Lee, R. C., Feinbaum, R. L., & Ambros, V. (1993). The C. elegans heterochronic gene lin-4 encodes small RNAs with antisense complementarity to lin-14. *Cell*, *75*(5), 843-854.

- Lee, Y., Jeon, K., Lee, J. T., Kim, S., & Kim, V. N. (2002). MicroRNA maturation: stepwise processing and subcellular localization. *Embo J*, *21*(17), 4663-4670.
- Lewis, B. P., Burge, C. B., & Bartel, D. P. (2005). Conserved seed pairing, often flanked by adenosines, indicates that thousands of human genes are microRNA targets. *Cell*, *120*(1), 15-20.
- Lewis, B. P., Shih, I. H., Jones-Rhoades, M. W., Bartel, D. P., & Burge, C. B. (2003). Prediction of mammalian microRNA targets. *Cell*, *115*(7), 787-798.
- Li, Y., Qiu, C., Tu, J., Geng, B., Yang, J., Jiang, T., & Cui, Q. (2014). HMDD v2.0: a database for experimentally supported human microRNA and disease associations. [Research Support, Non-U.S. Gov't]. *Nucleic Acids Res*, *42*(Database issue), D1070-1074. doi: 10.1093/nar/gkt1023
- Lihn, A. S., Pedersen, S. B., & Richelsen, B. (2005). Adiponectin: action, regulation and association to insulin sensitivity. [Research Support, Non-U.S. Gov't Review]. *Obes Rev*, *6*(1), 13-21. doi: 10.1111/j.1467-789X.2005.00159.x
- Lim, L. P., Lau, N. C., Garrett-Engele, P., Grimson, A., Schelter, J. M., Castle, J., . . . Johnson, J. M. (2005). Microarray analysis shows that some microRNAs downregulate large numbers of target mRNAs. *Nature*, *433*(7027), 769-773.
- Lin, F. T., & Lane, M. D. (1994). CCAAT/enhancer binding protein alpha is sufficient to initiate the 3T3-L1 adipocyte differentiation program. [In Vitro Research Support, Non-U.S. Gov't Research Support, U.S. Gov't, P.H.S.]. *Proc Natl Acad Sci U S A*, *91*(19), 8757-8761.
- Lingel, A., Simon, B., Izaurralde, E., & Sattler, M. (2003). Structure and nucleic-acid binding of the Drosophila Argonaute 2 PAZ domain. *Nature*, *426*(6965), 465-469.
- Liu, J., Carmell, M. A., Rivas, F. V., Marsden, C. G., Thomson, J. M., Song, J. J., . . . Hannon, G. J. (2004). Argonaute2 is the catalytic engine of mammalian RNAi. *Science*, *305*(5689), 1437-1441.
- Lowe, C. E., O'Rahilly, S., & Rochford, J. J. (2011). Adipogenesis at a glance. [Research Support, Non-U.S. Gov't Review]. *J Cell Sci*, *124*(Pt 16), 2681-2686. doi: 10.1242/jcs.079699

- Lu, C., Huang, X., Zhang, X., Roensch, K., Cao, Q., Nakayama, K. I., . . . Zhou, X. (2011). miR-221 and miR-155 regulate human dendritic cell development, apoptosis, and IL-12 production through targeting of p27kip1, KPC1, and SOCS-1. [Research Support, Non-U.S. Gov't]. *Blood*, *117*(16), 4293-4303. doi: 10.1182/blood-2010-12-322503
- Ma, J. B., Ye, K., & Patel, D. J. (2004). Structural basis for overhang-specific small interfering RNA recognition by the PAZ domain. *Nature*, *429*(6989), 318-322.
- Ma, J. B., Yuan, Y. R., Meister, G., Pei, Y., Tuschl, T., & Patel, D. J. (2005). Structural basis for 5'-end-specific recognition of guide RNA by the *A. fulgidus* Piwi protein. *Nature*, *434*(7033), 666-670.
- Maffei, M., Halaas, J., Ravussin, E., Pratley, R. E., Lee, G. H., Zhang, Y., . . . et al. (1995). Leptin levels in human and rodent: measurement of plasma leptin and ob RNA in obese and weight-reduced subjects. [Comparative Study Research Support, Non-U.S. Gov't Research Support, U.S. Gov't, P.H.S.]. *Nat Med*, *1*(11), 1155-1161.
- Mahabir, S., Baer, D., Johnson, L. L., Roth, M., Campbell, W., Clevidence, B., & Taylor, P. R. (2007). Body Mass Index, percent body fat, and regional body fat distribution in relation to leptin concentrations in healthy, non-smoking postmenopausal women in a feeding study. [Randomized Controlled Trial Research Support, Non-U.S. Gov't]. *Nutr J*, *6*, 3. doi: 10.1186/1475-2891-6-3
- Mahley, R. W. (1988). Apolipoprotein E: cholesterol transport protein with expanding role in cell biology. [Review]. *Science*, *240*(4852), 622-630.
- Mallory, A. C., Reinhart, B. J., Jones-Rhoades, M. W., Tang, G., Zamore, P. D., Barton, M. K., & Bartel, D. P. (2004). MicroRNA control of PHABULOSA in leaf development: importance of pairing to the microRNA 5' region. *Embo J*, *23*(16), 3356-3364.
- Marchesini, G., Bugianesi, E., Forlani, G., Cerrelli, F., Lenzi, M., Manini, R., . . . Rizzetto, M. (2003). Nonalcoholic fatty liver, steatohepatitis, and the metabolic syndrome. [Research Support, Non-U.S. Gov't]. *Hepatology*, *37*(4), 917-923. doi: 10.1053/jhep.2003.50161

- Maroney, P. A., Yu, Y., Fisher, J., & Nilsen, T. W. (2006). Evidence that microRNAs are associated with translating messenger RNAs in human cells. *Nat Struct Mol Biol*, *13*(12), 1102-1107.
- Martinez-Nunez, R. T., Louafi, F., Friedmann, P. S., & Sanchez-Elsner, T. (2009). MicroRNA-155 modulates the pathogen binding ability of dendritic cells (DCs) by down-regulation of DC-specific intercellular adhesion molecule-3 grabbing non-integrin (DC-SIGN). [Research Support, Non-U.S. Gov't]. *J Biol Chem*, *284*(24), 16334-16342. doi: 10.1074/jbc.M109.011601
- Mathonnet, G., Fabian, M. R., Svitkin, Y. V., Parsyan, A., Huck, L., Murata, T., . . . Sonenberg, N. (2007). MicroRNA inhibition of translation initiation in vitro by targeting the cap-binding complex eIF4F. *Science*, *317*(5845), 1764-1767.
- Matusue, K., Haluzik, M., Lambert, G., Yim, S. H., Gavrilova, O., Ward, J. M., . . . Gonzalez, F. J. (2003). Liver-specific disruption of PPARgamma in leptin-deficient mice improves fatty liver but aggravates diabetic phenotypes. [Research Support, Non-U.S. Gov't]. *J Clin Invest*, *111*(5), 737-747. doi: 10.1172/JCI17223
- Meister, G., Landthaler, M., Patkaniowska, A., Dorsett, Y., Teng, G., & Tuschl, T. (2004). Human Argonaute2 mediates RNA cleavage targeted by miRNAs and siRNAs. *Mol Cell*, *15*(2), 185-197.
- Mente, A., Razak, F., Blankenberg, S., Vuksan, V., Davis, A. D., Miller, R., . . . Anand, S. S. (2010). Ethnic variation in adiponectin and leptin levels and their association with adiposity and insulin resistance. [Research Support, Non-U.S. Gov't]. *Diabetes Care*, *33*(7), 1629-1634. doi: 10.2337/dc09-1392
- Miller, A. M., Gilchrist, D. S., Nijjar, J., Araldi, E., Ramirez, C. M., Lavery, C. A., . . . Kurowska-Stolarska, M. (2013). MiR-155 has a protective role in the development of non-alcoholic hepatosteatosis in mice. [Research Support, Non-U.S. Gov't]. *PLoS One*, *8*(8), e72324. doi: 10.1371/journal.pone.0072324
- Moller, D. E., & Kaufman, K. D. (2005). Metabolic syndrome: a clinical and molecular perspective. [Review]. *Annu Rev Med*, *56*, 45-62. doi: 10.1146/annurev.med.56.082103.104751

- Monteleone, P., Fabrazzo, M., Tortorella, A., Fuschino, A., & Maj, M. (2002). Opposite modifications in circulating leptin and soluble leptin receptor across the eating disorder spectrum. *Mol Psychiatry*, 7(6), 641-646. doi: 10.1038/sj.mp.4001043
- Naeem, H., Kuffner, R., Csaba, G., & Zimmer, R. (2010). miRSel: automated extraction of associations between microRNAs and genes from the biomedical literature. *BMC Bioinformatics*, 11, 135.
- Nakashima, Y., Plump, A. S., Raines, E. W., Breslow, J. L., & Ross, R. (1994). ApoE-deficient mice develop lesions of all phases of atherosclerosis throughout the arterial tree. [Research Support, Non-U.S. Gov't Research Support, U.S. Gov't, P.H.S.]. *Arterioscler Thromb*, 14(1), 133-140.
- Nazari-Jahantigh, M., Wei, Y., Noels, H., Akhtar, S., Zhou, Z., Koenen, R. R., . . . Schober, A. (2012). MicroRNA-155 promotes atherosclerosis by repressing Bcl6 in macrophages. [Research Support, Non-U.S. Gov't]. *J Clin Invest*, 122(11), 4190-4202. doi: 10.1172/JCI61716
- Neilsen, P. M., Noll, J. E., Mattiske, S., Bracken, C. P., Gregory, P. A., Schulz, R. B., . . . Callen, D. F. (2013). Mutant p53 drives invasion in breast tumors through up-regulation of miR-155. [Research Support, Non-U.S. Gov't]. *Oncogene*, 32(24), 2992-3000. doi: 10.1038/onc.2012.305
- Nielsen, C. B., Shomron, N., Sandberg, R., Hornstein, E., Kitzman, J., & Burge, C. B. (2007). Determinants of targeting by endogenous and exogenous microRNAs and siRNAs. *Rna*, 13(11), 1894-1910.
- Nottrott, S., Simard, M. J., & Richter, J. D. (2006). Human let-7a miRNA blocks protein production on actively translating polyribosomes. *Nat Struct Mol Biol*, 13(12), 1108-1114.
- O'Connell, R. M., Kahn, D., Gibson, W. S., Round, J. L., Scholz, R. L., Chaudhuri, A. A., . . . Baltimore, D. (2010). MicroRNA-155 promotes autoimmune inflammation by enhancing inflammatory T cell development. [Research Support, N.I.H., Extramural Research Support, Non-U.S. Gov't Research Support, U.S. Gov't, Non-P.H.S.]. *Immunity*, 33(4), 607-619. doi: 10.1016/j.immuni.2010.09.009
- Packard, R. R., Lichtman, A. H., & Libby, P. (2009). Innate and adaptive immunity in atherosclerosis. [Research Support, N.I.H., Extramural Research Support, Non-

U.S. Gov't Review]. *Semin Immunopathol*, 31(1), 5-22. doi: 10.1007/s00281-009-0153-8

- Paigen, B., Morrow, A., Brandon, C., Mitchell, D., & Holmes, P. (1985). Variation in susceptibility to atherosclerosis among inbred strains of mice. [Comparative Study Research Support, Non-U.S. Gov't Research Support, U.S. Gov't, P.H.S.]. *Atherosclerosis*, 57(1), 65-73.
- Parker, R., & Song, H. (2004). The enzymes and control of eukaryotic mRNA turnover. *Nat Struct Mol Biol*, 11(2), 121-127.
- Paschos, P., & Paletas, K. (2009). Non alcoholic fatty liver disease and metabolic syndrome. *Hippokratia*, 13(1), 9-19.
- Pelleymounter, M. A., Cullen, M. J., Baker, M. B., Hecht, R., Winters, D., Boone, T., & Collins, F. (1995). Effects of the obese gene product on body weight regulation in ob/ob mice. *Science*, 269(5223), 540-543.
- Petersen, C. P., Bordeleau, M. E., Pelletier, J., & Sharp, P. A. (2006). Short RNAs repress translation after initiation in mammalian cells. *Mol Cell*, 21(4), 533-542.
- Pillai, R. S., Bhattacharyya, S. N., Artus, C. G., Zoller, T., Cougot, N., Basyuk, E., . . . Filipowicz, W. (2005). Inhibition of translational initiation by Let-7 MicroRNA in human cells. *Science*, 309(5740), 1573-1576.
- Pogribny, I. P., Starlard-Davenport, A., Tryndyak, V. P., Han, T., Ross, S. A., Rusyn, I., & Beland, F. A. (2010). Difference in expression of hepatic microRNAs miR-29c, miR-34a, miR-155, and miR-200b is associated with strain-specific susceptibility to dietary nonalcoholic steatohepatitis in mice. *Lab Invest*, 90(10), 1437-1446. doi: 10.1038/labinvest.2010.113
- Poy, M. N., Eliasson, L., Krutzfeldt, J., Kuwajima, S., Ma, X., Macdonald, P. E., . . . Stoffel, M. (2004). A pancreatic islet-specific microRNA regulates insulin secretion. *Nature*, 432(7014), 226-230.
- Rabe, K., Lehrke, M., Parhofer, K. G., & Broedl, U. C. (2008). Adipokines and insulin resistance. [Research Support, Non-U.S. Gov't Review]. *Mol Med*, 14(11-12), 741-751. doi: 10.2119/2008-00058.Rabe

- Raitoharju, E., Lyytikainen, L. P., Levula, M., Oksala, N., Mennander, A., Tarkka, M., . . . Lehtimäki, T. (2011). miR-21, miR-210, miR-34a, and miR-146a/b are up-regulated in human atherosclerotic plaques in the Tampere Vascular Study. [Research Support, Non-U.S. Gov't]. *Atherosclerosis*, *219*(1), 211-217. doi: 10.1016/j.atherosclerosis.2011.07.020
- Rasmussen, K. D., Simmini, S., Abreu-Goodger, C., Bartonicek, N., Di Giacomo, M., Bilbao-Cortes, D., . . . O'Carroll, D. (2010). The miR-144/451 locus is required for erythroid homeostasis. *J Exp Med*, *207*(7), 1351-1358.
- Rees, D. A., & Alcolado, J. C. (2005). Animal models of diabetes mellitus. [Review]. *Diabet Med*, *22*(4), 359-370. doi: 10.1111/j.1464-5491.2005.01499.x
- Reilly, M. P., Lehrke, M., Wolfe, M. L., Rohatgi, A., Lazar, M. A., & Rader, D. J. (2005). Resistin is an inflammatory marker of atherosclerosis in humans. [Research Support, N.I.H., Extramural Research Support, Non-U.S. Gov't Research Support, U.S. Gov't, P.H.S.]. *Circulation*, *111*(7), 932-939. doi: 10.1161/01.CIR.0000155620.10387.43
- Roger, V. L., Go, A. S., Lloyd-Jones, D. M., Benjamin, E. J., Berry, J. D., Borden, W. B., . . . Turner, M. B. (2012). Heart disease and stroke statistics--2012 update: a report from the American Heart Association. *Circulation*, *125*(1), e2-e220.
- Romao, J. M., Jin, W., Dodson, M. V., Hausman, G. J., Moore, S. S., & Guan, L. L. (2011). MicroRNA regulation in mammalian adipogenesis. [Research Support, Non-U.S. Gov't Review]. *Exp Biol Med (Maywood)*, *236*(9), 997-1004. doi: 10.1258/ebm.2011.011101
- Roselaar, S. E., Kakkanathu, P. X., & Daugherty, A. (1996). Lymphocyte populations in atherosclerotic lesions of apoE ^{-/-} and LDL receptor ^{-/-} mice. Decreasing density with disease progression. [Research Support, Non-U.S. Gov't]. *Arterioscler Thromb Vasc Biol*, *16*(8), 1013-1018.
- Rosen, E. D., & MacDougald, O. A. (2006). Adipocyte differentiation from the inside out. [Review]. *Nat Rev Mol Cell Biol*, *7*(12), 885-896. doi: 10.1038/nrm2066
- Rosen, E. D., & Spiegelman, B. M. (2000). Molecular regulation of adipogenesis. [Research Support, U.S. Gov't, P.H.S. Review]. *Annu Rev Cell Dev Biol*, *16*, 145-171. doi: 10.1146/annurev.cellbio.16.1.145

- Rosen, E. D., Walkey, C. J., Puigserver, P., & Spiegelman, B. M. (2000). Transcriptional regulation of adipogenesis. [Research Support, Non-U.S. Gov't Research Support, U.S. Gov't, P.H.S. Review]. *Genes Dev*, *14*(11), 1293-1307.
- Ross, R. (1999). Atherosclerosis--an inflammatory disease. [Research Support, U.S. Gov't, P.H.S. Review]. *N Engl J Med*, *340*(2), 115-126. doi: 10.1056/NEJM199901143400207
- Rottiers, V., & Naar, A. M. (2012). MicroRNAs in metabolism and metabolic disorders. [Research Support, N.I.H., Extramural Review]. *Nat Rev Mol Cell Biol*, *13*(4), 239-250. doi: 10.1038/nrm3313
- Ruan, H., & Lodish, H. F. (2003). Insulin resistance in adipose tissue: direct and indirect effects of tumor necrosis factor-alpha. [Research Support, Non-U.S. Gov't Research Support, U.S. Gov't, P.H.S. Review]. *Cytokine Growth Factor Rev*, *14*(5), 447-455.
- Rudijanto, A. (2007). The role of vascular smooth muscle cells on the pathogenesis of atherosclerosis. [Review]. *Acta Med Indones*, *39*(2), 86-93.
- Saetrom, P., Heale, B. S., Snove, O., Jr., Aagaard, L., Alluin, J., & Rossi, J. J. (2007). Distance constraints between microRNA target sites dictate efficacy and cooperativity. *Nucleic Acids Res*, *35*(7), 2333-2342.
- Saltiel, A. R., & Kahn, C. R. (2001). Insulin signalling and the regulation of glucose and lipid metabolism. *Nature*, *414*(6865), 799-806. doi: 10.1038/414799a
- Sethupathy, P., Borel, C., Gagnebin, M., Grant, G. R., Deutsch, S., Elton, T. S., . . . Antonarakis, S. E. (2007). Human microRNA-155 on chromosome 21 differentially interacts with its polymorphic target in the AGTR1 3' untranslated region: a mechanism for functional single-nucleotide polymorphisms related to phenotypes. [Research Support, N.I.H., Extramural Research Support, Non-U.S. Gov't Research Support, U.S. Gov't, Non-P.H.S.]. *Am J Hum Genet*, *81*(2), 405-413. doi: 10.1086/519979
- Song, J. J., Liu, J., Tolia, N. H., Schneiderman, J., Smith, S. K., Martienssen, R. A., . . . Joshua-Tor, L. (2003). The crystal structure of the Argonaute2 PAZ domain reveals an RNA binding motif in RNAi effector complexes. *Nat Struct Biol*, *10*(12), 1026-1032.

- Song, J. J., Smith, S. K., Hannon, G. J., & Joshua-Tor, L. (2004). Crystal structure of Argonaute and its implications for RISC slicer activity. *Science*, *305*(5689), 1434-1437.
- Spalding, K. L., Arner, E., Westermark, P. O., Bernard, S., Buchholz, B. A., Bergmann, O., . . . Arner, P. (2008). Dynamics of fat cell turnover in humans. [Research Support, N.I.H., Extramural Research Support, Non-U.S. Gov't Research Support, U.S. Gov't, Non-P.H.S.]. *Nature*, *453*(7196), 783-787. doi: 10.1038/nature06902
- Steppan, C. M., Bailey, S. T., Bhat, S., Brown, E. J., Banerjee, R. R., Wright, C. M., . . . Lazar, M. A. (2001). The hormone resistin links obesity to diabetes. [Research Support, Non-U.S. Gov't Research Support, U.S. Gov't, P.H.S.]. *Nature*, *409*(6818), 307-312. doi: 10.1038/35053000
- Sun, K., Kusminski, C. M., & Scherer, P. E. (2011). Adipose tissue remodeling and obesity. [Research Support, N.I.H., Extramural Research Support, Non-U.S. Gov't Review]. *J Clin Invest*, *121*(6), 2094-2101. doi: 10.1172/JCI45887
- Tangirala, R. K., Rubin, E. M., & Palinski, W. (1995). Quantitation of atherosclerosis in murine models: correlation between lesions in the aortic origin and in the entire aorta, and differences in the extent of lesions between sexes in LDL receptor-deficient and apolipoprotein E-deficient mice. [Comparative Study Research Support, U.S. Gov't, P.H.S.]. *J Lipid Res*, *36*(11), 2320-2328.
- Tarantino, G., & Finelli, C. (2013). What about non-alcoholic fatty liver disease as a new criterion to define metabolic syndrome? [Review]. *World J Gastroenterol*, *19*(22), 3375-3384. doi: 10.3748/wjg.v19.i22.3375
- Thermann, R., & Hentze, M. W. (2007). Drosophila miR2 induces pseudo-polysomes and inhibits translation initiation. *Nature*, *447*(7146), 875-878.
- Trayhurn, P., & Beattie, J. H. (2001). Physiological role of adipose tissue: white adipose tissue as an endocrine and secretory organ. [Research Support, Non-U.S. Gov't Review]. *Proc Nutr Soc*, *60*(3), 329-339.
- Tsukada, J., Yoshida, Y., Kominato, Y., & Auron, P. E. (2011). The CCAAT/enhancer (C/EBP) family of basic-leucine zipper (bZIP) transcription factors is a multifaceted highly-regulated system for gene regulation. [Research Support, Non-U.S. Gov't Review]. *Cytokine*, *54*(1), 6-19. doi: 10.1016/j.cyto.2010.12.019

- Turner, M. L., Schnorfeil, F. M., & Brocker, T. (2011). MicroRNAs regulate dendritic cell differentiation and function. [Review]. *J Immunol*, *187*(8), 3911-3917. doi: 10.4049/jimmunol.1101137
- Valencia-Sanchez, M. A., Liu, J., Hannon, G. J., & Parker, R. (2006). Control of translation and mRNA degradation by miRNAs and siRNAs. *Genes Dev*, *20*(5), 515-524.
- Vigorito, E., Perks, K. L., Abreu-Goodger, C., Bunting, S., Xiang, Z., Kohlhaas, S., . . . Turner, M. (2007). microRNA-155 regulates the generation of immunoglobulin class-switched plasma cells. [Research Support, Non-U.S. Gov't]. *Immunity*, *27*(6), 847-859. doi: 10.1016/j.immuni.2007.10.009
- Wang, B., Majumder, S., Nuovo, G., Kutay, H., Volinia, S., Patel, T., . . . Jacob, S. T. (2009). Role of microRNA-155 at early stages of hepatocarcinogenesis induced by choline-deficient and amino acid-defined diet in C57BL/6 mice. [Research Support, N.I.H., Extramural]. *Hepatology*, *50*(4), 1152-1161. doi: 10.1002/hep.23100
- Wang, P., Mariman, E., Renes, J., & Keijer, J. (2008). The secretory function of adipocytes in the physiology of white adipose tissue. [Research Support, Non-U.S. Gov't Review]. *J Cell Physiol*, *216*(1), 3-13. doi: 10.1002/jcp.21386
- Wightman, B., Ha, I., & Ruvkun, G. (1993). Posttranscriptional regulation of the heterochronic gene *lin-14* by *lin-4* mediates temporal pattern formation in *C. elegans*. *Cell*, *75*(5), 855-862.
- Winter, J., Jung, S., Keller, S., Gregory, R. I., & Diederichs, S. (2009). Many roads to maturity: microRNA biogenesis pathways and their regulation. [Research Support, Non-U.S. Gov't Review]. *Nat Cell Biol*, *11*(3), 228-234. doi: 10.1038/ncb0309-228
- World Health Organization: Obesity Fact Sheet. (2014) Retrieved January 11th, 2014
- Wu, D., Molofsky, A. B., Liang, H. E., Ricardo-Gonzalez, R. R., Jouihan, H. A., Bando, J. K., . . . Locksley, R. M. (2011). Eosinophils sustain adipose alternatively activated macrophages associated with glucose homeostasis. [Research Support, N.I.H., Extramural]

- Research Support, Non-U.S. Gov't]. *Science*, 332(6026), 243-247. doi: 10.1126/science.1201475
- Xu, C. C., Han, W. Q., Xiao, B., Li, N. N., Zhu, D. L., & Gao, P. J. (2008). Differential expression of microRNAs in the aorta of spontaneously hypertensive rats. *Sheng Li Xue Bao*, 60(4), 553-560.
- Yan, K. S., Yan, S., Farooq, A., Han, A., Zeng, L., & Zhou, M. M. (2003). Structure and conserved RNA binding of the PAZ domain. *Nature*, 426(6965), 468-474.
- Yekta, S., Shih, I. H., & Bartel, D. P. (2004). MicroRNA-directed cleavage of HOXB8 mRNA. *Science*, 304(5670), 594-596.
- Yuan, Y. R., Pei, Y., Ma, J. B., Kuryavyi, V., Zhadina, M., Meister, G., . . . Patel, D. J. (2005). Crystal structure of A. aeolicus argonaute, a site-specific DNA-guided endoribonuclease, provides insights into RISC-mediated mRNA cleavage. *Mol Cell*, 19(3), 405-419.
- Zadelaar, S., Kleemann, R., Verschuren, L., de Vries-Van der Weij, J., van der Hoorn, J., Princen, H. M., & Kooistra, T. (2007). Mouse models for atherosclerosis and pharmaceutical modifiers. [Research Support, Non-U.S. Gov't Review]. *Arterioscler Thromb Vasc Biol*, 27(8), 1706-1721. doi: 10.1161/ATVBAHA.107.142570
- Zampetaki, A., & Mayr, M. (2012). MicroRNAs in vascular and metabolic disease. [Research Support, Non-U.S. Gov't Review]. *Circ Res*, 110(3), 508-522. doi: 10.1161/CIRCRESAHA.111.247445
- Zhang, S. H., Reddick, R. L., Burkey, B., & Maeda, N. (1994). Diet-induced atherosclerosis in mice heterozygous and homozygous for apolipoprotein E gene disruption. [Comparative Study Research Support, Non-U.S. Gov't Research Support, U.S. Gov't, P.H.S.]. *J Clin Invest*, 94(3), 937-945. doi: 10.1172/JCI117460
- Zuo, H., Shi, Z., Yuan, B., Dai, Y., Wu, G., & Hussain, A. (2013). Association between serum leptin concentrations and insulin resistance: a population-based study from China. [Research Support, Non-U.S. Gov't]. *PLoS One*, 8(1), e54615. doi: 10.1371/journal.pone.0054615